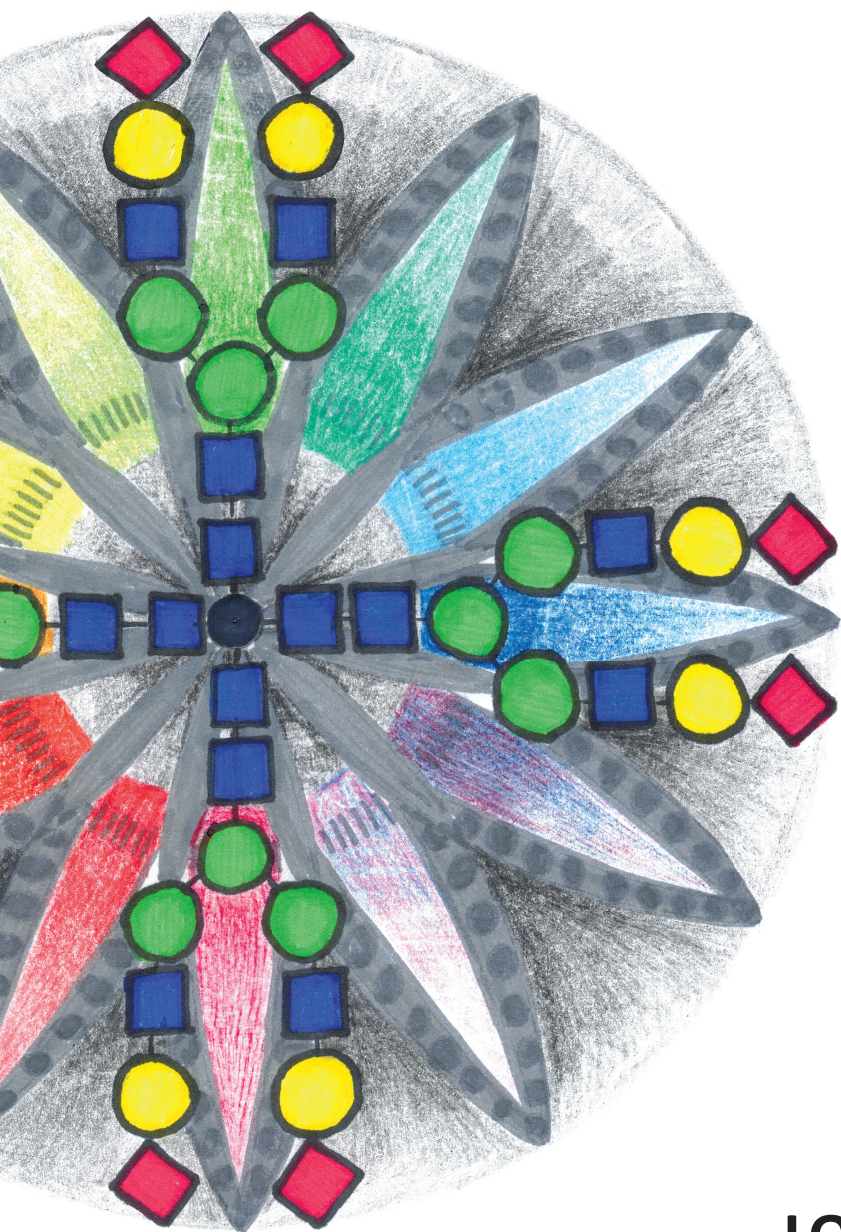


Liver disease in Congenital Disorders of Glycosylation



JOS JANSEN

Liver disease in Congenital Disorders of Glycosylation

Jos Jansen

ISBN: 978-94-6416-301-8

Coverdesign by: Arti Abhilakh Missier

Lay-out by: Publiss | www.publiss.nl

Printed by: Ridderprint | www.ridderprint.nl

© 2021 by Johannes Cornelis Jansen. All rights reserved. No part of this publication may be reproduced or transmitted in any form or by any means without written permission of the author, and, when appropriate, the publisher holding the copyright of the published manuscripts.

The production of this thesis was financially supported by Radboud University in Nijmegen, the Netherlands and Nederlandse Vereniging voor Hepatologie (NVH)

Liver disease in Congenital Disorders of Glycosylation

Proefschrift

ter verkrijging van de graad van doctor
aan de Radboud Universiteit Nijmegen
op gezag van de rector magnificus prof. dr. J.H.J.M. van Krieken,
volgens besluit van het college van decanen
in het openbaar te verdedigen op donderdag 21 januari 2021
om 16.30 uur precies

door

Johannes Cornelis Jansen
geboren op 30 november 1984
te Tiel

Promotoren

Prof. dr. J.P.H. Drenth

Prof. dr. D. J. Lefeber

Manuscriptcommissie

Prof. dr. Ir. R. Roepman

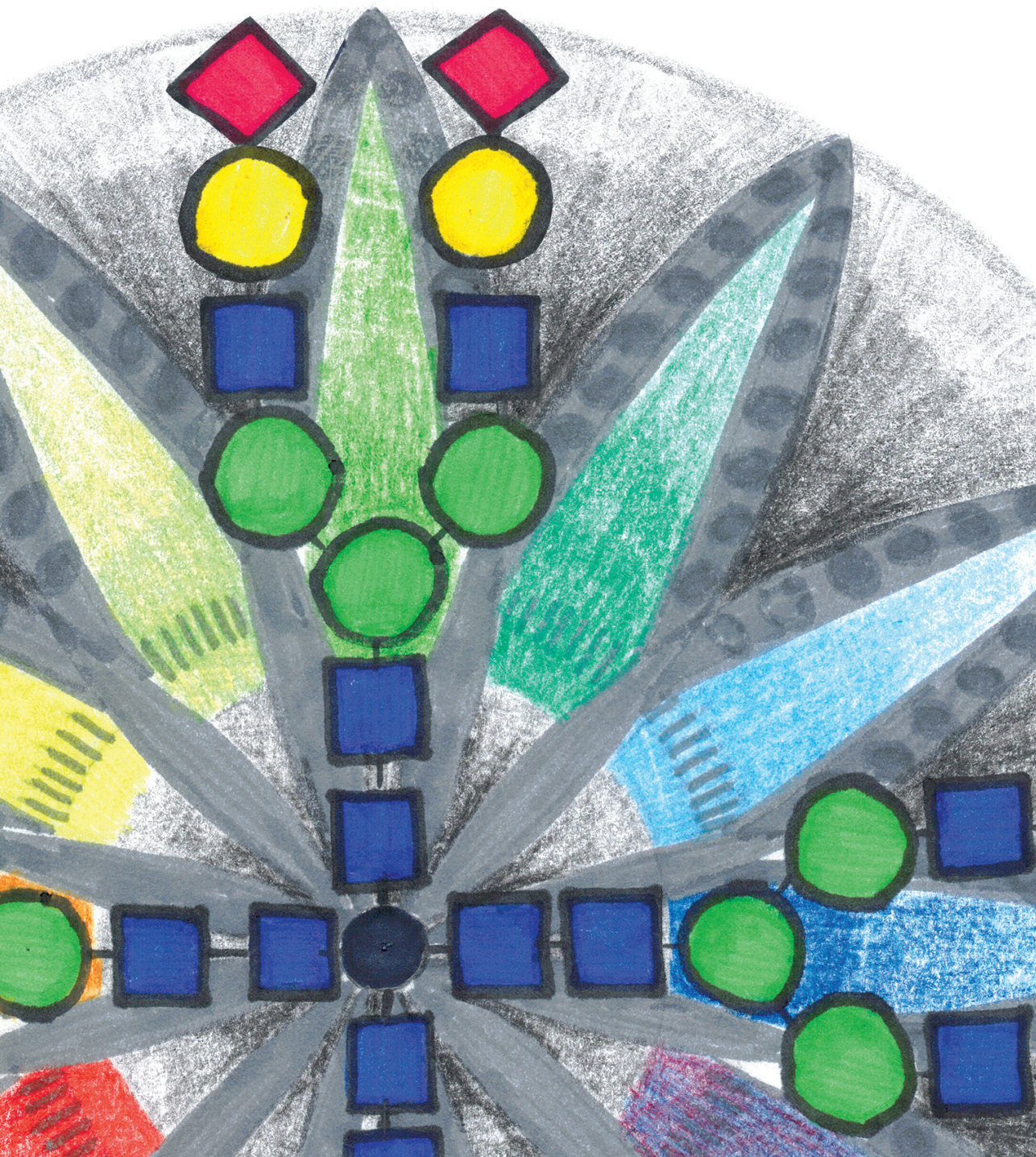
Dr. M.C.H. Janssen

Prof. dr. R. Shiri-Sverdlov (Universiteit Maastricht)

*Voor mijn lieve ouders,
ik weet hoe trots ze zouden zijn*

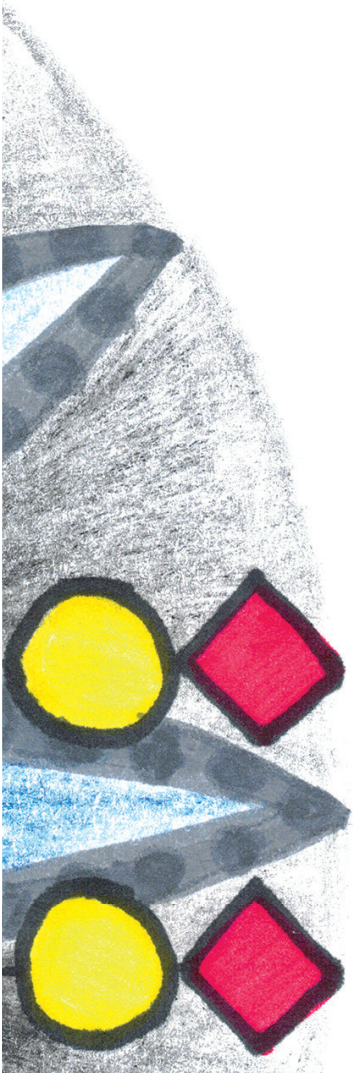
Table of Contents

Chapter 1	Introduction to hepatic congenital glycosylation disorders	9
Chapter 2	CCDC115 Deficiency Causes a Disorder of Golgi Homeostasis with Abnormal Protein Glycosylation <i>Am J Hum Genet. 2016 Feb 4;98(2):310-21</i>	27
Chapter 3	TMEM199 Deficiency Is a Disorder of Golgi Homeostasis Characterized by Elevated Aminotransferases, Alkaline Phosphatase, and Cholesterol and Abnormal Glycosylation <i>Am J Hum Genet. 2016 Feb 4;98(2):322-30</i>	65
Chapter 4	NAFLD Phenotype in Patients With V-ATPase Proton Pump Assembly Defects <i>Cell Mol Gastroenterol Hepatol. 2018 Jan 18;5(3):415-417.e1</i>	87
Chapter 5	Screening for Abnormal Glycosylation in a Cohort of Adult Liver Disease Patients <i>J Inherit Metab Dis. 2020 Jun 18</i>	109
Chapter 6	Discussion	131
Appendices	English summary	150
	Nederlandse samenvatting	152
	Dankwoord	154
	Curriculum vitae	158
	List of publications	159
	Research data management	160
	PhD portfolio	161



CHAPTER 1

Introduction to hepatic congenital glycosylation disorders



In 1865, the Czech friar Gregor Mendel conducted his pea-experiments and it was him who first described what is currently known as Mendelian inheritance.(1) With the publication of his 'Mendelian laws' he can be considered the founder of modern day genetics. Inborn error of metabolism (IEM) is a term coined in 1908 by Sir Archibald Garrod to describe monogenic diseases that affect metabolism. (2) He was the first to describe alkaptonuria, the first inborn error of metabolism that followed Mendelian laws in 1902.(3) Since then, pivotal discoveries such as DNA's double helix structure, the first genetic mapping of hereditary Huntington's disease, DNA amplification by polymerase chain reaction (PCR) and the mapping of the human genome in the HuGo project were advances that have completely changed the landscape of genetics.(4-7) In 2009, the technology of whole exome sequencing (WES or 'exome sequencing') was first published.(8) Exome sequencing is the nucleotide sequencing of all the protein-coding regions in a genome (or the 'exome').(9) This method proved especially useful in identifying pathogenic variants in monogenic diseases and quickly after its introduction, its application to inborn errors of metabolism resulted in the identification of novel IEMs.(10-12) Today, exome sequencing has become widely available in patient care and this is one of the reasons that the list of solved Mendelian diseases is growing exponentially, and Congenital Disorders of Glycosylation (CDG), an IEM with defective glycosylation, is no exception. (13)

Congenital Disorders of Glycosylation (CDG)

Glycosylation

Before describing CDG, a brief introduction to glycosylation is beneficial for understanding this specific group of IEM. Glycosylation is the attachment of glycans to newly formed proteins. A glycan is a compound containing different monosaccharides in a predefined arrangement. An overview is shown in Figure 1. Glycans perform several cellular functions such as protein-protein interactions and cell-cell interactions.(14) There are different glycosylation pathways such as N-glycosylation and O-glycosylation. In this thesis, I will focus on N-glycosylation and will refer to this process as 'glycosylation'. Glycosylation starts on the outer leaflet of the endoplasmic reticulum (ER) with assembly of the glycan and is then 'flipped' by RFT1 to the luminal side. In the lumen, the glycan is further modified and transferred *en bloc* to the newly formed protein by the oligosaccharyltransferase (OST) complex. The glycoprotein, which is highly mannosylated, is transferred to the Golgi apparatus (or simply 'Golgi').

Demannosylation with subsequent galactosylation and sialylation are steps that ultimately result in formation of the complete glycoprotein.

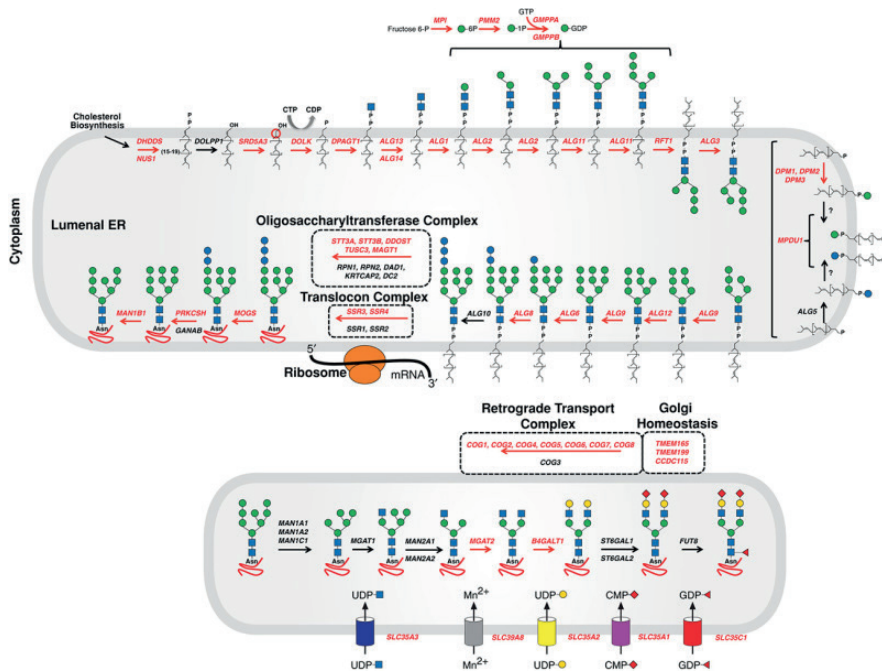


Figure 1. Overview of the glycosylation pathway and CDG due to defective steps in this pathway. Enzymes marked in red are known CDG. Derived from H.H. Freeze, Genetic Disorders of Glycosylation, 2015(15)

The secretory pathway

The secretory pathway is composed of organelles that serve a common purpose, namely excretion and sorting of newly synthesized proteins. It lies adjacent to the nucleus where nascent proteins are folded and checked for improper folding. If folded incorrectly, the protein is removed from the ER by the ER associated degradation (ERAD) mechanism.⁽¹⁶⁾ The ER is also the organelle where a new protein potentially receives the N-glycan, forming a glycoprotein. When the new protein passes quality criteria, it buds off and travels towards the ER-to-Golgi-intermediate compartment (ERGIC) via coatamer protein complex (COP)II vesicles. In the ERGIC the fate of the protein is decided.⁽¹⁷⁾ Most proteins will traffic to and fuse with the Golgi. Others will go to lipid droplets, the plasma membrane or other organelles. The Golgi is where modifications of the glycoprotein take place. The Golgi is composed of different stacks with a clear topology: an ER-orientated *cis*-part; a medial part; and a *trans*-part (or TGN,

trans-Golgi Network). How the new glycoproteins traffic between the stacks remains unclear and several theories exist. The most widely accepted version is the Golgi maturation model.(18) In this model, the Golgi stacks gain a specific set of enzymes, or 'mature', as they progress from the cis-part to the TGN. A consequence of this model is that enzymes, such as glycosyltransferases needed for glycosylation, are present in gradients. These gradients are maintained by coatamer protein complex (COPI) vesicles that provide retrograde transport between Golgi stacks and between the Golgi and the ER/ERGIC.(17) In the TGN new proteins are budded off in vesicles destined for intercellular or extracellular locations. This topic will not be part of this thesis.

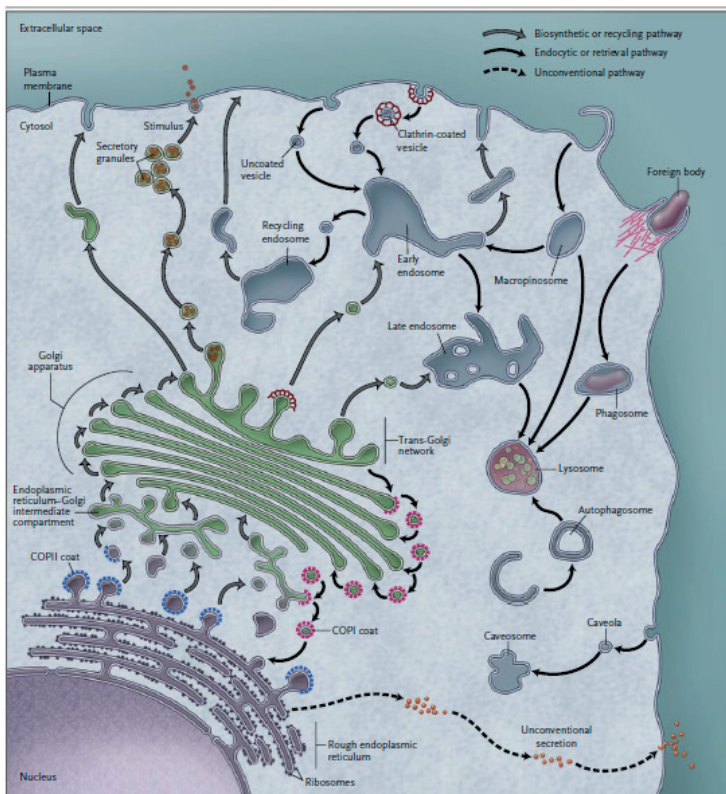


Figure 2. Overview of the secretory pathway. The nascent protein is formed in the ER, the purple tunnel complex in the lower left corner. Thereafter, the Golgi (the green stacks) further finetunes the protein before packing it in endosomes. These endosomes traffic to the cell membrane for endocytosis and release of the protein in the extracellular matrix. Derived from De Matteis and Luini, NEJM, 2011 (19)

Congenital Disorders of Glycosylation

CDG are first discovered by Dr. Jaeken in 1980.(20) CDG are a rare but quickly expanding group of monogenic diseases affecting glycosylation.(21) Since 1980, over 100 monogenic defects have been described affecting different aspects of glycosylation.(22) To date, all CDG are inherited in an autosomal recessive pattern. CDG are classified into two types based on the cellular location of the defective protein. Type 1 CDG affect the assembly of glycans in the ER, either by lowering the supply of substrates (e.g. PMM2-CDG) or by directly compromising enzyme function (e.g. ALG3-CDG). Type 2 CDG affect glycan modification in the Golgi. This can be caused by insufficient influx of sugars due to defects in transferases (e.g. B4GALT1-CDG) or by a defect that leads to an imbalance in Golgi homeostasis.(23) Examples of the latter are: the Conserved oligomeric Golgi (COG) complex defects, which cause mislocalization of glycosyltransferases due to incorrect trafficking between Golgi stacks, or TMEM165-CDG and ATP6V0A2-CDG which lead to abnormal pH and electrolyte imbalance.(24-26) An overview of different CDG and their place in the glycosylation pathway can be seen in Figure 1.

The phenotype of CDG patients

Classically, IEM can be characterized as multisystemic diseases and CDG are no exception to this rule. All body systems are associated with CDG symptoms with a notable exception for the pulmonary system.(27) Frequently dysmorphic features are present and these are accompanied by severe psychomotor disability and failure to thrive. Biochemical liver abnormalities are frequently seen in CDG but often not of primary concern for clinicians.(28) An exception is MPI-CDG, which presents predominantly with liver disease and protein-losing enteropathy.(29) On the other hand, abnormal glycosylation per se can be attributed to liver dysfunction.

Liver disease and abnormal glycosylation

The liver is the main organ responsible for protein synthesis and secretion, and an effect on protein glycosylation can be expected in case of liver disease. Multiple liver diseases are associated with abnormal glycosylation. (30) Here, I will highlight two of the frequent and well-studied liver diseases. The most well-known liver disease to cause abnormal glycosylation is alcoholic liver disease. In fact, the alcohol consumption test (CDT) is based on decreased activity of

β -Galactoside α 2,6-Sialyltransferase (*ST6GAL1*) leading to hyposialylation and a type I CDG pattern.(31, 32) Hepatocellular carcinoma (HCC) has been associated with increased fucosylation in multiple publications.(33) Most notably, the increase in activity of α 1-6-Fucosyl transferase (*FUT8*) results in hyperfucosylation of several proteins.(34) Of these proteins, α -fetoprotein (AFP) is used in diagnostics of HCC. Fucosylated AFP can better distinguish between HCC and non-HCC liver disease than non-fucosylated AFP.(35, 36)

Congenital metabolic liver diseases

As mentioned before, except for MPI-CDG, there are no CDG that present with isolated liver disease. Congenital metabolic liver diseases are a diverse group of diseases accounting for 6% of all liver transplantations in Europe in 2018.(37) This group is characterized by an autosomal dominant or recessive inherited pathogenic variant in a gene that codes for a hepatic enzyme. This can lead to an enzyme deficiency which leads to (1) structural liver disease with cirrhosis and ultimately liver related morbidity necessitating liver transplantation or (2) can cause injury to other organ systems.

The most well-known metabolic liver diseases that cause structural liver damage are alpha 1 antitrypsin deficiency, hereditary hemochromatosis and Wilson disease. In these three diseases, hepatic injury is the result of accumulation of respectively polymerized alpha-1 antitrypsin, iron or copper.(38-40) The mainstay of treatment is lowering hepatic concentrations of these substances. Lesser prevalent diseases that cause hepatic injury are the intrahepatic cholestasis syndromes which are caused by defective intrahepatic bilirubin transport.(41)

Metabolic liver diseases that additionally present with multisystemic disease symptoms can be attributed to defective metabolic pathways such as the urea cycle, glycogen storage, lipid metabolism, amino acid metabolism and carbohydrate metabolism. Liver transplantation is able to revert the liver phenotype in these patients in some cases.(42) As described in this thesis, the discovery of a CDG subgroup with a liver-dominant phenotype due to defects in assembly factors of the Vacuolar ATPase (V-ATPase) adds CDG to the list of congenital metabolic liver disease.

Diagnostic techniques in CDG

Exome sequencing

Filtering steps

As described in the first paragraph, exome sequencing allows analysis of all nucleotides in the exome. A nucleotide that differs from the most prevalent nucleotide is called a variant. As contemporary exome sequencing strategies generate ~80,000 variants, the sheer amount of data generated by exome sequencing requires rigorous filtering to identify the pathogenic variant. The most important filtering step for rare Mendelian disorders is based on the prevalence of a variant in the general population.⁽⁴³⁾ If a variant is more prevalent in the general population than the disorder itself, pathogenicity is unlikely. Databases with large cohorts of exomes (such as the Exome Aggregation Consortium (ExAC)) have been very important to facilitate this step.⁽⁴⁴⁾ After this first step, about hundred variants still remain. *In silico* tools such as Polyphen 2.0, SIFT and MutationTaster can be used to predict pathogenicity, however validation of these diagnostic tools demonstrated a limited sensitivity and specificity (60-80%).⁽⁴⁵⁾ For recessive disorders filtering based on familial segregation is a powerful adjunct. Homozygous or compound heterozygous variants must segregate within the family and preferably in multiple unrelated families.^(9, 46)

Limitations and challenges of exome sequencing

The most obvious limitation of exome sequencing is that only 1% of the genome is sequenced. Leaving out the other 99% undoubtedly results in loss of information. Another limitation is incomplete coverage of the exome due to low call rates. This was particularly the case for earlier kits (call rate of ~85%).⁽⁴⁷⁾ However, technical advances increased this percentage to ~95%.⁽⁴⁸⁾ Applied whole genome sequencing was first described in 2008 and its utility and technique is rapidly evolving.^(49, 50) Whole genome sequencing covers almost the whole genome. Its use has been proven in patients with intellectual disability where exome sequencing was inconclusive.⁽⁵¹⁾

An interesting outcome of a carrier screening study showed that 122 out of 460 (27%) of initially reported pathogenic variants were redefined as common polymorphisms or sequence errors.⁽⁵²⁾ The high false-positive rate in this study, and of other studies questioning causality of reported variants, led the American

Society for Human Genetics to publish strict guidelines for investigating causality. (53, 54) They recommend to provide firm functional evidence before a variant can be recognized as pathogenic.

Another challenge is that patient clustering is difficult because of a variable phenotype. One single genetic mutation may be associated with severe disease but also with mild disease with different clinical symptoms. Another challenge is the lack of knowledge regarding metabolic pathways, especially when many proteins are involved, such as the secretory pathway which encompasses at least 1000 proteins.

Methods to identify abnormal glycosylation

Isoelectric focusing

Diagnostics for CDG are based on the glycosylation profile of serum transferrin. Transferrin has two N-glycosylation sites at Asn432 and Asn630.(55) Isoelectric focusing (IEF) is an easily performed technique where protein isoforms are separated based on their isoelectric point. In most laboratory, it is the first step in CDG diagnostics. A glycan is negatively charged because of the two terminally located sialic acids. If both glycosylation sites of transferrin are occupied a total of four sialic acids are present. If glycosylation is incomplete, fewer sialic acids are present and this results in isoforms with a different isoelectric point. As already stated, type 1 CDG result in absence of complete glycans and thus accumulation of transferrin isoforms with two or zero sialic acids. Type 2 CDG, resulting in incomplete glycans, have an accumulation of isoforms with three, two, one or zero sialic acids. Advantages of IEF are low costs and high throughput. A disadvantage is the lack of information about other monosaccharides in the glycan, and about other glycan structural abnormalities, such as branching and fucosylation. A typical tIEF pattern is shown in Figure 3.

Whole serum mass spectrometry glycomics

Mass spectrometry of free serum glycans is an established method to analyze all glycans present in the serum.(56) For this, glycans are cleaved from the glycoprotein and the substrate injected into a MS. An advantage is the detailed information regarding the structure of the glycan, however due to the cleavage of the glycoprotein, it is not possible to attribute a glycan isoform to a specific

protein. Additionally, a lack of total glycans cannot be measured, rendering it less useful in the diagnostics for type 1 CDG. Additionally, because of the labile nature of the sialic acid, the glycan has to be derivatized to improve its stability during MS. This is less of a problem in recent LC-MS glycomics methods.

QTOF mass spectrometry analysis of intact transferrin

Efforts to overcome the limitations of IEF and whole serum N-glycan analysis lead to implementation and validation of mass spectrometry of the serum transferrin glycoprotein.(57) In short, serum transferrin is pulled down with anti-transferrin beads and injected on a LC system, before being sprayed into the Quadruple Time of Flight mass spectrometer (QTOF MS). A typical QTOF-MS spectrum of the intact transferrin is shown in Figure 3. Any peak with lower molecular mass represent incomplete glycans. The difference on the x-axis correlates to the weight of specific sugars. For example: loss of one sialic acid (296 amu), typical for type 2 CDG. Reference ranges of the percentage of the main peak have been determined for diagnostic purposes.

The advantage of mass spectrometric methods has been shown by the ability to unravel the pathogenic defect in several CDG subtypes. Two examples are MAN1B1-CDG and PGM1-CDG. MAN1B1 is the enzyme that cleaves off mannoses during glycan modification.(58) QTOF MS profiling showed accumulation of peaks associated with uncleaved mannose glycans. Another example is PGM1-CDG. (59) PGM1 catalyzes the bi-directional interconversion of glucose-1-phosphate and glucose-6-phosphate and is dually important for glucose metabolism and glycosylation. QTOF-MS showed a combination of type 1 and type 2 CDG, possibly due to effects on several events in the glycosylation pathway. Additionally, oral galactose supplementation in PGM1-CDG could be monitored by QTOF glycoprofiling. QTOF-MS can also be valuable in identification and grouping of CDG with an unknown genetic cause. Disadvantages are that only the glycosylation of transferrin can be measured. This implies that tissue- or protein-specific glycosylation defects, such as the Cohen syndrome, are missed. (60) This limitation extends to cell models as only hepatic cell lines produce transferrin and glycosylation of transferrin does not resemble physiological transferrin (unpublished observations).

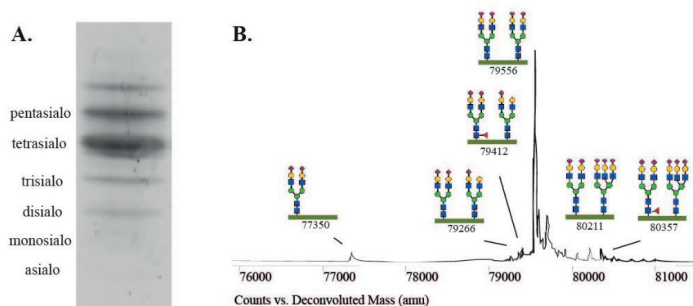


Figure 3. A. a typical tIEF pattern. The most abundant band is the Transferrin isoform with four sialic acids. B. QTOF MS of transferrin as a tool to define new groups of glycosylation disorders. The x-axis represents the deconvoluted atomic mass unit (amu) and the y-axis the abundance. The mass of the intact glycoprotein is 79.555 amu.

Outline of this thesis

In this thesis, I set out to obtain more insight in the association between abnormal glycosylation and liver disease in CDG. The incentive were patients from eight families with similar hepatic symptoms and a similar abnormal QTOF MS profile. Despite strong clinical and biochemical clues that these families had a mutation in the same gene (or a gene in the same pathway), regular genetic workup failed. This workup included linkage analysis, targeted sequencing for known Golgi homeostasis defects and exome sequencing.

The general aims of this thesis are to identify the pathogenic variants in these families, to identify more families, and to characterize the function of the newly found proteins. Another aim was to explore glycosylation in patients with severe liver transplantation. The following research questions were formulated:

Research question 1: can we find the pathogenic gene(s) in eight families with abnormal glycosylation

In **chapter 2** and **chapter 3** I describe how we used comparative genomics to identify the pathogenic variants in families with CDG. Available knowledge on Golgi proteins from *saccharomyces cerevisiae*, including the yeast Vacuolar H⁺-ATPase (V-ATPase), was used. The V-ATPase is an intracellular proton pump responsible for the pH gradient of the secretory pathway. This pump was particularly interesting because in human, mutations in a gene encoding one of the core subunits (*ATP6V0A2*) leads to abnormal glycosylation due to a Golgi homeostasis defect. This model was used with success to identify homozygous and compound heterozygous missense mutations in *CCDC115* and *TMEM199* in twelve patients from eight families. For *TMEM199*, these mutations were incompletely covered by exome sequencing. Yeast homologs of *CCDC115* and *TMEM199*, Vma22p and Vph2p, are ER-dedicated assembly factors of a subdomain of the V-ATPase. These two chapters cover the identification and confirmation of mutations in both genes. For the first time we show that both proteins are localized in the early secretory pathway in human. Additionally, the patient's phenotype, mostly hepatic, and glycosylation profile are described.

*Research question 2: can we correlate the phenotype of *CCDC115* and *TMEM199* deficiency to more common diseases*

Patients with mutations in *CCDC115* or *TMEM199* all have liver injury. In chapter 2 and chapter 3 we show that both proteins are located in the ERGIC organelle. This led to the hypothesis that both proteins are involved in trafficking of new proteins from the ER to the Golgi and back. Abnormal glycosylation can be hypothesized to be caused by an imbalance in Golgi homeostasis. However, the effect of disturbed ER-to-Golgi trafficking on the origin of steatosis remains unclear. In addition to *CCDC115* and *TMEM199* deficiency our group also identified *ATP6AP1* mutations in patients with similar symptoms. *ATP6AP1* is also a V-ATPase assembly factor. In **chapter 4** we wrote a narrative on the possible pathomechanism of V-ATPase assembly factor deficiencies. We hypothesized a model where disturbed trafficking via COPI vesicles results in hepatic steatosis.

Research question 3: can screening in a pre-selected liver patient group identify more patients with CDG?

In chapter 2 and 3 I describe eight families we discovered based on screening of genetically unsolved CDG patients that were sent to us via the EURO-CDG network, a European collaboration. However, because of the relative mild hepatic phenotype we set out to identify additional patients. For this we screened plasma or patient-derived serum samples stored in biobanks of three different liver transplantation centers and from the hepatitis biobank in the Radboudumc. **Chapter 5** describes this screening process. The results from this study were that 26% had abnormal glycosylation measured with IEF but no clear CDG profiles were detected with MS.

Research question 4: can we use our cohort to gain more insight in differences between primary and secondary glycosylation defects

Establishing a large cohort of patients with liver disease of various degrees left us with the unique opportunity to research glycosylation in liver disease. These data are useful as liver disease often interferes with CDG diagnostics. In **chapter 5** we show that especially hyperfucosylation occurs more frequently in liver disease compared with healthy controls. As hyperfucosylation is not a known phenomenon in CDG patients this could aid in diagnostics when a CDG is suspected in a patient with severe liver disease.

Chapter	Research question	Hypothesis	Research model
2, 3	Research question 1: can we find the pathogenic gene(s) in eight families with abnormal glycosylation	<p>1. Vph2p and Vma22p, two yeast proteins, have TMEM199 and CCDC115 as human orthologs</p> <p>2. pathogenic variants in <i>CCDC115</i> and <i>TMEM199</i> are causative for the geno- and phenotype in the investigated families</p> <p>3. CCDC115 and TMEM199 are located in the ERGIC</p>	<p>1. Comparative genomics</p> <p>2. WES, sanger sequencing, Western blot</p> <p>Immunofluorescence studies</p>
4	Research question 2: can we correlate the phenotype of CCDC115 and TMEM199 deficiency to more common diseases	Abnormal Golgi homeostasis due to CCDC115 and TMEM199 deficiency can be correlated to defective intracellular lipid transport via COP I and COP II vesicles	Narrative review
5	Research question 3: can screening in a pre-selected liver patient group identify more patients with CDG?	The a-priori chance of finding a CDG in patients with liver disease is higher	Retrospective screening study
5	Research question 4: can we use our cohort to gain more insight in differences between primary and secondary glycosylation defects	Hyposialylation and hyperfucosylation are more frequently seen in liver disease	tIEF and QTOF mass spectrometry

References

1. Ellis TH, Hofer JM, Timmerman-Vaughan GM, Coyne CJ, Hellens RP. Mendel, 150 years on. *Trends in plant science*. 2011;16(11):590-6.
2. Scriver CR. Garrod's Croonian Lectures (1908) and the charter 'Inborn Errors of Metabolism': albinism, alkaptonuria, cystinuria, and pentosuria at age 100 in 2008. *Journal of inherited metabolic disease*. 2008;31(5):580-98.
3. Garrod AE. The incidence of alkaptonuria: a study in chemical individuality. 1902 [classical article]. *The Yale journal of biology and medicine*. 2002;75(4):221-31.
4. Watson JD, Crick FH. Genetical implications of the structure of deoxyribonucleic acid. *Nature*. 1953;171(4361):964-7.
5. Mullis K, Faloona F, Scharf S, Saiki R, Horn G, Erlich H. Specific enzymatic amplification of DNA in vitro: the polymerase chain reaction. *Cold Spring Harbor symposia on quantitative biology*. 1986;51 Pt 1:263-73.
6. McPherson JD, Marra M, Hillier L, Waterston RH, Chinwalla A, Wallis J, et al. A physical map of the human genome. *Nature*. 2001;409(6822):934-41.
7. Gusella JF, Wexler NS, Conneally PM, Naylor SL, Anderson MA, Tanzi RE, et al. A polymorphic DNA marker genetically linked to Huntington's disease. *Nature*. 1983;306(5940):234-8.
8. Ng SB, Turner EH, Robertson PD, Flygare SD, Bigham AW, Lee C, et al. Targeted capture and massively parallel sequencing of 12 human exomes. *Nature*. 2009;461(7261):272-6.
9. Bamshad MJ, Ng SB, Bigham AW, Tabor HK, Emond MJ, Nickerson DA, et al. Exome sequencing as a tool for Mendelian disease gene discovery. *Nature reviews Genetics*. 2011;12(11):745-55.
10. Ng SB, Buckingham KJ, Lee C, Bigham AW, Tabor HK, Dent KM, et al. Exome sequencing identifies the cause of a mendelian disorder. *Nature genetics*. 2010;42(1):30-5.
11. Krawitz PM, Schweiger MR, Rodelsperger C, Marcelis C, Kolsch U, Meisel C, et al. Identity-by-descent filtering of exome sequence data identifies PIGV mutations in hyperphosphatasia mental retardation syndrome. *Nature genetics*. 2010;42(10):827-9.
12. Musunuru K, Pirruccello JP, Do R, Peloso GM, Guiducci C, Sougnez C, et al. Exome sequencing, ANGPTL3 mutations, and familial combined hypolipidemia. *The New England journal of medicine*. 2010;363(23):2220-7.
13. Yang Y, Muzny DM, Reid JG, Bainbridge MN, Willis A, Ward PA, et al. Clinical whole-exome sequencing for the diagnosis of mendelian disorders. *The New England journal of medicine*. 2013;369(16):1502-11.
14. Ohtsubo K, Marth JD. Glycosylation in cellular mechanisms of health and disease. *Cell*. 2006;126(5):855-67.
15. Freeze HH, Schachter H, Kinoshita T. Genetic Disorders of Glycosylation. In: rd, Varki A, Cummings RD, Esko JD, Stanley P, Hart GW, et al., editors. *Essentials of Glycobiology*. Cold Spring Harbor (NY)2015. p. 569-82.
16. Christianson JC, Ye Y. Cleaning up in the endoplasmic reticulum: ubiquitin in charge. *Nature structural & molecular biology*. 2014;21(4):325-35.
17. Brandizzi F, Barlowe C. Organization of the ER-Golgi interface for membrane traffic control. *Nature reviews Molecular cell biology*. 2013;14(6):382-92.
18. Farquhar MG, Palade GE. The Golgi apparatus: 100 years of progress and controversy. *Trends in cell biology*. 1998;8(1):2-10.
19. De Matteis MA, Luini A. Mendelian disorders of membrane trafficking. *The New England journal of medicine*. 2011;365(10):927-38.

20. Jaeken J. Familial psychomotor retardation with markedly fluctuating serum prolactin, FSH and GH levels, partial TBG-deficiency, increased serum arylsulphatase A and increased CSF protein: a new syndrome? *Pediatric research*. 1980;14(2):179.
21. Haeuptle MA, Hennet T. Congenital disorders of glycosylation: an update on defects affecting the biosynthesis of dolichol-linked oligosaccharides. *Human mutation*. 2009;30(12):1628-41.
22. Freeze HH, Chong JX, Bamshad MJ, Ng BG. Solving glycosylation disorders: fundamental approaches reveal complicated pathways. *American journal of human genetics*. 2014;94(2):161-75.
23. Guillard M, Morava E, de Ruijter J, Roscioli T, Penzien J, van den Heuvel L, et al. B4GALT1-congenital disorders of glycosylation presents as a non-neurologic glycosylation disorder with hepatointestinal involvement. *The Journal of pediatrics*. 2011;159(6):1041-3 e2.
24. Fisher P, Ungar D. Bridging the Gap between Glycosylation and Vesicle Traffic. *Frontiers in cell and developmental biology*. 2016;4:15.
25. Foulquier F, Amyere M, Jaeken J, Zeevaert R, Schollen E, Race V, et al. TMEM165 deficiency causes a congenital disorder of glycosylation. *American journal of human genetics*. 2012;91(1):15-26.
26. Kornak U, Reynders E, Dimopoulou A, van Reeuwijk J, Fischer B, Rajab A, et al. Impaired glycosylation and cutis laxa caused by mutations in the vesicular H⁺-ATPase subunit ATP6V0A2. *Nature genetics*. 2008;40(1):32-4.
27. Jaeken J. Congenital disorders of glycosylation (CDG): it's (nearly) all in it! *Journal of inherited metabolic disease*. 2011;34(4):853-8.
28. Janssen MJ, Waanders E, Woudenberg J, Lefeber DJ, Drenth JP. Congenital disorders of glycosylation in hepatology: the example of polycystic liver disease. *Journal of hepatology*. 2010;52(3):432-40.
29. Pelletier VA, Galeano N, Brochu P, Morin CL, Weber AM, Roy CC. Secretory diarrhea with protein-losing enteropathy, enterocolitis cystica superficialis, intestinal lymphangiectasia, and congenital hepatic fibrosis: a new syndrome. *The Journal of pediatrics*. 1986;108(1):61-5.
30. Blomme B, Van Steenkiste C, Callewaert N, Van Vlierberghe H. Alteration of protein glycosylation in liver diseases. *Journal of hepatology*. 2009;50(3):592-603.
31. Rao MN, Lakshman MR. Chronic ethanol consumption leads to destabilization of rat liver beta-galactoside alpha2,6-sialyltransferase mRNA. *Metabolism: clinical and experimental*. 1999;48(6):797-803.
32. Gong M, Garige M, Hirsch K, Lakshman MR. Liver Galbeta1,4GlcNAc alpha2,6-sialyltransferase is down-regulated in human alcoholics: possible cause for the appearance of asialoconjugates. *Metabolism: clinical and experimental*. 2007;56(9):1241-7.
33. Mehta A, Block TM. Fucosylated glycoproteins as markers of liver disease. *Disease markers*. 2008;25(4-5):259-65.
34. Noda K, Miyoshi E, Uozumi N, Yanagidani S, Ikeda Y, Gao C, et al. Gene expression of alpha1-6 fucosyltransferase in human hepatoma tissues: a possible implication for increased fucosylation of alpha-fetoprotein. *Hepatology*. 1998;28(4):944-52.
35. Shiraki K, Takase K, Tameda Y, Hamada M, Kosaka Y, Nakano T. A clinical study of lectin-reactive alpha-fetoprotein as an early indicator of hepatocellular carcinoma in the follow-up of cirrhotic patients. *Hepatology*. 1995;22(3):802-7.
36. Taketa K, Sekiya C, Namiki M, Akamatsu K, Ohta Y, Endo Y, et al. Lectin-reactive profiles of alpha-fetoprotein characterizing hepatocellular carcinoma and related conditions. *Gastroenterology*. 1990;99(2):508-18.
37. Adam R, Karam V, Cailliez V, JG OG, Mirza D, Cherqui D, et al. 2018 Annual Report of the

- European Liver Transplant Registry (ELTR) - 50-year evolution of liver transplantation. *Transplant international : official journal of the European Society for Organ Transplantation*. 2018;31(12):1293-317.
38. Kowdley KV, Brown KE, Ahn J, Sundaram V. ACG Clinical Guideline: Hereditary Hemochromatosis. *The American journal of gastroenterology*. 2019;114(8):1202-18.
 39. Patel D, Teckman JH. Alpha-1-Antitrypsin Deficiency Liver Disease. *Clin Liver Dis*. 2018;22(4):643-55.
 40. Roberts EA, Schilsky ML, American Association for Study of Liver D. Diagnosis and treatment of Wilson disease: an update. *Hepatology*. 2008;47(6):2089-111.
 41. Gunaydin M, Bozkurter Cil AT. Progressive familial intrahepatic cholestasis: diagnosis, management, and treatment. *Hepat Med*. 2018;10:95-104.
 42. Hansen K, Horslen S. Metabolic liver disease in children. *Liver transplantation : official publication of the American Association for the Study of Liver Diseases and the International Liver Transplantation Society*. 2008;14(4):391-411.
 43. Lelieveld SH, Veltman JA, Gilissen C. Novel bioinformatic developments for exome sequencing. *Human genetics*. 2016.
 44. Lek M, al. e. Analysis of protein-coding genetic variation in 60,706 humans. *bioRxiv*. 2015.
 45. Thusberg J, Olatubosun A, Vihinen M. Performance of mutation pathogenicity prediction methods on missense variants. *Human mutation*. 2011;32(4):358-68.
 46. Gilissen C, Hoischen A, Brunner HG, Veltman JA. Disease gene identification strategies for exome sequencing. *European journal of human genetics : EJHG*. 2012;20(5):490-7.
 47. Parla JS, Iossifov I, Grabill I, Spector MS, Kramer M, McCombie WR. A comparative analysis of exome capture. *Genome biology*. 2011;12(9):R97.
 48. Lelieveld SH, Spielmann M, Mundlos S, Veltman JA, Gilissen C. Comparison of Exome and Genome Sequencing Technologies for the Complete Capture of Protein-Coding Regions. *Human mutation*. 2015;36(8):815-22.
 49. Lupski JR, Reid JG, Gonzaga-Jauregui C, Rio Deiros D, Chen DC, Nazareth L, et al. Whole-genome sequencing in a patient with Charcot-Marie-Tooth neuropathy. *The New England journal of medicine*. 2010;362(13):1181-91.
 50. van Dijk EL, Jaszczyszyn Y, Naquin D, Thermes C. The Third Revolution in Sequencing Technology. *Trends in genetics : TIG*. 2018;34(9):666-81.
 51. Gilissen C, Hehir-Kwa JY, Thung DT, van de Vorst M, van Bon BW, Willemsen MH, et al. Genome sequencing identifies major causes of severe intellectual disability. *Nature*. 2014;511(7509):344-7.
 52. Bell CJ, Dinwiddie DL, Miller NA, Hateley SL, Ganusova EE, Mudge J, et al. Carrier testing for severe childhood recessive diseases by next-generation sequencing. *Science translational medicine*. 2011;3(65):65ra4.
 53. MacArthur DG, Manolio TA, Dimmock DP, Rehm HL, Shendure J, Abecasis GR, et al. Guidelines for investigating causality of sequence variants in human disease. *Nature*. 2014;508(7497):469-76.
 54. Richards S, Aziz N, Bale S, Bick D, Das S, Gastier-Foster J, et al. Standards and guidelines for the interpretation of sequence variants: a joint consensus recommendation of the American College of Medical Genetics and Genomics and the Association for Molecular Pathology. *Genetics in medicine : official journal of the American College of Medical Genetics*. 2015;17(5):405-24.
 55. Guillard M, Wada Y, Hansikova H, Yuasa I, Vesela K, Ondruskova N, et al. Transferrin mutations at the glycosylation site complicate diagnosis of congenital disorders of glycosylation type I. *Journal of inherited metabolic disease*. 2011;34(4):901-6.
 56. Guillard M, Morava E, van Delft FL, Hague R, Korner C, Adamowicz M, et al. Plasma N-glycan

- profiling by mass spectrometry for congenital disorders of glycosylation type II. *Clinical chemistry*. 2011;57(4):593-602.
57. van Scherpenzeel M, Steenbergen G, Morava E, Wevers RA, Lefeber DJ. High-resolution mass spectrometry glycoprofiling of intact transferrin for diagnosis and subtype identification in the congenital disorders of glycosylation. *Translational research : the journal of laboratory and clinical medicine*. 2015;166(6):639-49 e1.
 58. Van Scherpenzeel M, Timal S, Ryman D, Hoischen A, Wührer M, Hipgrave-Ederveen A, et al. Diagnostic serum glycosylation profile in patients with intellectual disability as a result of MAN1B1 deficiency. *Brain : a journal of neurology*. 2014;137(Pt 4):1030-8.
 59. Tegtmeier LC, Rust S, van Scherpenzeel M, Ng BG, Losfeld ME, Timal S, et al. Multiple phenotypes in phosphoglucomutase 1 deficiency. *The New England journal of medicine*. 2014;370(6):533-42.
 60. Duplomb L, Duvet S, Picot D, Jego G, El Chehadeh-Djebbar S, Marle N, et al. Cohen syndrome is associated with major glycosylation defects. *Human molecular genetics*. 2014;23(9):2391-9.

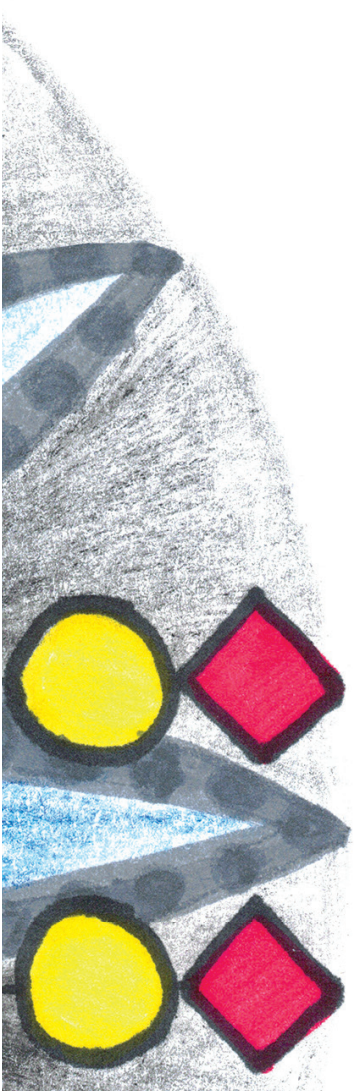


CHAPTER 2

CCDC115 Deficiency Causes a Disorder of Golgi Homeostasis with Abnormal Protein Glycosylation

Jos C. Jansen, Sebahattin Cirak, Monique van Scherpenzeel, Sharita Timal, Janine Reunert, Stephan Rust, Belén Pérez, Dorothée Vicogne, Peter Krawitz, Yoshinao Wada, Angel Ashikov, Celia Pérez-Cerdá, Celia Medrano, Andrea Arnoldy, Alexander Hoischen, Karin Huijben, Gerry Steenbergen, Dulce Quelhas, Luisa Diogo, Daisy Rymen, Jaak Jaeken, Nathalie Guffon, David Cheillan, Lambertus P. van den Heuvel, Yusuke Maeda, Olaf Kaiser, Ulrike Schara, Patrick Gerner, Marjolein A.W. van den Boogert, Adriaan G. Holleboom, Marie-Cécile Nassogne, Etienne Sokal, Jody Salomon, Geert van den Bogaart, Joost P.H. Drenth, Martijn A. Huynen, Joris A. Veltman, Ron A. Wevers, Eva Morava, Gert Matthijs, François Foulquier, Thorsten Marquardt, and Dirk J. Lefeber

Am J Hum Genet. 2016 Feb 4;98(2):310-21



Abstract

Disorders of Golgi homeostasis form an emerging group of genetic defects. The highly heterogeneous clinical spectrum is not explained by our current understanding of the underlying cell-biological processes in the Golgi. Therefore, uncovering genetic defects and annotating gene function are challenging. Exome sequencing in a family with three siblings affected by abnormal Golgi glycosylation revealed a homozygous missense mutation, c.92T>C (p.Leu31Ser), in coiled-coil domain containing 115 (*CCDC115*), the function of which is unknown. The same mutation was identified in three unrelated families, and in one family it was compound heterozygous in combination with a heterozygous deletion of *CCDC115*. An additional homozygous missense mutation, c.31G>T (p.Asp11Tyr), was found in a family with two affected siblings. All individuals displayed a storage-disease-like phenotype involving hepatosplenomegaly, which regressed with age, highly elevated bone-derived alkaline phosphatase, elevated aminotransferases, and elevated cholesterol, in combination with abnormal copper metabolism and neurological symptoms. Two individuals died of liver failure, and one individual was successfully treated by liver transplantation. Abnormal N- and mucin type O-glycosylation was found on serum proteins, and reduced metabolic labeling of sialic acids was found in fibroblasts, which was restored after complementation with wild-type *CCDC115*. PSI-BLAST homology detection revealed reciprocal homology with Vma22p, the yeast V-ATPase assembly factor located in the endoplasmic reticulum(ER). Human *CCDC115* mainly localized to the ERGIC and to COPI vesicles, but not to the ER. These data, in combination with the phenotypic spectrum, which is distinct from that associated with defects in V-ATPase core subunits, suggest a more general role for *CCDC115* in Golgi trafficking. Our study reveals *CCDC115* deficiency as a disorder of Golgi homeostasis that can be readily identified via screening for abnormal glycosylation in plasma.

Introduction

Congenital Disorders of glycosylation (CDG) are a heterogeneous group of monogenic diseases affecting the glycosylation of proteins and lipids. Approximately 100 CDG have been described so far, and they affect multiple glycosylation pathways.(1) CDG with abnormal protein N-linked glycosylation can be divided into type 1 CDG, affecting glycan assembly in the endoplasmic reticulum (ER), and type 2 CDG, affecting glycan modification in the Golgi apparatus. Identification of disease-associated genes in the latter group is complicated by the complexity of the Golgi apparatus and the heterogeneous phenotype of individuals with CDG, making phenotypic clustering difficult. Type 2 CDG can be further grouped on the basis of disease mechanism. Mutations in genes encoding for proteins directly involved in Golgi glycosylation (e.g., SLC35A1 [MIM: 605634], B4GALT1 [MIM: 137060], and MGAT2 [MIM: 602616]) were the first to be discovered.(2–4) Another group of type 2 CDG are caused by disturbances in Golgi homeostasis. This group encompasses several conserved oligomeric Golgi (COG)-CDG, TMEM165-CDG (MIM: 14726) and ATP6V0A2-CDG (MIM:611716). The COG complex is involved in retrograde Golgi transport, and mutations lead to abnormal distribution of proteins involved in the glycosylation machinery, such as glycosyltransferases.(5) TMEM165 mutations were recently described in individuals with skeletal symptoms and linked with deficient Ca²⁺ and pH homeostasis.(6,7) ATP6V0A2 mutations were described in autosomal-recessive cutis laxa type 2 (ARCL2 [MIM: 219200]).(8) ATP6V0A2 encodes a subunit of the vacuolar H⁺ ATPase (V-ATPase), which is primarily responsible for acidification of organelles within the secretory pathway and endolysosomal system.(9) Fibroblasts from ARCL2-affected individuals show delayed retrograde Golgi transport, in accordance with the versatile role of the V-ATPase and its involvement in multiple cellular processes.(10,11)

Traditionally, diagnostics for protein N-glycosylation defects is performed with isoelectric focusing (IEF) of serum transferrin (Tf). This method is used to distinguish between type 1 and type 2 CDG.(12) Additionally, IEF of serum apolipoprotein C-III (ApoC-III) can detect abnormal mucin-type O-glycosylation.(13) Recently, we described the use of a high resolution nanochip-C8 QTOF mass spectrometry method for annotation of glycan structures on intact serum Tf.(14)

This method provides additional glycan information, such as loss of galactose.

Here, we report the identification of pathogenic mutations in coiled-coil domain containing 115 (CCDC115 [GenBank: NM_032357.3], UCSC Genome Browser [GRCh37/hg19], chr2:131,095,506–131,099,956) in five unrelated families with abnormal N- and mucin type O-glycosylation, suggestive of a Golgi homeostasis defect.

Materials and methods

Participating Individuals

Blood and, if obtained, fibroblasts of participating individuals were sent to the Radboud University Medical Center, Translational Metabolic Laboratory, for CDG diagnostics, based on clinical suspicion for an inborn error of metabolism. All participating affected individuals or their legal representatives gave informed consent for exome sequencing. Tissue and samples were obtained in accordance with the Declaration of Helsinki. Exome Sequencing and Interpretation Next-generation sequencing and analysis were performed as described earlier.⁽¹⁵⁾ The SureSelect Human All Exon 50 Mb Kit (v.4, Agilent) was used for exome enrichment, covering ~21,000 genes. The exome library was sequenced on a 5500xl SOLiD

sequencer (Life Technologies). Color space reads were iteratively mapped to the hg19 reference genome with the SOLiD LifeScope software v.2.1. We used our in-house annotation pipeline for annotation of called variants and indels. ⁽¹⁶⁾ Variants were excluded based on a frequency of >0.2% in our inhouse database of >1,300 exomes. Also, synonymous variants, deep intronic variants, and variants in UTRs were excluded. Quality criteria were applied and included variants called more than five times and with variation of more than 20% for heterozygous variants and 80% for homozygous variants. Bioinformatics Amino acid sequences of human CCDC115 and homologs of other species were aligned and visualized with Jalview v.2.8 (see Web Resources). The following accession numbers were used for the alignment in Figure 1B: GenBank: NP_115733.2 (*H. sapiens*); GenBank: NP_081435.1 (*M. musculus*); GenBank: NP_001013313.1 (*D. rerio*); GenBank: NP_649550.1 (*D. melanogaster*); GenBank: NP_011927.1 (*S. cerevisiae* S288c); GenBank: NP_173500.1 (*A. thaliana*).

Mutation Analyses

In silico analysis was done with Alamut v.2.4.6 (Interactive Biosoftware) and the effects of mutations were predicted with SIFT, PolyPhen, and MutationTaster (see Web Resources). The Exome Aggregation Consortium (ExAC) database (see Web Resources) was used for allele frequency. Primers (Biolegio and Sigma-Aldrich) flanked with universal M13 tags were constructed with the help of the UCSC Genome Browser, Primer3, and SNPCheck3 (see Web Resources).(17,18) For a list of primers used, see Table S1. Sanger sequencing was performed

on DNA isolated from peripheral blood or cultured fibroblasts, according to standard protocols. DNA was amplified with a T100 ThermoCycler (Bio-Rad). An ABI 3730 DNA Analyzer (Life Technologies) was used for sequencing. Data analysis was done with Sequencher 4.8 (Gene Codes). Multiplex ligation-dependent probe amplification (MLPA) was performed as described previously. (19) In short, combinations of two adjacently annealing oligonucleotide probes were hybridized and ligated. After ligation, the common ends of the probes served as a template for PCR amplification with one primer pair, and due to the fluorescent labeling of the primer, the resulting products could be separated according to size via capillary electrophoresis on an ABI3130 Genetic Analyzer (Applied Biosystems). Fragment data were analyzed in GeneScan (Applied Biosystems). Peak heights of samples from affected individuals were compared with those from control individual probes, and ratios were calculated for all fragments (originating from *CCDC115*, *PTPN18*, and *SMPD4* exons) via an Excel spreadsheet. Thresholds for deletions and duplications were set at 0.75 and 1.25 respectively, and all samples were tested at least twice. All reagents for the MLPA reaction and subsequent PCR amplification were purchased from MRC-Holland, with exception of the *CCDC115*, *PTPN18*, *SMPD4*, and control primers (Biolegio). Primer sequences are described in Table S1.

Cell Culture

Skin fibroblasts from participants and healthy control individuals were cultured at 37.0°C under 5.0% CO₂ in culture medium E199, supplemented with 10% fetal calf serum, and 1% penicillin/streptomycin. All cultures were tested for mycoplasma infection prior to cultivation.

Cloning Studies

CCDC115 Wild-Type Sequence in pLIB-GSKBrd for Transfection in Skin-Derived Fibroblasts

A retroviral pLIB construct was purchased from Clontech, and a PGK-Blasticidin resistant cassette was introduced to create a pLIB-PGKBsr vector. Human *CCDC115* was then cloned into this vector. Skin fibroblasts from individual F1-II4 were transfected with either pLIB2-pgkBsr construct (empty vector) or pLIB2-*CCDC115*-PGKBsr construct.

pcDNA3.1-CCDC115-V5-His for Transfection in HeLa cells

CCDC115 cDNA was obtained from healthy control fibroblasts with the Transcriptor First Strand cDNA Synthesis Kit (Roche) and primers spanning the whole cDNA (see Table S1 for primer sequences). cDNA was sequenced and cloned into the mammalian expression vector pcDNA3.1_V5_HisTOPO-TA (Life Technologies). The construct was checked via Sanger sequencing and transformed in competent *E. coli*. DNA was extracted with the Birnboim method and checked for correct placement of the *CCDC115* strand.⁽²⁰⁾ Plasmid purification was done with the Plasmid Midi Kit (QIAGEN) according to the manual. Transfection was done with FuGENE HD Transfection Reagent (Promega) on coverslips coated with poly-Llysine (Sigma) and incubated overnight in DMEM (GIBCO) with 30%–50% confluency for immunofluorescence studies.

Immunofluorescence

48 hr. after transfection of HeLa cells with pcDNA3.1-*CCDC115*-V5-His, cells were fixed with 3.7% paraformaldehyde (PFA) for 12 min, washed three times in PBS, and permeabilized with 0.1% Triton in 3% BSA/13 PBS at 4°C for 10 min. After washing in PBS, cells were blocked for 30 min with 3% BSA/13 PBS solution. Primary antibodies were diluted in 3% BSA/13 PBS. Cells were incubated with primary antibody in a wet environment for 1 hr. at room temperature (RT) and, after washing with PBS, incubated for 1.5 hr. with secondary antibodies in 3% BSA/13 PBS. After washing the cells three times with PBS and once with distilled water, they were mounted on a slide with Prolong Gold antifade with DAPI (Life Technologies) and left to dry at RT for at least 24 hr. Under identical settings, the cells were visualized with a confocal Leica SP8 (Leica Microsystems) with 603 water immersion and 1.2 NA objective. Picture processing was done with ImageJ

software v.1.46 (see Web Resources). Primary antibodies used are as follows: anti-V5-Tag (1:200, Life Technologies, #R960-25), anti-beta COP (1:1,000, Abcam, #ab2899), anti-SEC31A (1:500, Sigma-Aldrich, #HPA005457), anti-Giantin (1:1,000, BioLegend, #prb-114c), anti-ERGIC53/p58 (1:200, Sigma-Aldrich, #E1031), anti-PDI (1:500, Abcam, #ab3672), anti-Calnexin (1:200, StressMarq Biosciences, #SPC-108). Secondary antibodies are as follows: Alexa Fluor 488-conjugated goat antimouse IgG (H+L) (1:1,000, Life Technologies, #A-11029) and Alexa Fluor 568-conjugated goat anti-rabbit IgG (H+L) (1:1,000, Life Technologies, #A-11011).

IEF of Tf and ApoC-III

Tf IEF was performed as previously described.⁽²¹⁾ In short, 10 ml serum or plasma sample was added to a solution containing iron and NaHCO₃, electrophorized on a 5–7 pH gradient gel, and incubated with 60 µl polyclonal rabbit anti-Tf antibody (Dako, #A0061). Quantification of the gel was done with Image Quant software (TotalLab). Neuraminidase treatment was performed when a Tf polymorphism was suspected as described earlier.⁽²¹⁾ ApoC-III IEF was performed as described, but with small modifications. ⁽¹³⁾ In short, 2 µl of serum/plasma was 15x diluted with saline solution. Before electrophoresis, the gel was rehydrated in a solution containing 8 M urea. After blotting on a nitrocellulose membrane filter, the blot was washed and blocked before incubation with anti-ApoC-III (1:2,000, Rockland, #600-101-114). After incubation with the secondary anti-goat-HRP antibody (1:5,000, Thermo Scientific, #31402) and ECL reagent (Pierce), the blot was visualized on a LAS3000 imaging system (Fujifilm). Blot quantification was done with Image Quant software.

MALDI-LTQ Mass Spectrometry

Mass spectrometry of total plasma N-glycans was performed as described earlier.⁽²²⁾ To summarize, glycans from 10 µl plasma were cleaved with PNGaseF (NE Biolabs) and incubated overnight. After purification on graphitized carbon SPE columns, the glycans were permethylated, purified again, and eluted in 50 µl of 75% v/v aqueous acetonitrile. The glycans were dried and resuspended in a methanol/sodium acetate mixture for spotting. Measurements were done on a vMALDI-LTQ (Thermo Scientific).

Nanochip-C8 QTOF Mass Spectrometry of Intact Tf

For high-resolution mass spectrometry of the intact Tf protein, 10 μ l of serum sample was incubated with anti-Tf beads before injection, and the eluate was analyzed on a microfluidic nanoLC-C8-chip 6540 QTOF instrument (Agilent Technologies).(14) Agilent Mass Hunter Qualitative Analysis Software B.04.00 was used for data analysis. For deconvolution of the charge distribution raw data, Agilent BioConfirm Software was used.

Metabolic Labeling with Alkyne-Tagged Modified Sugar

Metabolic labeling was performed as described before.(23) Primary skin fibroblasts were maintained in DMEM supplemented with 10% fetal bovine serum (Lonza), at 37°C under 5% CO₂ atmosphere. Fibroblasts were grown overnight on glass coverslips (12 mm diameter). Medium was then changed with pre-warmed medium containing 500 mM of alkynyl-modified sugar (ManNAI, provided by Dr. Y. Geurardel and Prof. C. Biot). Labeling lasted 8 hr or 6 hr. The labeling was stopped by fixing the cells with 4% PFA. Cells were then permeabilized in 0.5% Triton X-100 for 10 min. After washes, cells were incubated in the click chemistry buffer containing CuSO₄, 5H₂O-BTTAA-ascorbate-potassium phosphate, and azide-fluor 545 (Sigma, #760757). The pool of fluorescent glycoconjugates was visualized through an inverted Leica TCS-SP5 confocal microscope. Pictures were taken with the Leica Application Suite Advanced Fluorescence (LAS AF) software (Leica Microsystems). For comparison purposes, each picture was taken under the same settings. TISGolgi was used to automatically detect the Golgi area and measure the Golgi fluorescence. This homemade ImageJ plugin was developed by TISBio (see Web Resources). Three different fields of two independent experiments were examined.

Results

Clinical Phenotype

All affected individuals (see pedigrees in Figure 1A and overview in Table 1) had a similar phenotype with storage-disease-like symptoms at a younger age. These included hepatosplenomegaly, hypotonia, elevated serum aminotransferases (ATs, composed of aspartate and alanine aminotransferases [AST, ALT]), and elevated serum alkaline phosphatase (ALP). Additional symptoms included psychomotor disability (PMD), mild hypercholesterolemia, and low serum ceruloplasmin.

Siblings F1-II1 (female, born in 2000) and F1-II2 (male, born in 2004) from family F1 were from Turkish ancestry and have been described previously.²⁴ Their parents are first cousins. During our studies, a younger affected sister was born (individual F1-II4, female, born in 2012). Overall, their symptoms were dominated by PMD, hypotonia, and hepatosplenomegaly with elevated AT and ALP. Metabolic screening revealed a type 2 CDG profile.

Individual F1-II1 was first seen at the age of nine years. Her neonatal period was unremarkable. At examination there was a generalized hypotonia and PMD. She showed mild dysmorphic features. Over the years her AT and ALP fluctuated but were always elevated (AST 130–158 U/l [normal range, 0–50 U/l], ALT 85–101 U/l [normal range, 0–50 U/l], and ALP 1,016–1,193 U/l [normal range, < 360 U/l]). Isotype analysis showed that ALP was mostly bone derived, as seen in defects of glycosylphosphatidylinositol (GPI)-anchor biosynthesis. However, surface expression of GPI-anchored proteins CD59 and CD55 in EBV-transformed lymphoblasts did not confirm a GPI-anchor defect (data not shown). Additional biochemical analysis showed low serum ceruloplasmin (4 mg/dl [normal range, 15–60 mg/dl]), decreased coagulation factors, and elevated creatine kinase. Total cholesterol and low-density lipoprotein (LDL-C) were normal.

Her brother, F1-II2, was also seen in 2009 at the age of five years. He shared the same phenotype as his sister but had additional dysmorphic features (long face, ptosis, blue sclera, and down-slanting palpebral fissures). In addition to generalized hypotonia, muscle atrophy was present. Biochemically, elevated AT and ALP (AST 96–436 U/l, ALT 140–995 U/l, and ALP 1,070–1,577 U/l), low ceruloplasmin (4 mg/dl), hypercholesterolemia (289 mg/dl [normal range, 120–200 mg/dl]), and abnormal coagulation factors were seen over time.

Table 1 Overview of the genetic and clinical features of the CDC115-deficient families

Family	IV (y.o.b.)	Zygoty	Allele frequency (ExAc browser)	gDNA change (chr2(GRCh37))	cDNA change	Protein change	CDG		Elevated cholesterol and LDL-C	Elevated ALP	Ceruloplasmin	Hepatic phenotype	Neurological phenotypic type
							N	O					
1	1.1 (00)	Homozygous	8.253e-06	g:131099607A>G	c:[92T>C];	p.[Leu31Ser];	+	+	++	+	low	cirrhosis, hepatomegaly	Hypotonia, PMD
	1.2 (04)				[92T>C]	[Leu31Ser]							
	1.3 (12)					u31Ser]							
2	2.1 (08)	Homozygous	8.253e-06	g:131099607A>G	c:[92T>C];	p.[Leu31Ser];	+	+	++	+	low	hepatomegaly, dry cop-per	PMD
					[92T>C]	[Leu31Ser]							
3	3.1 (89)	Homozygous	8.253e-06	g:131099607A>G	c:[92T>C];	p.[Leu31Ser];	+	-	++	+	low	fibrosis, steatosis, necrotic lesions	Hypotonia, PMD, seizures
					[92T>C]	[Leu31Ser]							
4 ¹	4.1 (02)	Homozygous	0	g:131099668C>A	c:[31G>T];	p.[Asp11Tyr];	+	-	++	+	n.d.	liver failure ²	-
	4.2 (03)				[31G>T]	[Asp11Tyr]							
5 ³	5.1 (14)	Compound Heterozygous	8.253e-06	g:131099607A>G / g:(130939272_131096872)_ (131116671_?)del	c:[92T>C]; [(?_258)_ (*1245_?) del]	p.[Leu31Ser]; [p.0?]	+	+	++	++	n.d.	liver failure	hypotonia

Abbreviations are as follows: y.o.b., year of birth; CDG, Congenital Disorders of Glycosylation; N, N-glycosylation measured by isoelectric focusing of serum transferrin; O, O-glycosylation measured by isoelectric focusing of serum apoCIII; LDL-C, low-density lipoprotein; AT, serum aminotransferases; ALP, serum alkaline phosphatase; PMD, psychomotor disability; n.d., not determined.

¹ Sibling 4.1 died at the age of 9 years due to liver failure after repeated liver transplantation.

² Both siblings needed liver transplantation

³ Individual 5.1 died of liver failure at the age of 7 months

Individual F1-II4 was last seen in 2014 at the age of two years. The most prominent finding was PMD. Hypotonia was not present. Hepatic evaluation showed elevated AST (1,089 U/l), ALT (591 U/l), ALP (1,251 U/l), and profound hepatosplenomegaly, similar to lysosomal storage disorders in the first years of life. Organ size normalized with increasing age. Individual F2-II1 (male, born in 2008) from family F2 was the only child of unrelated Italian parents. As a neonate, he suffered from prolonged neonatal jaundice and elevated AST, ALT, and hepatosplenomegaly. Low serum ceruloplasmin and hypercholesterolemia were found. On suspicion of Wilson disease (WD [MIM: 277900]), zinc treatment was started but proved unsuccessful. Genetic screening for WD failed to detect mutations in ATP7B (MIM: 606882). At the age of two years, examinations showed mild PMD and mild dysmorphic features. Biochemical analysis revealed elevated AT and ALP (AST 422 U/l, ALT 588 U/l, ALP 976 U/l), low ceruloplasmin (3.3 mg/dl), high cholesterol (381 mg/dl), and high LDL-C (332 mg/dl [normal range, 50–130 mg/dl]). Metabolic diagnostics showed a type 2 CDG pattern. A liver biopsy at the age of three years showed an increased hepatic copper concentration of 125 mg/g dry weight (normal range, <40 mg/g dry weight; WD, >250 mg/g dry weight).

Individual F3-II2 (female, born in 1989) from family F3 was the second child of unrelated French parents. She had an uncomplicated birth but developed neonatal jaundice, which was treated successfully by phototherapy. This was accompanied by elevated AT and ALP. She was hospitalized at the age of one year due to persistent moderate hypotonia.

Biochemically, she had elevated AST (1,780 U/l), ALT (390 U/l), and ALP (950 U/l, with increased bone fraction). Steatosis, fibrosis, and necrotic lesions were seen on liver biopsy. During childhood, she developed PMD with hypotonia and seizures. Biochemically, elevated AT and ALP persisted. At a later age, she developed hypercholesterolemia. CDG screening showed a type 2 pattern. During her last visit at the age of twenty-five years, she still suffered from PMD, as well as additional behavioral problems such as aggressiveness, agitation, and psychotic behavior, for which she is being treated with risperidone. Her seizures persisted despite treatment with lamotrigine. Serum AT and ALP remain elevated (AST 82 U/l, ALT 76 U/l, ALP 180 U/l) and ceruloplasmin low (10 mg/dl).

Individuals F4-II1 (male, born in 2002, died in 2011) and F4-II2 (female, born in 2003) are brother and sister and were born to consanguineous Turkish

parents. As a neonate, individual F4-II1 showed neonatal jaundice. Progressive cholestatic liver disease was diagnosed at an early age. Due to progressive liver failure, sibling F4-II1 underwent a liver transplantation at the age of three years and ten months, and sibling F4-II2 at the age of eight years. Unfortunately, the transplant of sibling F4-II1 was rejected twice, and he died at the age of nine years. Both siblings showed mild dysmorphic features and individual F4-II1 had a mild PMD. They showed elevated AT and ALP during several check-ups (F4-II1: AST 192–669 U/l, ALT 83–308 U/l, ALP 702 U/l; F4-II2: AST 98–422 U/l, ALT 98–178 U/l, ALP 710–985 U/l). Ceruloplasmin was never measured. After liver transplantation, individual F4-II2 is doing well. Among other parameters, her AT and CDG profile have normalized.

Individual F5-II1 (female, born in 2014, died after seven months) was the only child of non-consanguineous Portuguese parents. Jaundice was noticed since the first day of life. At five months, jaundice persisted and she developed hepatosplenomegaly, failure to thrive, redundant skin, poor muscle volume, and generalized hypotonia. There were no signs of PMD. Her parents refused a liver biopsy. Intermittent episodes of hypoglycemia and hyperammonemia ensued. Subsequently, she developed progressive cholestatic liver disease (bilirubin 41.3 mg/dl, 40% conjugated) and liver failure. Investigation showed increased ATs (AST 207–972 U/l, ALT 48–153 U/l) and ALP (850–1,031 U/l). Additional biochemical analysis revealed hypercholesterolemia (431 mg/dl) and elevated LDL-C (314 mg/dl), abnormal coagulation factors (low FVII and high FVIII, INR 0.79–3.0), and anemia (Hb 7 g/dl) with acanthocytes and 7% reticulocytes. Interestingly, a bone marrow biopsy showed dyserythropoiesis, some lipidic histiocytes, and erythrophagocytosis. Later on, generalized cell vacuolization and few erythroblasts with perinuclear deposition of iron were seen. CDG screening revealed a type 2 pattern. Liver transplantation was not attempted due to rapid deterioration with multi-organ failure and encephalopathy. She died at the age of seven months. Postmortem liver analysis revealed severe cholestatic hepatitis with complete septal fibrosis and cirrhosis.

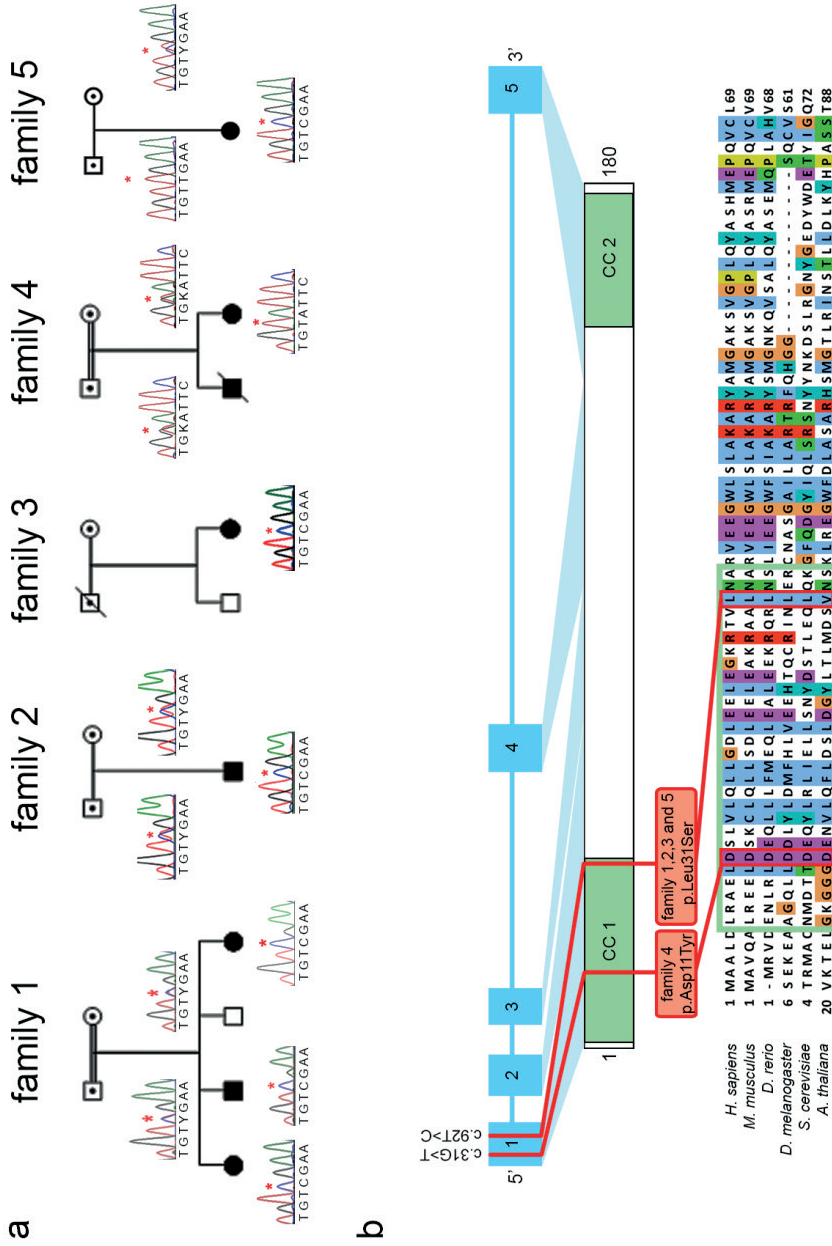


Figure 1. Pedigrees and overview of the structure, variants and conservation of CCDC115.(A) The pedigrees of families 1 to 5 are shown. Partial chromatograms show autosomal recessive segregation for all families except family 4 where no parental DNA was available. The red asterisk indicate respective nucleotide changes. (B) Schematic representation of the intron-exon structure of CCDC115 and the encoded protein. The red lines indicate the mutations within the families. The green regions indicate two predicted coiled-coil regions (CC1 and CC2).

Mutational Analyses

To uncover the genetic defect, we performed exome sequencing of individuals F1-II1 and F1-II2 from index family F1. Eight possible candidates were identified on the basis of having autosomal-recessive inheritance (Table S2). Among these candidates was a homozygous missense variant in *CCDC115* (c.92T>C [p.Leu31Ser]) (Table 1). We performed a profile-based method, Position-Specific Iterated (PSI)-BLAST,²⁵ to identify possible homologs of the candidate variants and identified Vma22p (GenBank: NP_011927.1) as the yeast homolog of *CCDC115* (GenBank: NP_115733.2) in the second iteration with an E-value of $2e-14$ and a reciprocal E-value of $3e-11$. Vma22p is a dedicated ER-localized assembly factor of the V-ATPase.^(9,26,27) Importantly, Vma22p and *CCDC115* were found as each others' best hits. This suggests that, apart from being homologs, they are likely orthologs with overlapping functions in humans.²⁸ Based on the link between the V-ATPase and abnormal glycosylation, this variant was considered our most likely candidate.⁷ This was further supported by homozygosity mapping, indicating a small homozygous region on chromosome 2, in which *CCDC115* was located (Figure S1). In silico analysis of the p.Leu31Ser substitution with SIFT, PolyPhen-2, and MutationTaster predicted pathogenicity (Table S3). The ExAC database showed a very low allele frequency of $8.253e-06$. Sanger sequencing confirmed homozygosity for the affected individuals, heterozygosity for both parents, and homozygous wild-type sequence for a healthy sibling, confirming complete segregation in the family (Figure 1A). Western blotting of fibroblasts derived from individual F1-II4 demonstrated a protein level similar to that of healthy control individuals (Figure S2).

For individuals F2-II1 and F5-II1, exome sequencing revealed multiple genetic variants, among which was the same c.92T>C homozygous missense variant (Table 1). Sanger sequencing for individual F2-II1 confirmed homozygosity and heterozygosity for the parents (Figure 1A). For individual F5-II1, Sanger sequencing of parental DNA revealed a maternal heterozygous missense mutation and a paternal wild-type sequence (Figure 1A). We suspected a paternal deletion as possible explanation, given that haplotype analysis excluded non-paternity. MLPA of DNA from individual F5-II1 displayed a heterozygous deletion for all exons of *CCDC115* and on the studied position in upstream *PTPN18* (Table S4). We did not observe a deletion for the position we investigated within downstream *SMPD4*. Segregation analysis showed that the deletion originated

from the paternal allele. This complete deletion of *CCDC115* is in agreement with the severe phenotype of individual F5-II1.

Sanger sequencing of additional individuals with unsolved Golgi glycosylation defects identified missense mutations in *CCDC115* in individuals from two unrelated families: individual F3-II2 with the same homozygous c.92T>C mutation and siblings F4-II1 and F4-II2 with a homozygous missense mutation, c.31G>T, leading to a p.Asp11Tyr substitution (Figure 1A and Table 1). The p.Asp11Tyr substitution was also predicted to be pathogenic by SIFT, PolyPhen-2, and MutationTaster (Table S3). The allele frequency in the ExAC database was 0.

In total, we found two missense mutations and one deletion in eight individuals from five families. *CCDC115* is located on the negative strand, contains five exons, and encodes coiled-coil domain containing 115 with 180 amino acids and two predicted coiled-coil domains (Figure 1B). Both *CCDC115* missense mutations are located in the first predicted coiled-coil domain and affect highly conserved positions. *CCDC115* is widespread among eukaryotes, including *Arabidopsis thaliana*, indicating its origin at the root of the eukaryotic tree.

Glycosylation Studies

Global defects in glycosylation can be detected by IEF of serum Tf (N-glycosylation) and serum ApoC-III (mucin type O-glycosylation). Tf has two N-glycosylation sites, and the most abundant fraction corresponds with four sialic acids. ApoC-III has one mucin-type O-linked glycan that can host one or two sialic acids. An increase in fractions associated with hyposialylated Tf or ApoC-III is indicative of abnormal N- or O-glycosylation. All individuals showed a similarly abnormal type 2 N-glycosylation profile of Tf (see Figure 2A and Table S5 for quantifications). ApoC-III IEF was abnormal for all tested individuals (see Figure 2A and Table S6 for quantifications).

We performed MALDI-LTQ mass spectrometry of total plasma N-glycans of individual F1-II1 and compared the spectrum with that of a healthy control individual. Most notably, the glycans with theoretical masses of 2,433 m/z and 2,229 m/z were increased, indicating loss of either one sialic acid (2,433 m/z) or one sialic acid plus one galactose (2,229 m/z) (Figure 2B).

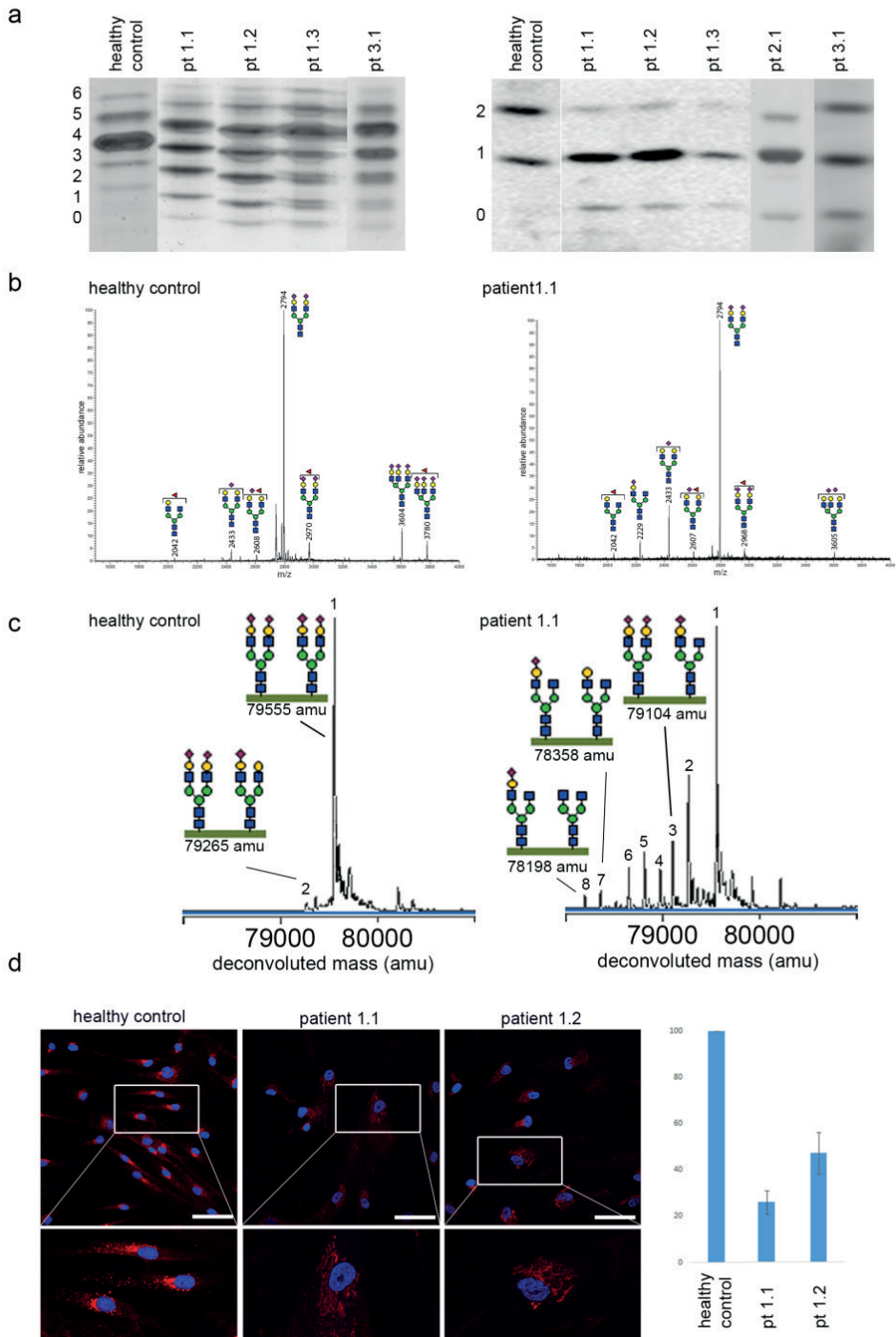
In accordance with total plasma N-glycan analysis, nanochip-C8 QTOF mass spectrometry of intact serum Tf (79,555 amu, peak 1) showed accumulation of

incomplete glycans lacking sialic acid (79,265 amu, peak 2), galactose (79,104 amu, peak 3), and additional minor isoforms lacking sialic acid and/or galactose in individual F1-II1 (Figure 2C, peaks 4–8, see Table S7 for a list of all annotated glycan structures). This pattern is compatible with an overall detrimental effect on Golgi glycosylation. Together with abnormal O-glycosylation, these data are suggestive of a Golgi homeostasis defect and a combined disorder of N-glycosylation and mucin-type O-glycosylation.

Metabolic Labeling of Sialic Acids

We further assessed glycosylation efficiency in skin-derived fibroblasts by metabolic labeling of sialic acids with alkyne tagged synthetic sugar analogs. These alkyne-tagged sialic acids are incorporated into nascent glycoproteins by the cell allowing for specific detection with fluorescently labeled azides.⁽²³⁾ In CCDC115-deficient individuals F1-II1 and F1-II2, the pool of glycoconjugates was located to the Golgi, and immunofluorescence signal quantification in the Golgi showed a clear reduction for all individuals, in agreement with less efficient Golgi glycosylation (Figures 3A and 3B). Additionally, we observed a dispersed pattern of the glycoconjugates, suggestive of dilatation of the Golgi (Figure 3B).

► **Figure 2. Glycosylation abnormalities in CCDC115 deficient patients.** (A) The isofocusing profiles (IEF) of serum transferrin (Tf) and serum apolipoprotein CIII (aCIII). Tf has two N-glycosylation sites and the most abundant fraction corresponds with four sialic acids. aCIII has one O-linked glycan that can host one or two sialic acids. The accompanying numbers represent the total number of sialic acids in the different protein isoforms. All patients show a relative increase of isoforms Tf-2 and Tf-3 and of aCIII-1. For patient 2.1 HPLC was used to assess Tf glycosylation status. (B) MALDI mass spectrometry profiles of total serum N-glycans of a healthy control and CCDC115 deficient patient 1.1. An increase in hypoglycosylated glycans can be seen for all patients when compared to the control. Most notably the glycans with theoretical masses of 2433 m/z and 2228 m/z are increased, indicating loss of one sialic acid (2433) or one sialic acid plus one galactose (2228). (C) The nanochip-C8-QTOF mass profile is shown of the intact transferrin protein with two attached glycans at 79555 amu (peak 1). Any subsequent sialic acid and/or hexose loss can be calculated based on mass difference with the main peak (i.e., loss of one sialic acid (purple diamond, peak 2). Patient 1.1 shows a reduction in sialic acid and galactose residues (peaks 3 to 8). (D) Incubation of healthy control fibroblasts with the alkynyl-tagged sialic acid precursor ManNAI which can be labeled with azide-conjugated fluorophores. A reduced fluorescent signal can be visualized for patient 1.1 and 1.2. Scale bars indicate 75 μm . Percentage reduction in metabolic labeling for the analyzed patients compared to control cells (approximately 100 cells were counted per condition).



To investigate whether we could rescue the phenotype of individual F1-II4, we transfected skin fibroblasts with a construct containing either a mock construct or *CCDC115* wild-type sequence. As seen in Figures 3C and 3D, fibroblasts transfected with a mock construct have a non-detectable fluorescence intensity in the Golgi, in contrast to fibroblasts transfected with a construct containing wild-type *CCDC115*. In addition to metabolic labeling, we stained healthy control fibroblasts and fibroblasts from affected individual F2-II1 with anti-calnexin antibody to visualize the ER (Figure 3E). Individual F2-II1 fibroblasts showed a dilated ER in 60% of counted cells, in comparison to 20% in healthy control fibroblasts.

Localization

To define the subcellular location of *CCDC115*, we constructed a pcDNA3.1-*CCDC115*-V5 plasmid for transient expression of C-terminally V5-tagged *CCDC115* in HeLa cells. Confocal imaging revealed clear localization to the ER-Golgi intermediate compartment (ERGIC) and coat protein complex I (COPI) vesicles (Figure 4). Also, in immortalized human hepatocytes (HepaRG), *CCDC115* located to the ERGIC and COPI vesicles (data not shown). Partial co-localization was seen in both cell types with COPII and Golgi markers. No co-localization was seen with the ER marker PDI (Figure 4). We conclude that *CCDC115* predominantly localizes to the ER-to-Golgi region but not to the ER, in contrast to yeast *Vma22p*.

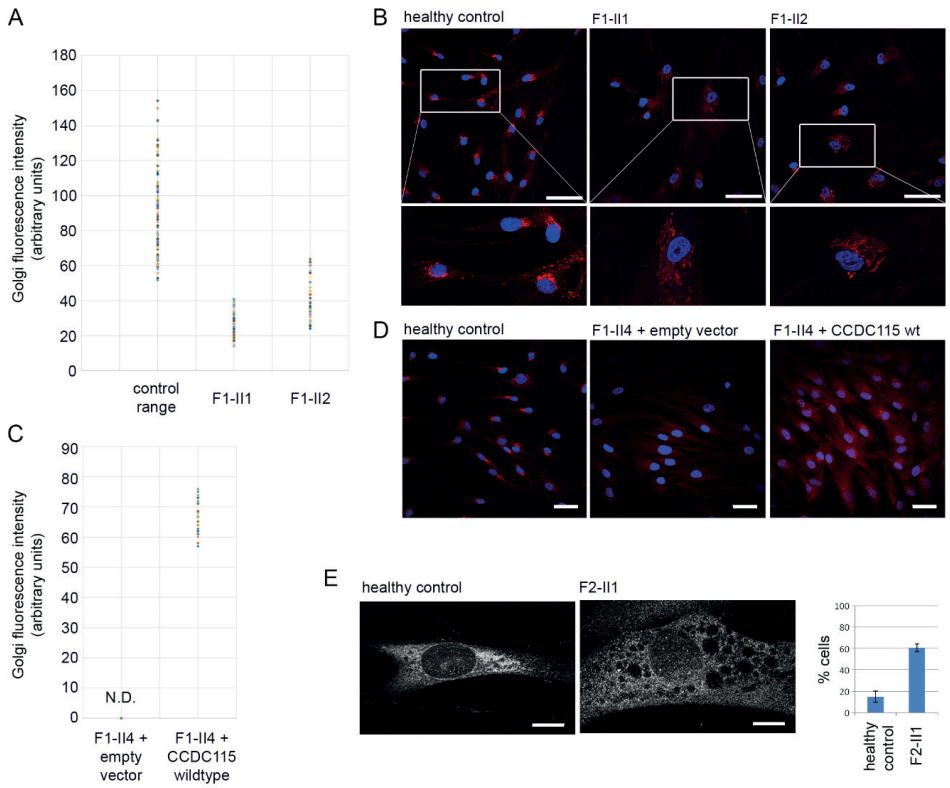


Figure 3. Metabolic Labeling of Sialic Acids Shows Decreased Glycosylation in CCDC115-Deficient Fibroblasts (A and B) Metabolic labeling of fibroblasts with alkyne-tagged sialic acid precursor ManNAI for 8 hr. Fibroblasts from three healthy controls were used, and the experiment was performed twice. A reduced absolute Golgi fluorescence signal was observed for siblings F1-II1 and F1-II2. Scale bars indicate 75 μ m. (C and D) Fibroblasts of F1-II4, transfected with empty vector or wild-type *CCDC115*, were incubated with ManNAI for 6 hr, followed by fluorescent staining. The graphs indicate the absolute Golgi fluorescence intensity in a.u. Scale bars indicate 50 μ m. (E) Healthy control fibroblasts and fibroblasts from CCDC115-deficient individual F2-II1 were stained with anti-calnexin antibody. The graph shows the percentage of cells with a dilated ER. Approximately 50 cells were counted, and the experiment was performed twice. The graph shows the percentage of cells (mean \pm SEM) with a dilated ER. Scale bars indicate 10 μ m. N.D., not detectable.

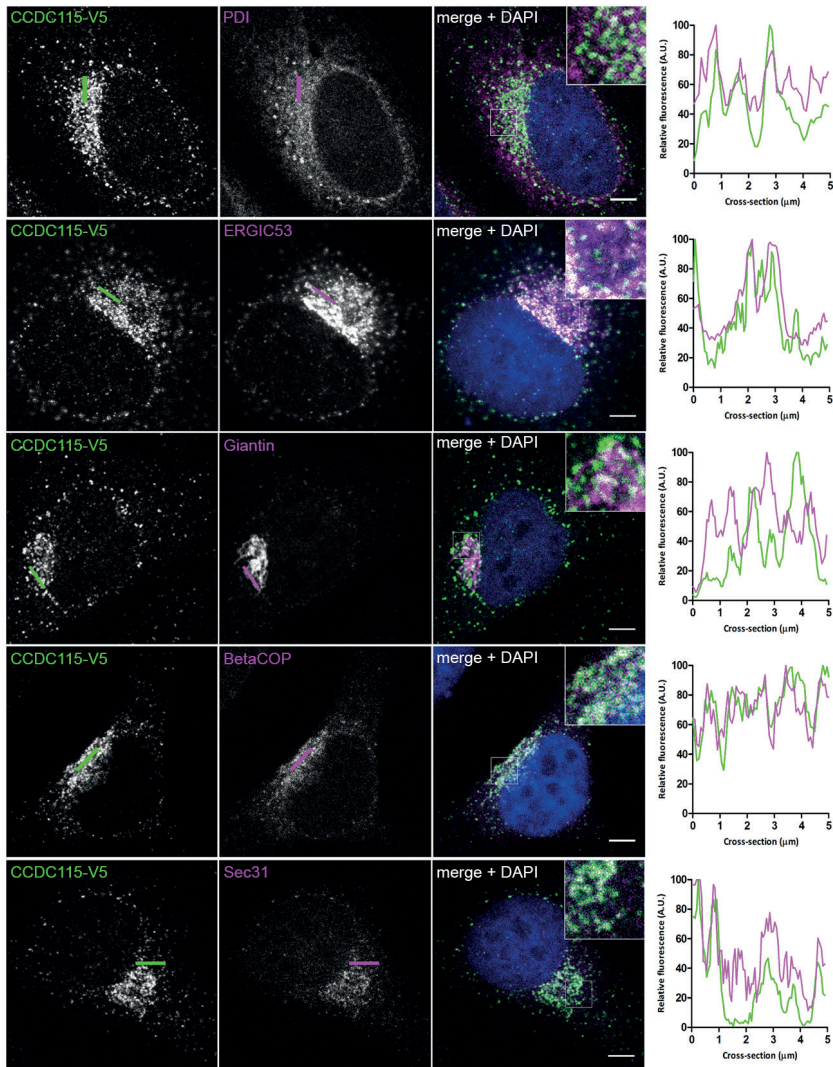


Figure 4. Immunofluorescence staining and localization of CCDC115-V5 in HeLa cells. HeLa cells were transiently transfected with a V5-tagged CCDC115 construct and then fixed and stained with immunofluorescently labeled antibodies against V5 (green in merge) and different organelle markers (magenta in merge). Shown are representative cells stained for CCDC115 organelle markers, and a merge with DAPI stain (blue), including a 3-fold magnification. Co-localization is indicated by white color in the merged channel. The graphs show the fluorescence intensity profiles along the crosssections indicated. Scalebars represent 5 μm .

Discussion

We identified *CCDC115* mutations in eight individuals from five unrelated families, and we provide evidence that these mutations affect protein N- and mucin-type O-glycosylation via their effect on Golgi homeostasis. Also, we showed that *CCDC115* is localized to the ER-to-Golgi region. However, the question remains—what is the function of *CCDC115* and how does its deficiency result in abnormal protein glycosylation and clinical symptoms?

Previous studies in mice suggest localization of *CCDC115* to the lysosomal-endosomal system and upregulation of *Ccdc115* in mouse cortical neurons after fibroblast growth factor 2 (FGF2) stimulation.(29) Overexpression of *Ccdc115* in mouse embryonic fibroblasts has been shown to have a positive effect on cell proliferation.(30) Our data suggest a physiological role for *CCDC115* in Golgi homeostasis, and loss-of-function mutations lead to the inability of the Golgi to perform its core functions: post-translational modification and protein secretion and sorting. A disturbance in Golgi homeostasis is indicated by the combined defect of N- and O-glycosylation. Detailed structural studies on N-glycans revealed an accumulation of incomplete glycans lacking both sialic acid and galactose. These data indicate a general disturbance in Golgi homeostasis with an effect on multiple glycosylation pathways, for example, via incorrect targeting and/or recycling of glycosyltransferases and nucleotide-sugar transporters. Previously, deficient vesicular transport has been proposed as explanation for abnormal Golgi glycosylation in COG and ATP6V0A2 defects.(5,10) Localization of *CCDC115* to, among others, COPI vesicles that are involved in ER-to-Golgi transport and sorting of cargo proteins, could indicate a similar mechanism.

Based on comparative genomics, it is likely that *CCDC115* and the yeast protein Vma22p are orthologs and have, at least partially, overlapping functions. Vma22p is involved in assembly of the V-ATPase proton pump by stabilizing the V0 domain during early assembly in the ER. Vma22 knockout yeast showed diminished V-ATPase activity and destabilization of the V0 domain.(31) Possibly, mutations in *CCDC115* could exert part of the effect via alteration of V-ATPase assembly or function. Vma22p exerts its function as a V-ATPase assembly factor by interacting with Vph2p (also called Vma12p [GenBank: NP_012803]) and Vma21p (GenBank: NP_011619.3).(27) In another study in this issue, we have identified TMEM199 (also known as C17orf32 [GenBank: NP_689677.1]) as the human homolog of Vph2p, and recently VMA21 (GenBank: NP_001017980.1)

has been described as the human homolog of Vma21p.(32,33) Individuals with TMEM199 deficiency showed partial clinical and biochemical overlap with CCDC115-deficient individuals, although symptoms seem to be milder. TMEM199-deficient individuals presented in adolescence with a phenotype of elevated ATs and ALP, hypercholesterolemia, hepatic steatosis, and low ceruloplasmin. Profound hepatosplenomegaly and PMD, as seen in CCDC115 deficiency, were absent.

Compared to known V-ATPase associated disorders, CCDC115 deficiency (and TMEM199 deficiency) is the first that predominantly affects the liver. (34) Mutations in *VMA21* cause X-linked myopathy with excessive autophagy (XMEA [MIM: 310440]). XMEA is a disorder associated with progressive muscle weakness.(35,36) Mutations in V-ATPase subunits TCIRG1 (also called ATP6V0A3) and ATP6V0A4 cause tissue-specific symptoms (osteopetrosis [MIM: 259700] and distal renal tubular acidosis [MIM: 602722]).(37,38) A hallmark clinical feature of ATP6V0A2-affected individuals is cutis laxa.(39) Biochemically, ATP6V0A2 deficiency is highly similar to CCDC115 (and TMEM199) deficiency with defective N- and O-glycosylation.(10,40) Interestingly, the most severely affected individual (F5-II1) was diagnosed with redundant skin and poor muscle volume, symptoms characteristic of ATP6V0A2 and VMA21 deficiency, respectively. This hints at a phenotypical continuum among several V-ATPase-associated disorders.

The storage-disease-like phenotype of CCDC115 deficiency resembles that of lysosomal disease, such as Niemann-Pick disease type C (NPC, caused by mutations in *NPC1* and *NPC2* [MIM: 257220]). NPC is characterized by hepatosplenomegaly and neurologic manifestations.(41) Lysosomal accumulation of cholesterol and sphingomyelin due to impaired cholesterol trafficking is the hallmark of NPC; hence, NPC can be regarded as a cholesterol trafficking disease.(42) NPC1 and NPC2 work in conjunction with each other and are involved in the transport of cholesterol from late endosomes and lysosomes to the plasma membrane and ER. Interestingly, binding of cholesterol to NPC2 is improved in an acidic environment, and this could be a possible link between CCDC115 deficiency and NPC, given that the V-ATPase is the main acidifier of lysosomal pH.(43) Alternatively, altered trafficking of lysosomal proteins could explain the clinical resemblance.

All individuals had elevated serum ALP on biochemical analysis. This was determined to be bone derived for the investigated individuals. Discrepantly

high bone-derived ALP can be observed in individuals with defects of GPI anchor biosynthesis.(44,45) However, this is not supported for CCDC115 deficiency. Trafficking of GPI-anchored proteins, which might include ALP, is suggested to occur through a COPII-dependent process from ER exit sites.(46) In *Vma22p* mutant yeast, trafficking of ALP to the yeast vacuole is not majorly altered. (31) However, yeast ALP is membrane bound and not a GPI-anchored protein. Treatment of yeast with bafilomycin A1, a potent V-ATPase inhibitor known to block vacuole acidification, did not show any effect on trafficking and maturation of membrane-bound yeast ALP.(47) This suggests that transport of vacuolar membrane proteins, including ALP, in yeast is independent from acidification. A study in mouse pituitary corticotrope tumor cells showed decreased trafficking of cargo proteins, independent of pH, after incubation with Concamycin A (ConA), another V-ATPase inhibitor. Although knockdown of the V-ATPase showed an overlapping phenotype with ConA treatment, this was not investigated for protein secretion. Additionally, processing of the investigated protein, PC1, begins in the trans-Golgi network and could therefore not be representative for Golgi trafficking.(48) Based on the localization of CCDC115 in the ER-to-Golgi region, it could be speculated that CCDC115 has a role in protein cargo sorting or trafficking of alkaline phosphatase in addition to a possible role in V-ATPase assembly.

In conclusion, we describe eight individuals with a type 2 CDG from five unrelated families affected by mutations in *CCDC115*. The phenotype consists of elevated aminotransferases and alkaline phosphatase and hepatosplenomegaly in combination with psychomotor disability, hypercholesterolemia, and hypotonia. Based on homology detection, glycosylation studies, and cellular co-localization, we propose a role for CCDC115 in Golgi homeostasis.

Accession Numbers

The accession numbers for the pathogenic variants c.92T>C, c.31G>T, and c.92T>C and the *CCDC115* deletion reported in his paper are ClinVar: SCV000257472, SCV000257474, and SCV000257477, respectively.

Acknowledgments

We would like to thank all individuals and their families for their participation in this study. We would also like to thank the group of Prof. C. Biot and Dr. Y. Guerardel for their generous donation of ManNAI and Dr. F. Pellicano and Dr. T. Iwata for their generous donation of the anti-CCDC115 antisera. This work was financially supported by grants from the Institute of Genetic and Metabolic Disease (D.J.L., J.A.V., and R. J. Rodenburg), the Dutch Organization for Scientific Research (ZONMW Medium Investment grant 40-00506-98-9001, VIDI grant 91713359 to D.J.L., and VENI grant to A.G.H.), the AMC graduate school PhD scholarship (M.A.W.v.d.B.), the Metakids foundation (J.C.J., M.V.S., J.D., D.J.L.), the Dr. Karel-Lodewijk Verleysen Award (J.D.), the Spanish Ministry of Economy and Competitiveness (grant PI11/01254 to B.P., C.P.C., and C.M.), the German Research Foundation (S.C.), Muscular Dystrophy Association (S.C.), the French national agency (ANR-SOLV_CDG to F.F.), and the ERA-Net for Research Programs on Rare Diseases Joint Transnational Call 2011 (EUROCDG, grant ERARE11-135 to G.M. and F.F.).

Web Resources

The URLs for data presented herein are as follows:

BLAST, <http://blast.ncbi.nlm.nih.gov/Blast.cgi>

COILS, http://www.ch.embnet.org/software/COILS_form.html

dbSNP, <http://www.ncbi.nlm.nih.gov/projects/SNP/>

ExAC Browser, <http://exac.broadinstitute.org>

ImageJ, <http://imagej.nih.gov/ij>

Jalview, <http://www.jalview.org>

MutationTaster, <http://www.mutationtaster.org/>

OMIM, <http://www.omim.org/>

PolyPhen-2, <http://genetics.bwh.harvard.edu/pph2/>

SIFT, <http://sift.jcvi.org>

SNPcheck, <https://secure.ngsl.org.uk/SNPCheck/snpcheck.htm>

TISGolgi, tisbio.wix.com/tisbio

UCSC Human Genome Browser, <http://genome-euro.ucsc.edu/index.html>

References

1. Freeze, H.H., Chong, J.X., Bamshad, M.J., and Ng, B.G. (2014). Solving glycosylation disorders: fundamental approaches reveal complicated pathways. *Am. J. Hum. Genet.* 94, 161–175.
2. Ng, B.G., Buckingham, K.J., Raymond, K., Kircher, M., Turner, E.H., He, M., Smith, J.D., Eroshkin, A., Szybowska, M., Losfeld, M.E., et al.; University of Washington Center for Mendelian Genomics (2013). Mosaicism of the UDP-galactose transporter SLC35A2 causes a congenital disorder of glycosylation. *Am. J. Hum. Genet.* 92, 632–636.
3. Guillard, M., Morava, E., de Ruijter, J., Roscioli, T., Penzien, J., van den Heuvel, L., Willemsen, M.A., de Brouwer, A., Bodamer, O.A., Wevers, R.A., et al. (2011). B4GALT1-congenital disorders of glycosylation presents as a non-neurologic glycosylation disorder with hepatointestinal involvement. *J. pediatr.* 159, 1041–1043 e1042.
4. Tan, J., Dunn, J., Jaeken, J., and Schachter, H. (1996). Mutations in the MGAT2 gene controlling complex N-glycan synthesis cause carbohydrate-deficient glycoprotein syndrome type II, an autosomal recessive disease with defective brain development. *Am. J. Hum. Genet.* 59, 810–817.
5. Miller, V.J., and Ungar, D. (2012). Re'COG'nition at the Golgi. *Traffic* 13, 891–897.
6. Foulquier, F., Amyere, M., Jaeken, J., Zeevaert, R., Schollen, E., Race, V., Bammens, R., Morelle, W., Rosnoblet, C., Legrand, D., et al. (2012). TMEM165 deficiency causes a congenital disorder of glycosylation. *Am. J. Hum. Genet.* 91, 15–26.
7. Demaegd, D., Foulquier, F., Colinet, A.S., Gremillon, L., Legrand, D., Mariot, P., Peiter, E., Van Schaftingen, E., Matthijs, G., and Morsomme, P. (2013). Newly characterized Golgi-localized family of proteins is involved in calcium and pH homeostasis in yeast and human cells. *Proc. Natl. Acad. Sci. USA* 110, 6859–6864.
8. Kornak, U., Reynders, E., Dimopoulou, A., van Reeuwijk, J., Fischer, B., Rajab, A., Budde, B., Nürnberg, P., Foulquier, F., Lefeber, D., et al.; ARCL Debré-type Study Group (2008). Impaired glycosylation and cutis laxa caused by mutations in the vesicular H⁺-ATPase subunit ATP6V0A2. *Nat. Genet.* 40, 32–34.
9. Forgac, M. (2007). Vacuolar ATPases: rotary proton pumps in physiology and pathophysiology. *Nat. Rev. Mol. Cell Biol.* 8, 917–929.
10. Huchtagowder, V., Morava, E., Kornak, U., Lefeber, D.J., Fischer, B., Dimopoulou, A., Aldinger, A., Choi, J., Davis, E.C., Abuelo, D.N., et al. (2009). Loss-of-function mutations in ATP6V0A2 impair vesicular trafficking, tropoelastin secretion and cell survival. *Hum. Mol. Genet.* 18, 2149–2165.
11. Marshansky, V., Rubinstein, J.L., and Grüber, G. (2014). Eukaryotic V-ATPase: novel structural findings and functional insights. *Biochim. Biophys. Acta* 1837, 857–879.
12. Wopereis, S., Grünewald, S., Huijben, K.M., Morava, E., Mollicone, R., van Engelen, B.G., Lefeber, D.J., and Wevers, R.A. (2007). Transferrin and apolipoprotein C-III isofocusing are complementary in the diagnosis of N- and O-glycan biosynthesis defects. *Clin. Chem.* 53, 180–187.
13. Wopereis, S., Grünewald, S., Morava, E., Penzien, J.M., Briones, P., García-Silva, M.T., Demacker, P.N., Huijben, K.M., and Wevers, R.A. (2003). Apolipoprotein C-III isofocusing in the diagnosis of genetic defects in O-glycan biosynthesis. *Clin. Chem.* 49, 1839–1845.
14. van Scherpenzeel, M., Steenbergen, G., Morava, E., Wevers, R.A., and Lefeber, D.J. (2015). High-resolution mass spectrometry glycoprofiling of intact transferrin for diagnosis and subtype identification in the congenital disorders of glycosylation. *Transl. Res.* 166, 639–649.
15. Stránecký, V., Hoischen, A., Hartmannová, H., Zaki, M.S., Chaudhary, A., Zudaire, E., Nosková, L., Baresová, V., Pristoupilová, A., Hodanová, K., et al. (2013). Mutations in ANTXR1 cause GAPO syndrome. *Am. J. Hum. Genet.* 92, 792–799.

16. Vissers, L.E., de Ligt, J., Gilissen, C., Janssen, I., Steehouwer, M., de Vries, P., van Lier, B., Arts, P., Wieskamp, N., del Rosario, M., et al. (2010). A de novo paradigm for mental retardation. *Nat. Genet.* 42, 1109–1112.
17. Untergasser, A., Cutcutache, I., Koressaar, T., Ye, J., Faircloth, B.C., Remm, M., and Rozen, S.G. (2012). Primer3—new capabilities and interfaces. *Nucleic Acids Res.* 40, e115.
18. Koressaar, T., and Remm, M. (2007). Enhancements and modifications of primer design program Primer3. *Bioinformatics* 23, 1289–1291.
19. White, S.J., Vink, G.R., Kriek, M., Wuyts, W., Schouten, J., Bakker, B., Breuning, M.H., and den Dunnen, J.T. (2004). Two-color multiplex ligation-dependent probe amplification: detecting genomic rearrangements in hereditary multiple exostoses. *Hum. Mutat.* 24, 86–92.
20. Birnboim, H.C., and Doly, J. (1979). A rapid alkaline extraction procedure for screening recombinant plasmid DNA. *Nucleic Acids Res.* 7, 1513–1523.
21. Guillard, M., Wada, Y., Hansikova, H., Yuasa, I., Vesela, K., Ondruskova, N., Kadoya, M., Janssen, A., Van den Heuvel, L.P., Morava, E., et al. (2011). Transferrin mutations at the glycosylation site complicate diagnosis of congenital disorders of glycosylation type I. *J. Inherit. Metab. Dis.* 34, 901–906.
22. Guillard, M., Morava, E., van Delft, F.L., Hague, R., Körner, C., Adamowicz, M., Wevers, R.A., and Lefeber, D.J. (2011). Plasma N-glycan profiling by mass spectrometry for congenital disorders of glycosylation type II. *Clin. Chem.* 57, 593–602.
23. Vanbeselaere, J., Vicogne, D., Matthijs, G., Biot, C., Foulquier, F., and Guerardel, Y. (2013). Alkynyl monosaccharide analogues as a tool for evaluating Golgi glycosylation efficiency: application to Congenital Disorders of Glycosylation (CDG). *Chem. Commun. (Camb.)* 49, 11293–11295.
24. Mohamed, M., Guillard, M., Wortmann, S.B., Cirak, S., Marklova, E., Michelakakis, H., Korsch, E., Adamowicz, M., Koletzko, B., van Spronsen, F.J., et al. (2011). Clinical and diagnostic approach in unsolved CDG patients with a type 2 transferrin pattern. *Biochim. Biophys. Acta* 1812, 691–698.
25. Altschul, S.F., Madden, T.L., Schäffer, A.A., Zhang, J., Zhang, Z., Miller, W., and Lipman, D.J. (1997). Gapped BLAST and PSI-BLAST: a new generation of protein database search programs. *Nucleic Acids Res.* 25, 3389–3402.
26. Ho, M.N., Hill, K.J., Lindorfer, M.A., and Stevens, T.H. (1993). Isolation of vacuolar membrane H⁽⁺⁾-ATPase-deficient yeast mutants; the VMA5 and VMA4 genes are essential for assembly and activity of the vacuolar H⁽⁺⁾-ATPase. *J. Biol. Chem.* 268, 221–227.
27. Graham, L.A., Hill, K.J., and Stevens, T.H. (1998). Assembly of the yeast vacuolar H⁺-ATPase occurs in the endoplasmic reticulum and requires a Vma12p/Vma22p assembly complex. *J. Cell Biol.* 142, 39–49.
28. Szklarczyk, R., Wanschers, B.F., Cuypers, T.D., Esseling, J.J., Riemersma, M., van den Brand, M.A., Gloerich, J., Lasonder, E., van den Heuvel, L.P., Nijtmans, L.G., and Huynen, M.A. (2012). Iterative orthology prediction uncovers new mitochondrial proteins and identifies C12orf62 as the human ortholog of COX14, a protein involved in the assembly of cytochrome c oxidase. *Genome Biol.* 13, R12.
29. Pellicano, F., Inglis-Broadgate, S.L., Pante, G., Ansoorge, W., and Iwata, T. (2006). Expression of coiled-coil protein 1, a novel gene downstream of FGF2, in the developing brain. *Gene Expr. Patterns* 6, 285–293.
30. Pellicano, F., Thomson, R.E., Inman, G.J., and Iwata, T. (2010). Regulation of cell proliferation and apoptosis in neuroblastoma cells by ccp1, a FGF2 downstream gene. *BMC Cancer* 10, 657.
31. Hill, K.J., and Stevens, T.H. (1995). Vma22p is a novel endoplasmic reticulum-associated protein required for assembly of the yeast vacuolar H⁽⁺⁾-ATPase complex. *J. Biol. Chem.* 270, 22329–22336.

32. Ramachandran, N., Munteanu, I., Wang, P., Ruggieri, A., Rilstone, J.J., Israelian, N., Naranian, T., Paroutis, P., Guo, R., Ren, Z.P., et al. (2013). VMA21 deficiency prevents vacuolar ATPase assembly and causes autophagic vacuolar myopathy. *Acta Neuropathol.* 125, 439–457.
33. Jansen, J.C., Timal, S., Van Scherpenzeel, M., Michelakakis, H., Vicogne, D., Moraitou, M., Hoischen, A., Huijben, K., Steenbergen, G., van den Boogaard, M.A.W., et al. (2015). TMEM199 deficiency causes a Golgi homeostasis disorder characterized by elevated aminotransferases, alkaline phosphatase, and cholesterol and abnormal glycosylation. *Am. J. Hum. Genet.* 98, this issue, 329–337.
34. Janssen, M.J., Waanders, E., Woudenberg, J., Lefeber, D.J., and Drenth, J.P. (2010). Congenital disorders of glycosylation in hepatology: the example of polycystic liver disease. *J. Hepatol.* 52, 432–440.
35. Mercier, S., Magot, A., Caillon, F., Isidor, B., David, A., Ferrer, X., Vital, A., Coquet, M., Penttilä, S., Udd, B., et al. (2015). Muscle magnetic resonance imaging abnormalities in X-linked myopathy with excessive autophagy. *Muscle Nerve* 52, 673–680.
36. Ruggieri, A., Ramachandran, N., Wang, P., Haan, E., Kneebone, C., Manavis, J., Morandi, L., Moroni, I., Blumbergs, P., Mora, M., and Minassian, B.A. (2015). Non-coding VMA21 deletions cause X-linked myopathy with excessive autophagy. *Neuromuscul. Disord.* 25, 207–211.
37. Frattini, A., Orchard, P.J., Sobacchi, C., Giliiani, S., Abinun, M., Mattsson, J.P., Keeling, D.J., Andersson, A.K., Wallbrandt, P., Zecca, L., et al. (2000). Defects in TCIRG1 subunit of the vacuolar proton pump are responsible for a subset of human autosomal recessive osteopetrosis. *Nat. Genet.* 25, 343–346.
38. Smith, A.N., Skaug, J., Choate, K.A., Nayir, A., Bakkaloglu, A., Ozen, S., Hulton, S.A., Sanjad, S.A., Al-Sabban, E.A., Lifton, R.P., et al. (2000). Mutations in ATP6N1B, encoding a new kidney vacuolar proton pump 116-kD subunit, cause recessive distal renal tubular acidosis with preserved hearing. *Nat. Genet.* 26, 71–75.
39. Fischer, B., Dimopoulou, A., Egerer, J., Gardeitchik, T., Kidd, A., Jost, D., Kayserili, H., Alanay, Y., Tancheva-Poor, I., Mangold, E., et al. (2012). Further characterization of ATP6V0A2-related autosomal recessive cutis laxa. *Hum. Genet.* 131, 1761–1773.
40. Guillard, M., Dimopoulou, A., Fischer, B., Morava, E., Lefeber, D.J., Kornak, U., and Wevers, R.A. (2009). Vacuolar H⁺-ATPase meets glycosylation in patients with cutis laxa. *Biochim. Biophys. Acta* 1792, 903–914.
41. Vanier, M.T. (2010). Niemann-Pick disease type C. *Orphanet J. Rare Dis.* 5, 16.
42. Vanier, M.T. (2015). Complex lipid trafficking in Niemann-Pick disease type C. *J. Inher. Metab. Dis.* 38, 187–199.
43. Storch, J., and Xu, Z. (2009). Niemann-Pick C2 (NPC2) and intracellular cholesterol trafficking. *Biochim. Biophys. Acta* 1791, 671–678.
44. Howard, M.F., Murakami, Y., Pagnamenta, A.T., Daumer-Haas, C., Fischer, B., Hecht, J., Keays, D.A., Knight, S.J., Kölsch, U., Krüger, U., et al. (2014). Mutations in PGAP3 impair GPI-anchor maturation, causing a subtype of hyperphosphatasia with mental retardation. *Am. J. Hum. Genet.* 94, 278–287.
45. Krawitz, P.M., Murakami, Y., Hecht, J., Krüger, U., Holder, S.E., Mortier, G.R., Delle Chiaie, B., De Baere, E., Thompson, M.D., Roscioli, T., et al. (2012). Mutations in PIGO, a member of the GPI-anchor-synthesis pathway, cause hyperphosphatasia with mental retardation. *Am. J. Hum. Genet.* 91, 146–151.
46. Muñoz, M., and Zurzolo, C. (2014). Sorting of GPI-anchored proteins from yeast to mammals—common pathways at different sites? *J. Cell Sci.* 127, 2793–2801.

47. Klionsky, D.J., and Emr, S.D. (1989). Membrane protein sorting: biosynthesis, transport and processing of yeast vacuolar alkaline phosphatase. *EMBO J.* 8, 2241–2250.
48. Sobota, J.A., Bäck, N., Eipper, B.A., and Mains, R.E. (2009). Inhibitors of the V0 subunit of the vacuolar H⁺-ATPase prevent segregation of lysosomal- and secretory-pathway proteins. *J. Cell Sci.* 122, 3542–355

Supplementary files

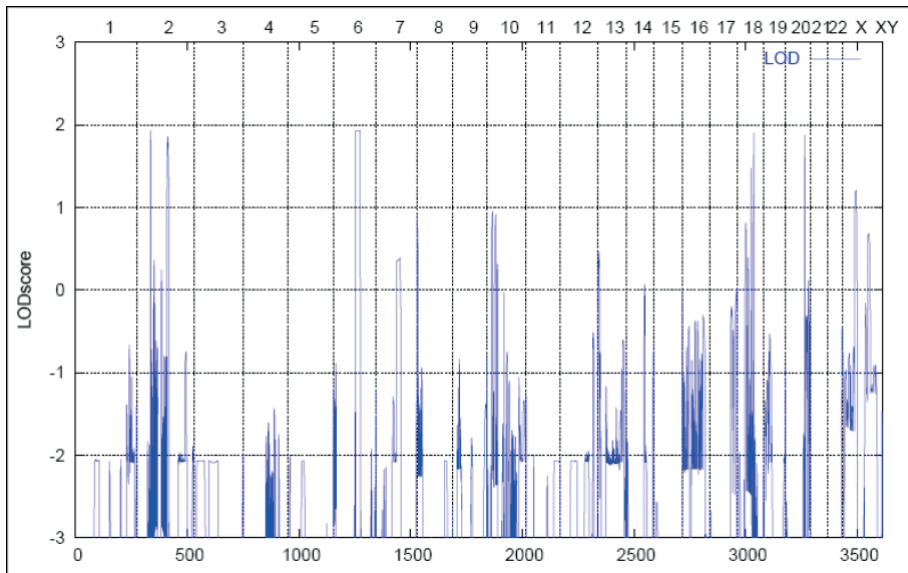


Figure S1. Linkage analysis of CCDC115 deficient family F1 Homozygosity mapping in family F1 (F1-II1 and F1-II2, the unaffected sibling F1-II3 and both parents) was done with the XBA142 10K SNP array (Affymetrix) according to manufacturer's instructions. After quality control (including Pedcheck) parametric linkage analysis was performed using AllegroV2 under a recessive disease model. We found homozygous regions with the theoretical maximum lodscore of 1.93 in this small core pedigree.(1,2)

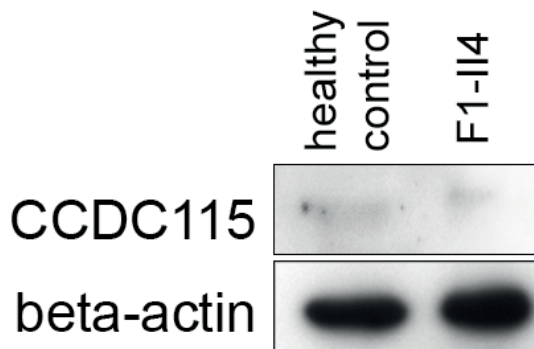


Figure S2. CCDC115 Western Blot We used polyclonal anti-CCDC115 antiserum (provided by Dr. F. Pellicano and Dr. T. Iwata) and HRP-conjugated anti-rabbit secondary antibody. Monoclonal mouse anti- β -actin antibody (Santa Cruz, #SC-81178) was used for loading control with an HRP-conjugated anti-mouse secondary antibody for ECL detection.

Table S1. Primer overview

		Forward 5'	3'	Reverse 5'	3'
Primers for Sanger sequencing					
<i>CCDC115</i>	exon 1	CCACTCTTCCCTCAACCAAA		TCCATGTGGGAAGCATACTG	
<i>CCDC115</i>	exon 2	AGAAGGAAGAGGGGGCTCAC		CAGATCTGGAGGTGTGTCCA	
<i>CCDC115</i>	exon 3	CCCAGTGTAAGCAACTACC		TCTACCGCTTTCCTCTCC	
<i>CCDC115</i>	exon 4	TTTGATGGAGGAAAACCTG		GTTTCCTGGAACCCCAAAGT	
<i>CCDC115</i>	exon 5	GGCTGAGTACGGTTTTCTCC		CCTCAGGGTCTGGAGCAG	
	M13 tag	tgtaaacgacggccagt		caggaaacagctatgacc	
Primers for cloning of the pcDNA3.1-CCDC115-V5 construct					
<i>CCDC115</i>	cDNA	GGCAGCCCCAGGCTCCAG		ATGGCGGCCTTGACCTGC	
Primers for MLPA					
<i>CCDC115</i>	5' Exon 1	gggttcctaagggttgaACCAACAG-GAGAACCCAATGGGCAAGGAA		AACGGCCGGCAAGCATTGGAAAGAC-GCTtctagattggatcttctgtgac	
<i>CCDC115</i>	Exon 1-2	gggttcctaagggttgaAGGAGGGTACACG-GGCGTAAACTGA		GTCTCACCGCTTTCCTCTCCCTG-CAtctagattggatcttctgtgac	
<i>CCDC115</i>	Exon 3	gggttcctaagggttgaTTCTCGTCTTCAG-CGAGGCCAGGA		GGGACTCCAGAAGTTCAAGGTGGT-GAgcgctatagggtgccgtggttcttagattgatcttctgtgac	
<i>CCDC115</i>	Exon 4	gggttcctaagggttgaCAGGCTCAAG-CAAGCTTCGGGATGGTGAGTG		GACCGTGTGTTTGGCTCTGTGGC-CCTCAGACggcgctatagggtgccgtggttga-atctagattggatcttctgtgac	
<i>CCDC115</i>	Exon 5	gggttcctaagggttgaATCCAGATCCTCCT-GGGTCGTGTGTACTACTAC		AGATACCATGGT-GACCTTCTCTCTTTCCTCCAtctagattgatcttctgtgac	
<i>SMPD4</i>	Exon 1	gggttcctaagggttgaGCCTTCGTTTGC-GCACGCGCCTTTTGAGGT		AACGGCCCAAAGAGGTGGAAGC-GCTTTTCCggcgctatagggtgccgtg-gttctagattggatcttctgtgac	
<i>PTPN18</i>	Exon 2-3	gggttcctaagggttgaTAGCTGAAAGC-CAGCAGGGGACCACACATGC		AGAGATCCCACCAAGGTGCCCTTGTG-GGCTGCTgtggcgctatagggtgccgtggttga-agtggcttagattggatcttctgtgac	

Table S2. Candidate gene list of exome sequencing data for CCDC115 deficient siblings F1-II1 and F1-II2

chromosome [hg19]	Genomic position	Reference nucleotide	Variant nucleotide	Coverage F1-II1 / F1-II2	%Variant reads F1-II1 / F1-II2	%Variant reads F1-II2	SNP ID	SNP Frequency [%]	In-house db	Gene	Isoform ID	Strand	Protein position	cdna position	PhyloP	Grantam dis-tance
Homozygous variants																
2	131099607	A	G	12/16	11/16	92/100		0	0	CCDC115	NM_032357	-	L31S	92A>G	2.27	145
6	112575045	C	T	54/64	54/64	100/100		0	0	LAMA4	NM_001105209	-	S103N	308C>T	-0.052	46
6	112441491	G	A	75/45	74/45	99/100		0	0	LAMA4	NM_001105206	-	H1554Y	4639G>A	5.611	83
6	109787164	T	C	27/33	26/33	96/100		0	0	ZBTB24	NM_014797	-	T662A	1984T>C	0.573	58
7	104751219	C	A	99/64	99/64	100/100		0	0	MLL5	NM_018682	+	D1324E	3972C>A	-0.137	45
10	72509677	C	T	33/34	33/34	100/100		0.15	1	ADAMTS14	NM_139155	+	A788V	2372C>T	0.476	64
10	102256987	C	T	87/84	86/83	99/99	rs149827193	0.15	1	SEC31B	NM_015490	-	E681K	2041C>T	2.207	56
Compound heterozygous variants																
2	182767128	C	T	78/96	41/44	52/46	rs184179348	0.001	0	SSFA2	NM_001130445	+	P450S	1348C>T	2.349	74
2	182783319	T	C	63/92	14/47	22/51	rs193034331	0.001	0	SSFA2	NM_006751	+	No protein	-	0.267	0
12	56349606	C	T	31/25	14/9	45/36	rs76045902	0.021	0	PMEL	NM_001200054	-	G505S	1513G>A	0.669	56
12	56349121	A	G	271/201	117/151	43/38	rs57990974	0.021	0	PMEL	NM_001200054	-	V603A	1787A>G	1.326	64

Table S3. *In silico* predictions for CCDC115 mutations

Affected individuals	F1-II1, F1-II2, F1-II4, F2-II1, F3-II2, F5-II1	F4-II1, F4-II2	F5-II1
Mutation	c.[92T>C]	c.[31G>T]	c.[(?_-258)_(*1245_?)del]
Protein change	p.Leu31Ser	p.Asp11Tyr	p.0?
PhyloP	2.22	2.47	NA
SIFT	Not tolerated	Not tolerated	NA
PolyPhen 2.0	Probably damaging (score 0.999)	Probably damaging (score 1.000)	NA
Mutation taster	Disease causing	Disease causing	NA
Grantham distance	145	160	NA

Abbreviations: NA, not applicable

Table S4. Dosage quotients for the MLPA analysis of family F5

	F5-II1 (affected child)	F5-I1 (father)	F5-I2 (mother)	average of 9 control samples
PTPN18 exon 2-3	0.50 ↓	0.52 ↓	1.05	0.99
CCDC115 exon 1	0.39 ↓	0.38 ↓	1.14	1.03
CCDC115 exon 2	0.56 ↓	0.54 ↓	1.04	1.00
CCDC115 exon 3	0.56 ↓	0.56 ↓	1.09	1.00
CCDC115 exon 4	0.52 ↓	0.60 ↓	1.07	1.00
CCDC115 exon 5	0.55 ↓	0.51 ↓	1.02	1.01
SMPD4 exon 1	1.08	1.08	0.95	1.00

Table S5. Quantification of transferrin IEF

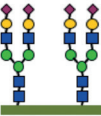
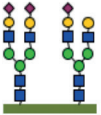
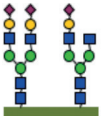
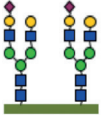
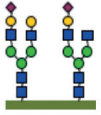
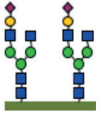
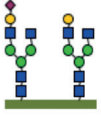
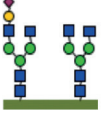
Family	Individual	0-sialo (%)	1-sialo (%)	2-sialo (%)	3-sialo (%)	4-sialo (%)	5-sialo (%)	6-sialo (%)
Control range (n=60)		0.0-3.2	0.0-5.0	3.3-7.6	4.9-10.6	47.3-62.7	18.7-31.5	3.2-7.8
F1	II1	2.25	7.57 †	21.24 †	29.27 †	29.86 †	7.88 †	1.93 †
	II2	3.42 †	9.90 †	19.69 †	26.36 †	27.49 †	10.66 †	2.48 †
	II4	3.68 †	8.57 †	13.77 †	17.03 †	35.90 †	17.35 †	3.70
F2	II1*	1.86	4.60	13.67 †	33.14 †	42.85 †	3.88 †	
F3	II2	no data available						
F4	II1	2.4	6.3 †	15.8 †	24.6 †	35.5 †	12.6 †	2.7 †
	II2	no data available						
F5	II1	no data available						

* Transferrin isoforms were measured with HPLC

Table S6. Quantification of ApoCIII IEF

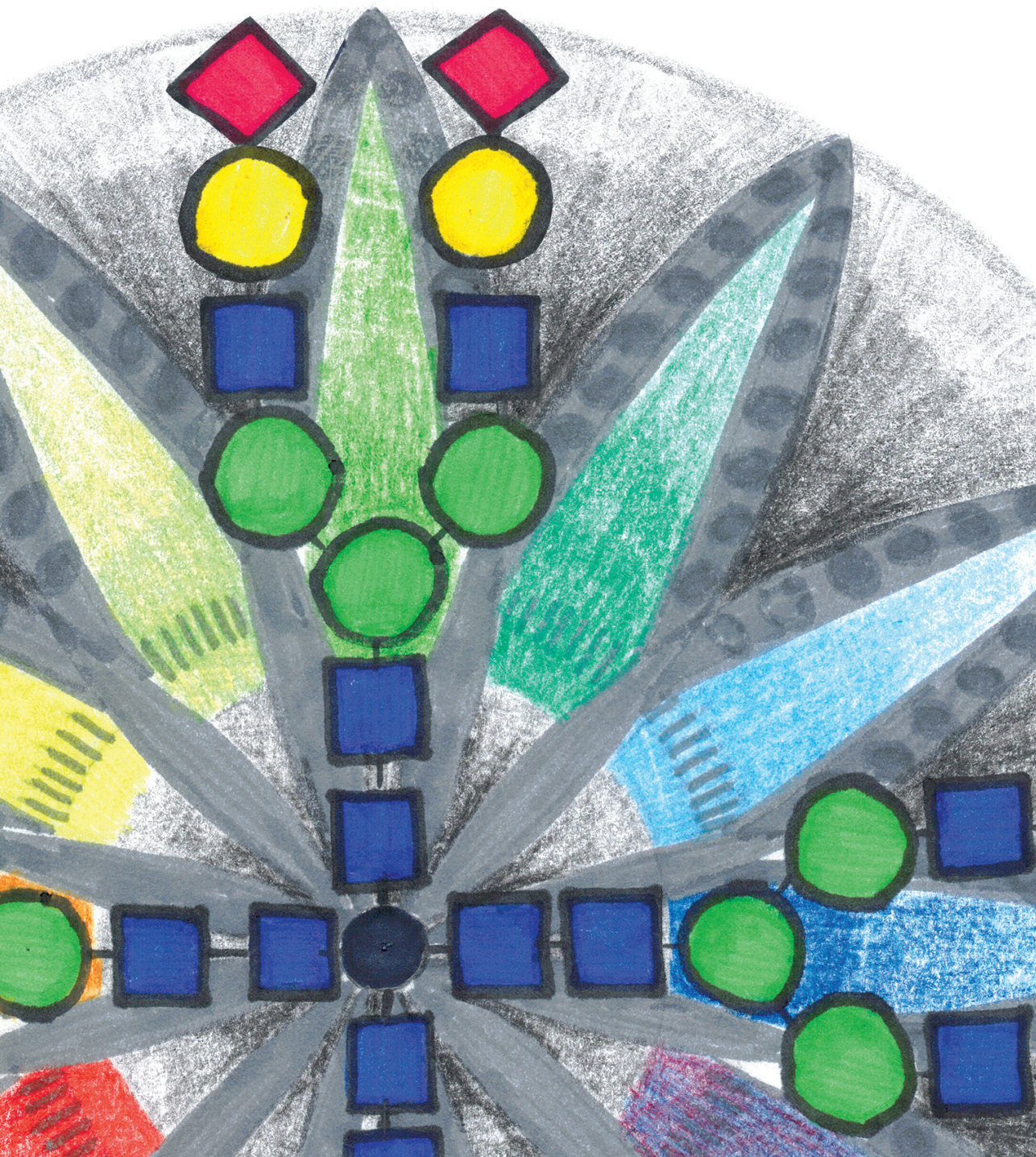
Family	individual	Age	0-sialo (%)	1-sialo (%)	2-sialo (%)
Control range	Age 0-1		0.2-4.5	42.7-69.8	26.2-56.7
	Age 1-18		1.4-9.5	48.5-75.2	21.0-45.8
	Age >18		1.8-7.6	47.4-73.6	20.2-46.5
F1	II1	5	10.5 †	81.5 †	8.0 ↓
	II2	5	7.4	85.9 †	6.7 ↓
	II4	1	8.6	73.1 †	18.3 ↓
F2	II1	3	18.6 †	63.22	18.1 ↓
F3	II2		no data available		
F4	II1	12	12.2 †	58	29.8
	II2		no data available		
F5	II1		no data available		

Table S7. Glycan structures (peak numbers associated with Figure 2C)

peak	structure	predicted mass (amu)
1		79555
2		79265
3		79104
4		78973
5		78811
6		78649
7		78358
8		78200

References

1. Gudbjartsson, D.F., Thorvaldsson, T., Kong, A., Gunnarsson, G., and Ingolfsson, A. (2005). Allegro version 2. *Nature genetics* 37, 1015-1016.
2. O'Connell, J.R., and Weeks, D.E. (1998). PedCheck: a program for identification of genotype incompatibilities in linkage analysis. *American journal of human genetics* 63, 259-266.

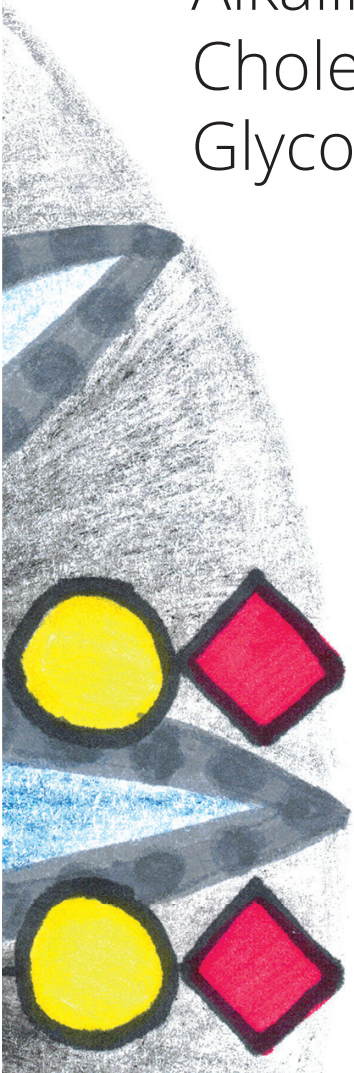


CHAPTER 3

TMEM199 Deficiency is a Disorder of Golgi Homeostasis Characterized by Elevated Aminotransferases, Alkaline Phosphatase, and Cholesterol and Abnormal Glycosylation

Jos C. Jansen, Sharita Timal, Monique van Scherpenzeel, Helen Michelakakis, Dorothée Vicogne, Angel Ashikov, Marina Moraitou, Alexander Hoischen, Karin Huijben, Gerry Steenbergen, Marjolein A.W. van den Boogert, Francesco Porta, Pier Luigi Calvo, Mersyni Mavrikou, Giovanna Cenacchi, Geert van den Bogaart, Jody Salomon, Adriaan G. Holleboom, Richard J. Rodenburg, Joost P.H. Drenth, Martijn A. Huynen, Ron A. Wevers, Eva Morava, François Foulquier, Joris A. Veltman, and Dirk J. Lefeber

Am J Hum Genet. 2016 Feb 4;98(2):322-30



Abstract

Congenital Disorders of glycosylation (CDG) form a genetically and clinically heterogeneous group of diseases with aberrant protein glycosylation as a hallmark. A subgroup of CDG can be attributed to disturbed Golgi homeostasis. However, identification of pathogenic variants is seriously complicated by the large number of proteins involved. As part of a strategy to identify human homologs of yeast proteins that are known to be involved in Golgi homeostasis, we identified uncharacterized transmembrane protein 199 (TMEM199, previously called C17orf32) as a human homolog of yeast V-ATPase assembly factor Vph2p (also known as Vma12p). Subsequently, we analyzed raw exome-sequencing data from families affected by genetically unsolved CDG and identified four individuals with different mutations in *TMEM199*. The adolescent individuals presented with a mild phenotype of hepatic steatosis, elevated aminotransferases and alkaline phosphatase, and hypercholesterolemia, as well as low serum ceruloplasmin. Affected individuals showed abnormal N- and mucin-type O-glycosylation, and mass spectrometry indicated reduced incorporation of galactose and sialic acid, as seen in other Golgi homeostasis defects. Metabolic labeling of sialic acids in fibroblasts confirmed deficient Golgi glycosylation, which was restored by lentiviral transduction with wild-type TMEM199. V5-tagged TMEM199 localized with ERGIC and COPI markers in HeLa cells, and electron microscopy of a liver biopsy showed dilated organelles suggestive of the endoplasmic reticulum and Golgi apparatus. In conclusion, we have identified TMEM199 as a protein involved in Golgi homeostasis and show that TMEM199 deficiency results in a hepatic phenotype with abnormal glycosylation.

The introduction of exome sequencing in genetics has had an enormous impact on the identification of Mendelian disorders.(1) However, genetic variants can appear to be falsely positive, and a considerable percentage of cases still remains genetically unsolved.(2,3) The availability of functional data improves candidate gene selection in the case of well-known biochemical pathways.(4) However, this is more complicated for complex pathways with many unknown proteins, such as the secretory pathway, which is composed of the endoplasmic reticulum (ER), the Golgi apparatus, and secretory vesicles. Multiple monogenic disorders have been associated with abnormal membrane trafficking, resulting in diverse clinical phenotypes.(5) Protein glycosylation also occurs in the secretory pathway: assembly and quality control of the glycoprotein occurs in the ER and further glycan modification in the Golgi.(6) Congenital Disorders of glycosylation (CDG) form a group of >100 monogenic diseases affecting glycosylation.(7) In a subgroup of CDG, abnormal glycosylation of serum proteins is caused by a disturbance of Golgi homeostasis. Examples are abnormal retrograde Golgi transport of glycosyltransferases (conserved oligomeric Golgi [COG] complex defects), abnormal ion transport (TMEM165 deficiency [MIM: 614727]), and abnormal Golgi pH regulation (ATP6V0A2 deficiency [MIM: 219200]).(8-12) ATP6V0A2 is a subunit of the vacuolar H⁺-ATPase (V-ATPase), the proton pump responsible for acidification of the secretory pathway, among other functions. (13)

Identification of more genes involved in this emerging group of Golgi homeostasis defects will generate biological insights into organelle homeostasis and vesicular transport. However, this is challenging given the large number of proteins involved, many of these with unknown functions. We set out to identify human Golgi-related proteins by using a bioinformatics search for human homologs of yeast proteins with a known role in ER-to-Golgi transport and/or Golgi glycosylation, including the V-ATPase. Yeast-to-human comparative genomics via a profile-based method, Position-Specific Iterated (PSI)-BLAST,(14) revealed transmembrane protein 199 (TMEM199, also known as C17orf32 [GenBank: NP_689677.1]) as a human homolog for yeast Vph2p (also known as Vma12p [GenBank: NP_012803]). Both proteins were identified as each other's best hit in the third iteration with an E-value of 3e-08 and a reciprocal E-value of 6e-18, suggesting that both proteins are orthologs.(15) Vph2p localizes to the ER and has a confirmed role as a V-ATPase assembly factor.(16,17) Subsequently, we searched for *TMEM199* mutations in individuals with genetically unsolved Golgi glycosylation defects.

DNA of individuals F1-II2, F1-II3 and F2-II2 was isolated from fibroblasts and subjected to whole-exome sequencing as described.(18) All individuals, or their legal representatives, participating in this study provided informed consent, and all biological materials were obtained in accordance with the Declaration of Helsinki.

Our in-house bioinformatics pipeline was used to annotate called variants and indels.(19) A frequency of >0.2% in an in-house database of over 1,300 exomes was set for exclusion of variants. We searched for non-synonymous variants located in exons and canonical splice sites. As quality criteria, we only included variants called more than five times and with a frequency of more than 20% for heterozygous variants and 80% for homozygous variants. According to a model of autosomal-recessive inheritance, no obvious candidate genes could be identified. For brothers F1-II2 and F1-II3 from family F1, previous homozygosity mapping and targeted chip-based gene sequencing of all genes in the largest homozygous intervals did not reveal a clear candidate gene either. Inspection of the raw exome-sequencing data of both brothers was carried out with the Integrative Genomics Viewer (IGV, v.2.3.14, Broad Institute). Zooming in on all *TMEM199* exons (GenBank: NM_152464.2) revealed a missense mutation, c.20C>A (p.Ala7Glu), in exon 1 (Figure 1). This variant had a sequence depth of three reads in one sibling and no coverage for the other affected sibling. Sanger sequencing confirmed the missense mutation to be homozygous in DNA from both affected siblings and heterozygous in both parents. The mutation was absent from a healthy sister, thereby showing complete segregation of the mutation in the family, in agreement with autosomal-recessive inheritance (Figure 2A).

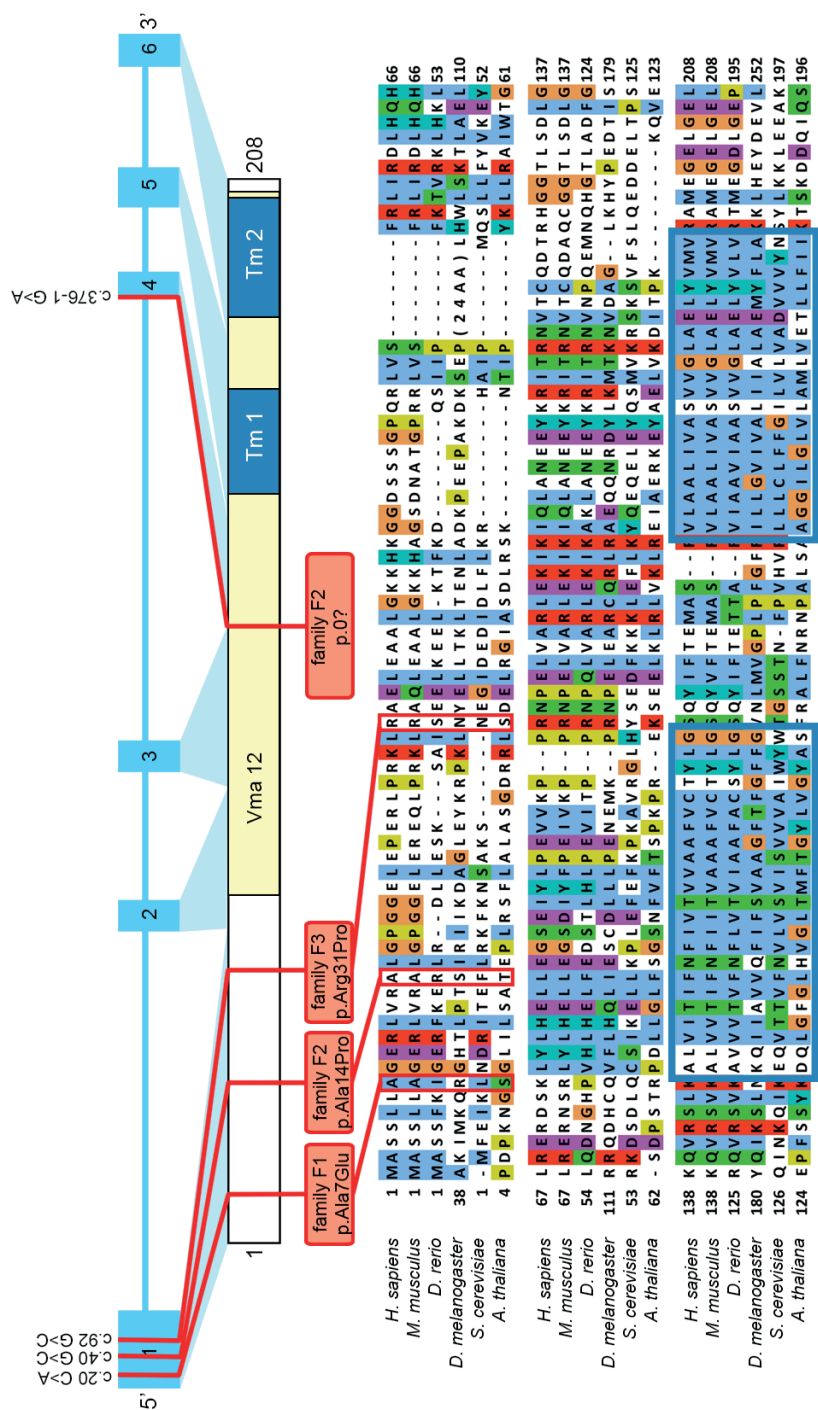


Figure 1. TMEM199 Domain Structure, Genetic Variants, and Conservation Schematic representation of the intron-exon structure of TMEM199 and the encoded protein. The mutations and substitutions within the different families are indicated by red lines. The yellow region indicates the conserved Vma12 domain ([PFam: PF11712] amino acids 78–203). The two predicted transmembrane regions (Tm1 and Tm2) are indicated by a blue box.

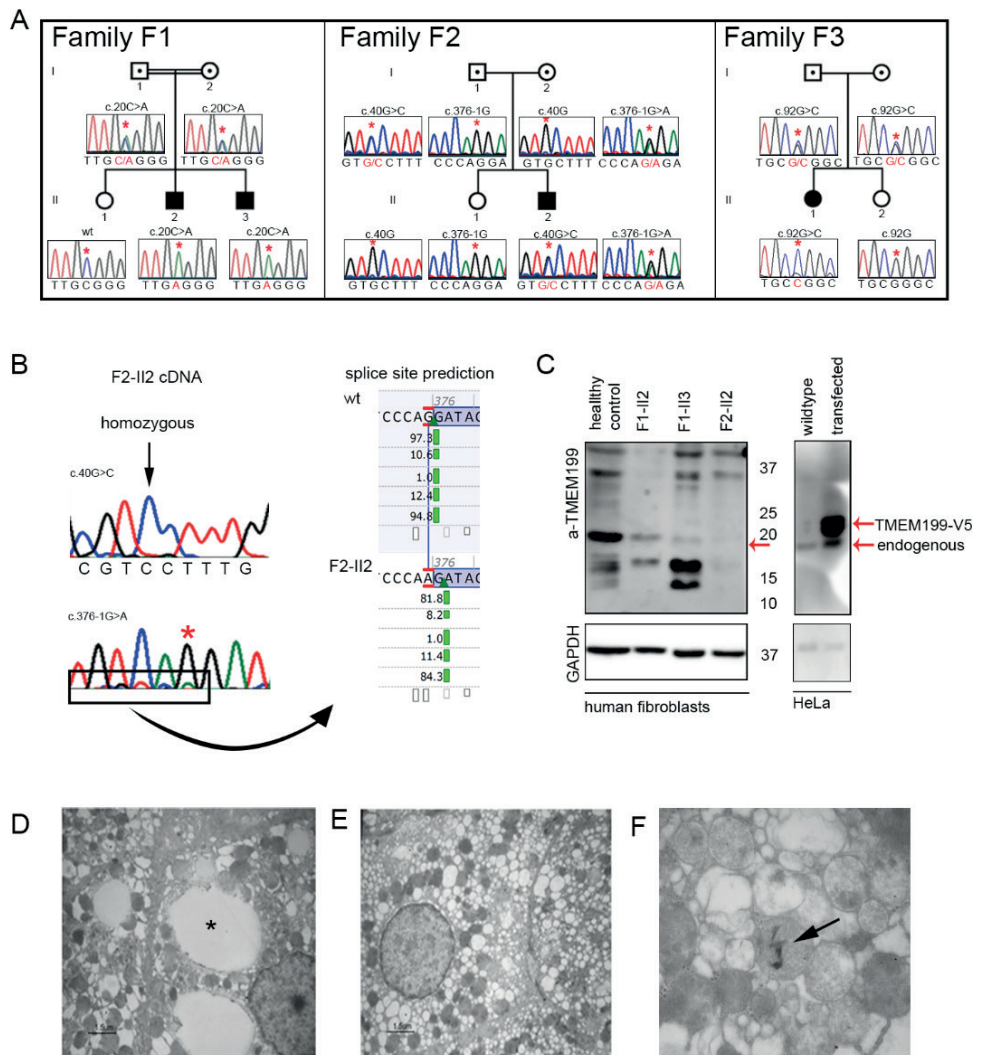


Figure 2. *TMEM199* Mutations, *TMEM199* Levels, and Liver Ultrastructure (A) Pedigrees and sequence profiles of *TMEM199* mutations in families F1 to F3. (B) Sequencing of *TMEM199* cDNA from individual F2-II2 showed homozygosity for the c.40G>C missense mutation. The insert shows the splice site prediction according to Alamut v.2.5.1 (Interactive Biosoftware), indicating a new splice site one nucleotide downstream. (C) Western blot analysis of *TMEM199* levels was performed on fibroblasts from healthy control individuals and affected individuals with anti-*TMEM199* antibody (1:250, Sigma, #HPA027051) (left). *TMEM199*-V5 was overexpressed in HeLa cells and the Western blot incubated with anti-*TMEM199* antibody (right). As a protein loading control, the same blot was incubated with mouse anti-GAPDH antibody (1:2,500, Calbiochem, #CB1001). (D-F) Transmission electron microscopy of liver tissue from individual F2-II2. (D) Focally, lipid vacuoles were present in the paranuclear area (asterisk). (E) Enlarged hepatocytes show diffuse and severe vacuolization most likely derived from rough ER, smooth ER, and/or Golgi apparatus. (F) Mitochondria featured fragmented cristae and an altered inner matrix appearing as granulo-filamentous material. Sometimes electron-dense crystal-like structures were included in the mitochondria (arrow).

For individual F2-II2, standard filtering of the whole exome sequencing data indicated a heterozygous variant in the splice acceptor site of *TMEM199* exon 4 (c.376-1G>A) (Figure 1). The raw exome-sequencing data revealed an uncalled heterozygous missense variant in exon 1 (c.40G>C [p.Ala14Pro]). Sequencing of parental DNA showed heterozygosity for the c.40G>C mutation in the father and heterozygosity for the c.376-1G>A mutation in the mother. A healthy sister did not show any of these mutations (Figure 2A). To further study the effect of the splice site mutation, we extracted mRNA from skin fibroblasts, synthesized cDNA, and sequenced it by Sanger sequencing. The resulting cDNA sequence showed the c.40G>C variant in homozygous form (Figure 2B), suggesting nonsense mediated decay of mRNA transcribed from the allele with the splice site mutation. Splice site prediction software (Alamut Visual v.2.5.1, Interactive Biosoftware) predicted the mutation to induce a stop codon 14 positions downstream by skipping one nucleotide (Figure 2B).

Sanger sequencing of *TMEM199* in a cohort of individuals with genetically unsolved Golgi glycosylation disorders revealed an additional individual in family F3 with a homozygous missense mutation in *TMEM199* exon 1 (c.92G>C [p.Arg31Pro]). This variant was heterozygous in both parents (Figures 1 and 2A).

Western blot analysis of *TMEM199* was performed in fibroblasts of affected individuals from families F1 and F2, and reduced protein levels were observed (Figure 2C, left). Specificity was demonstrated by detection of *TMEM199*-V5 with an anti-*TMEM199* antibody after overexpression of a *TMEM199*-V5 construct in HeLa cells, showing a slightly higher molecular weight than endogenous *TMEM199* (Figure 2C, right).

TMEM199 (UCSC Genome Browser [GRCh37/hg19], chr17:26,684,687–26,689,089) contains six exons and encodes a protein of 208 amino acids, which includes a conserved Vma12 domain (Pfam: PF11712) at the C terminus. The Vma12 domain is widespread among eukaryotes, including *Arabidopsis thaliana*, and includes two transmembrane helices as predicted by the CCTOP server (see Figure 1 and Web Resources). Interestingly, three of four mutations alter residues in the N terminus, which seems to be conserved only in higher eukaryotes. The missense mutations were variably predicted to be pathogenic by different prediction programs (Table 1). The Exome Aggregation Consortium (ExAC, see Web Resources) database showed an absence of all variants except the c.92G>C variant, which had a very low frequency (5.002e-05).

Individuals with mutations in *TMEM199* (Table 1) showed a mild clinical presentation with hypercholesterolemia and elevated low-density lipoprotein cholesterol (LDL-C), elevated alkaline phosphatase (ALP, bone-derived) and aminotransferases (ATs, consisting of aspartate aminotransferase [AST] and alanine aminotransferase [ALT]). Liver biopsy showed lipid degeneration and mild steatosis with minimal fibrosis. In addition, slight abnormalities of copper metabolism were noted. However, sequencing of *ATP7B* (MIM: 606882) for a diagnosis of Wilson disease (WD [MIM: 277900]) failed to detect a mutation. Total cholesterol levels were in between those of control individuals and individuals with familial hypercholesterolemia (FH [MIM: 143890]). Inspection of the raw exome-sequencing data from three individuals revealed no mutations in genes known to be associated with FH (*LDLR* [MIM: 606945], *APOB* [MIM: 107730], *PCSK9* [MIM: 607786]), although coverage was very poor for exon 1 of these three genes and for exon 10 of *PCSK9*. Total cholesterol levels of the parents were not measured.

The birth and early childhood of brothers F1-II2 and F1-II3, born 1990 and 1998, respectively, to Greek consanguineous parents, was unremarkable. During a routine blood test at fourteen and six years of age, respectively, elevated serum ATs and ALP were noticed (F1-II2: ALT 54 U/l [normal range, 0–50 U/l], AST 73 U/l [normal range, 0–50 U/l], ALP 745 U/l [normal range, < 360 U/l]; F1-II3: ALT 210 U/l, AST 246 U/l, ALP 1162 U/l). Gammaglutamyl transferase (gGT) and bilirubin levels were normal. A liver ultrasound was normal and liver biopsy showed steatosis. Their clinical appearance was unremarkable, and their growth and psychomotor development were normal. Isoelectric focusing (IEF) of transferrin (Tf) showed a type 2 CDG profile. Further biochemical analysis showed low serum ceruloplasmin for individual F1-II2 (11.5 mg/dl [normal range, 15–60 mg/dl]) and low-normal ceruloplasmin for individual F1-II3 (15.6 mg/dl). On suspicion of WD, a slightly elevated 24 hr urinary copper/creatinine ratio was found (86.9 and 72.8 mg/g creatinine [normal range, < 60 mg/g creatinine]). However, Kayser-Fleischer rings were absent, and genetic testing for *ATP7B* found no mutations, therefore a diagnosis of WD was discarded. Additionally, both siblings had elevated levels of total cholesterol (F1-II2: 253 mg/dl [normal range, 120–200 mg/dl]; F1-II3: 336 mg/dl) and LDL-C (F1-II2: 188 mg/dl [normal range, 50–130 mg/dl]; F1-II3: 277 mg/dl). Several coagulation factors were slightly decreased (antithrombin-III, factor XI, factor XIII, and protein S), but the international normalized ratio was normal. During subsequent years, ATs, ALP, and total cholesterol fluctuated from normal to approximately 1.5 times the upper level of normal.

Table 1. Genotype and phenotype of TMEM199 deficient families

	Family F1	Family F2	Family F3
Individuals (y.o.b.)	F1-II2 ('90) F1-II3 ('98)	F2-II2 ('74)	F3-II1 ('92)
Genotype			
Genomic change (Chr17(GRCh37))	g.26684713C>A	g.26684733G>C / g.26687551G>A	g.26684785G>C
cDNA change	Homozygous c.20C>A	Compound heterozygous c.40G>C / c.376-1G>A	Homozygous c. 92G>C
Protein change	p.Ala7Glu	p.Ala14Pro / p.0?	p.Arg31Pro
Allele frequency (ExaC browser)	0	0 / 0	5.002e-05
PhyloP	0.29	3.19 / NA	1.09
SIFT	Not tolerated	Tolerated / NA	Tolerated
PolyPhen 2.0 (score)	Possibly damaging (score 0.609)	Probably damaging (score 0.990) / NA	Probably damaging (score 0.991)
MutationTaster	Polymorphism	Disease causing / NA	Disease causing
Grantham distance	107	27/ NA	103
Phenotype			
Elevated aminotransferases	+	+	+
Elevated alkaline phosphatase	++	++	++
Steatosis	+	+	n.d.
Elevated cholesterol & LDL-C	+	+	+
Low ceruloplasmin	+	+	+
Glycosylation profile	Abnormal N- and O-glycosylation	Abnormal N-glycosylation	Abnormal N- and O-glycosylation

Abbreviations are as follows: y.o.b., year of birth; LDL-C, low-density lipoprotein cholesterol; NA, not applicable; n,d, not determined

During their last visit at the ages of 23 and 15 years, respectively, ALT and AST were within the normal range, but ALP was still slightly elevated. Lipid levels of individual F1-II2 had normalized, but for individual F1-II3, hypercholesterolemia persisted. Ceruloplasmin levels remained low for both individuals.

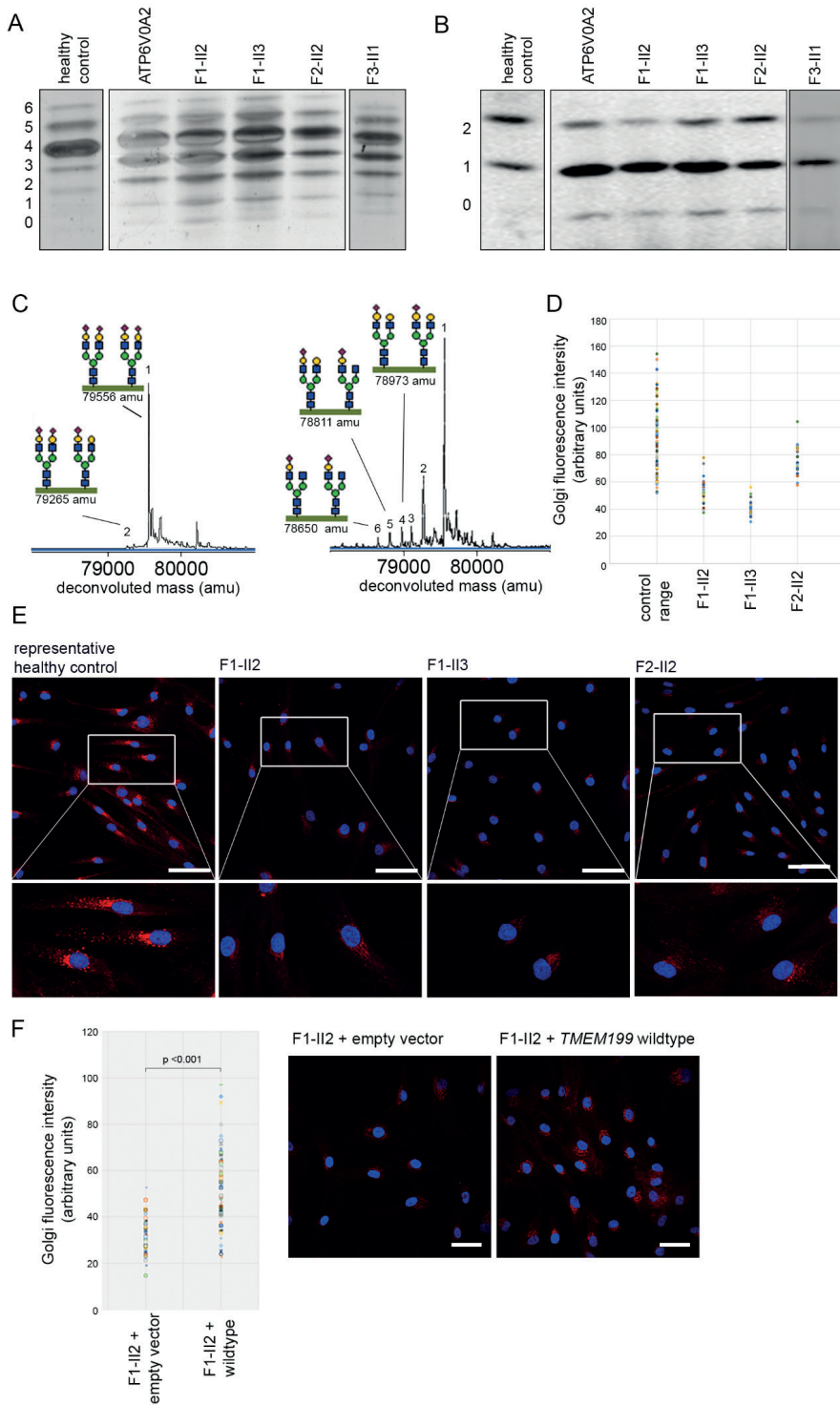
Individual F2-II2 is a 41-year-old male with a clinical history of unexplained elevation of ATs and ALP. His clinical presentation has been described before.²⁰ During routine pre-operative investigations for inguinal hernia surgery at the age of 11, incidentally, elevated ATs and ALP were found (ALT 190 U/l, AST 153 U/l, and ALP 718 U/l). At age 31, after 21 years of unexplained elevated ATs and ALP, a liver biopsy showed steatosis and minimal fibrosis with a hepatic dry copper weight of 90 mg/g (normal range, <40 mg/g; for WD, >250 mg/g). Serum ceruloplasmin was decreased (8.8 mg/dl) and urinary copper levels were normal. Kayser-Fleischer rings were absent. Based on these parameters, WD was discarded as a diagnosis. Additionally, hypercholesterolemia (204–337 mg/dl) and elevated LDL-C (182–226 mg/dl) were present. Over the course of years, ATs regressed to normal (ALT 46–159 U/l, AST 40–110 U/l), but high ALP persisted (365–557 U/l). Metabolic screening showed a type 2 CDG pattern.

Individual F3-II1 is a 23-year-old female born to Greek parents originating from the same small town. Her neonatal period was unremarkable. She was first seen by a clinician at the age of three months with hypotonia, which persisted during the following years. At the age of one year old, the diagnosis of benign infantile hypotonia was made. During early childhood, she also suffered from psychomotor disability. Brain MRI at the ages of four years and eleven years was normal. Due to attention deficit, carbamazepine was started at the age of six years but was discontinued after two years due to elevation of her liver enzymes, thought to be drug induced. Over the course of years, ATs and ALP remained elevated (ALT 36–172 U/l, AST 31–119 U/l, ALP 132–1,528 U/l) with low-normal ceruloplasmin (17–24 mg/dl). The lipid spectrum was normal until the age of five years, but cholesterol (231–257 mg/dl) and LDL-C (161–171 mg/dl) increased when she got older. At the age of 13 years, metabolic screening revealed abnormal N- and O-glycosylation, in agreement with a diagnosis of type 2 CDG. Subunit analysis of the COG complex failed to detect mutations. Unfortunately, she was lost for follow-up until 2014. In 2014 she was doing well and her ALT, AST, and ALP were only slightly elevated (58 U/l, 52 U/l, and 132 U/l). Serum ceruloplasmin was low (18 mg/dl) and hypercholesterolemia persisted.

We performed ultrastructural analysis of liver tissue from individual F2-II2, directly fixed with 2.5% glutaraldehyde in 0.1 M phosphate buffer. Hepatocytes were enlarged with cytoplasmic degeneration. Severe vacuolization was observed, as well as the presence of large lipid vacuoles, in agreement with optical microscopy analysis (Figure 2D). A marked dilation and vesiculation of the Golgi and/or ER was seen (Figure 2E). In addition, mitochondria featured fragmented cristae, an altered inner matrix appearing as a granulo-filamentous material, and sometimes included electron-dense crystal-like structures (Figure 2F).

All individuals were identified during routine metabolic diagnostics with abnormal glycosylation of serum Tf in CDG screening. Tf IEF showed increased disialo- and trisialotransferrin (see Figure 3A and Table S1 for quantification and ranges), indicating abnormal N-glycosylation. In addition, IEF of serum apolipoprotein C-III (ApoC-III) for analysis of mucin-type O-glycosylation showed an abnormal ApoC-III-1 profile for families F1 and F3 (see Figure 3B and Table S2 for quantification and ranges). To gain further insight into the aberrant N-glycan structures, we performed nanochip-C8 QTOF mass spectrometry of the intact Tf protein, which showed an accumulation of incompletely synthesized glycans lacking galactose and sialic acid for individual F1-II2, in comparison to the spectrum of a healthy individual (Figure 3C, peaks 2–6). Mass spectrometry of total plasma N-glycans showed a similar pattern, with an increase of glycans lacking galactose and sialic acid (Figure S1). Individuals with ATP6V0A2 deficiency show very similar glycosylation abnormalities of Tf, apoC-III, and total plasma N-glycans (Figures 3A and 3B).(11)

Next, we labeled sialic acids with alkyne-tagged synthetic sugar analogs, as reported before.(21) These sialic acid precursors (alkyne-tagged mannosamine [ManNAI]) are incorporated into nascent glycoproteins by the cell, allowing specific detection with fluorescently labeled azides. The immunofluorescent intensity of the azides is a marker for Golgi glycosylation efficiency. As in previous studies, the main pool of labeled glycoproteins located to the Golgi apparatus in healthy control fibroblasts (Figure 3E).(21) Quantification of the immunofluorescence signal with TISGolgi, an ImageJ plugin, showed a clear reduction of absolute Golgi fluorescence intensity in individuals F1-II2, F1-II3, and F2-II2 (Figures 3D and 3E). Subsequently, fibroblasts from individual F1-II2 were complemented by transduction with either a pLenti6.2-GFP-V5 (mock) or a pLenti6.2-TMEM199-V5 (wild-type *TMEM199*) vector. .



◀**Figure 3. Glycosylation Abnormalities in TMEM199-Deficient Individuals** (A) Glycosylation screening by IEF of serum Tf. The accompanying numbers represent the total number of sialic acids in the different protein isoforms. Representative N-glycosylation profiles from a healthy control individual, an ATP6V0A2-deficient individual, and TMEM199-deficient individuals are shown. (B) Glycosylation screening by IEF of serum ApoC-III. ApoC-III has one mucintype O-linked glycan with one or two sialic acids. For normal ranges and quantification of Tf-IEF and ApoC-III-IEF, see Tables S1 and S2. (C) The nanochip-C8 QTOF mass spectrum of a healthy control individual (left spectrum) and individual F1-II2 (right spectrum) are shown. Peak 1 (79,556 amu) represents the intact Tf protein with two attached complete glycans. Any subsequent loss of sialic acid and/or galactose can be calculated based on the mass difference with the main peak (i.e., loss of one sialic acid [purple diamond, peak 2]). For glycan structural annotation of peaks 1 to 6, see Table S3. (D–E) Fibroblasts from healthy control individuals and individuals F1-II2, F1-II3, and F2-II2 were incubated with ManNAI for metabolic labeling of sialic acids. The fluorescent signal indicates incorporation of sialic acids in glycoconjugates. Three healthy control fibroblasts were pooled for experiments performed twice. Scale bars indicate 75 μm . (F) Fibroblasts of individual F1-II2 were transduced with an empty vector or *TMEM199* wild-type construct and incubated with ManNAI, similarly to (D) and (E). Scale bars indicate 50 μm .

As shown in Figure 3F, the overall Golgi fluorescence intensity increased after transduction with wildtype *TMEM199* but not with the mock vector. Together, these data confirm a generalized defect in Golgi processing of protein-linked glycans due to deficiency of *TMEM199*

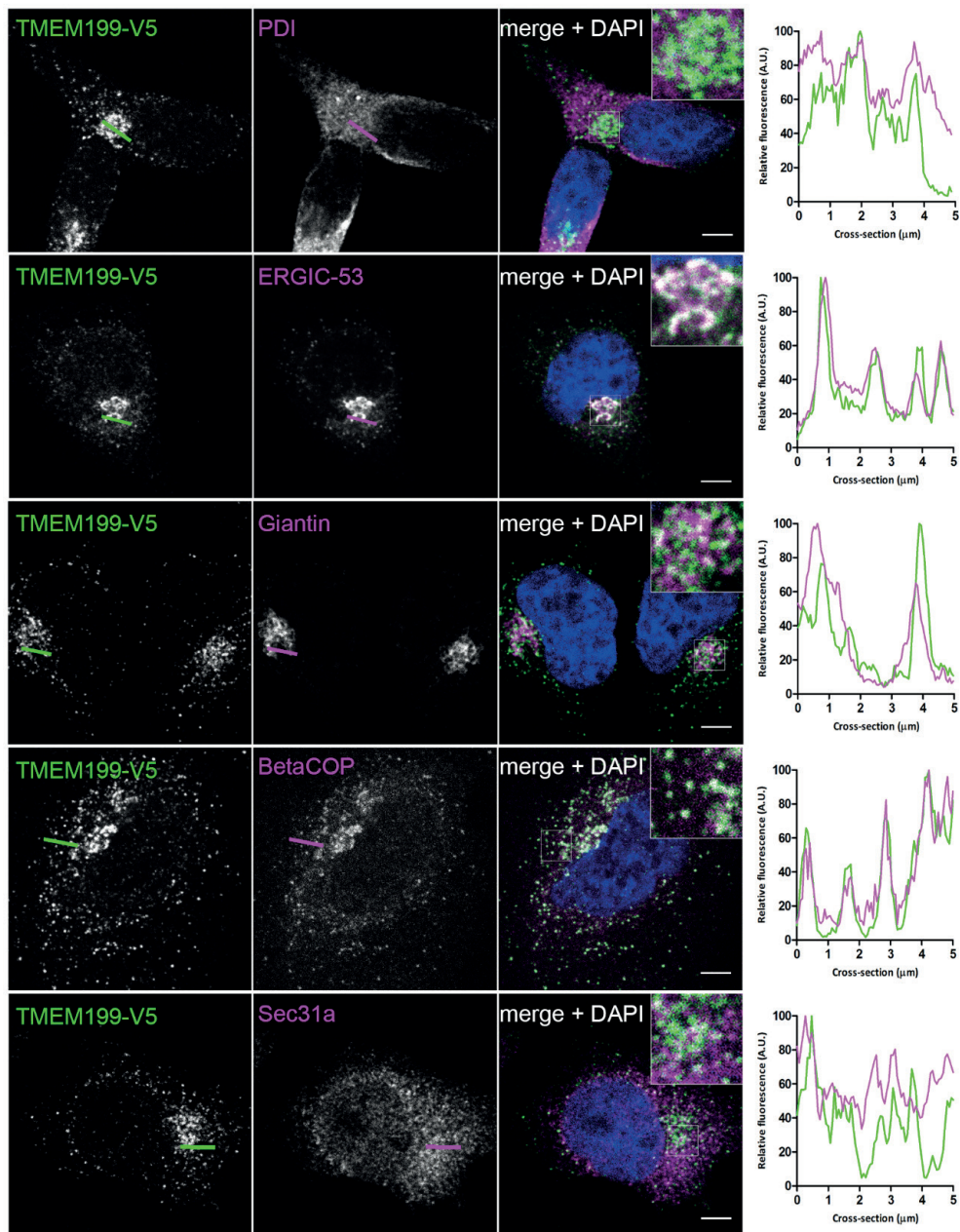
Our study indicated *TMEM199* as the human homolog of yeast V-ATPase assembly factor Vph2p. In yeast, V-ATPase assembly factors Vph2p, Vma21p, Pkr1p, and Vma22p are localized to the ER.(17) To define the subcellular location of *TMEM199*, a pLenti6.2-*TMEM199*-V5 plasmid for expression of C-terminally V5-tagged proteins was transiently overexpressed in HeLa cells. Imaging was done with a Leica SP8 (Leica Microsystems) confocal microscope with 603 water immersion 1.2 NA objective. Figure 4 shows clear co-localization of V5-tagged *TMEM199* with ER-Golgi intermediate compartment (ERGIC) and coat protein complex I (COPI) vesicle markers. In addition, partial co-localization was seen with giantin, a Golgi marker, but not with markers for ER or COPII vesicles. On the basis of these results, we conclude that *TMEM199* predominantly localizes to the ER-to-Golgi region, but not to the ER.

In parallel with identification of *TMEM199* mutations, we identified mutations in *CCDC115* in a cohort of individuals with abnormal Golgi glycosylation and a storage disease-like clinical phenotype including hepatosplenomegaly, neurological symptoms, elevated ATs, alkaline phosphatase, and hypercholesterolemia (see the related paper in this issue of AJHG).(22) *CCDC115* was predicted to be homologous to yeast V-ATPase assembly factor Vma22p. In yeast, Vph2p and Vma22p are localized to the ER and cooperatively stabilize the V0 domain during early assembly of the V-ATPase in the ER.(16,17) The human V-ATPase proton pump consists of 14 subunits divided between the membranebound V0 domain and a cytosolic V1 domain.(13) It participates in the acidification of the

secretory pathway or the extracellular matrix in specialized cells. However, it has numerous additional functions and associations with other cellular mechanisms and pathways.(13) A few human disorders involving defects in V-ATPase proteins are known, including X-linked myopathy with excessive autophagy due to mutations in *VMA21* (MIM: 310440),(23) renal tubular acidosis with deafness due to mutations in the kidney-specific isoforms ATP6V1B1 (MIM: 267300) or ATP6V0A4 (MIM: 602722),(24–26) Zimmerman- Laband syndrome 2 due to mutations in ATP6V1B2 (MIM: 616455),(27) osteopetrosis due to mutations in the osteoclast-specific V0a3 subunit (MIM: 259700) and cutis laxa due to mutations in ATP6V0A2.(24,28,29) ATP6V0A2 encodes the $\alpha 2$ subunit of the V0 domain, which localizes the V-ATPase complex to the Golgi apparatus, and is the only core subunit thus far associated with abnormal glycosylation.(11,30) The glycosylation profile seen in ATP6V0A2 deficiency is similar to that of *TMEM199* deficiency; however, the clinical symptoms are clearly different. In addition, a clear effect of *TMEM199* mutations was observed on organelle ultrastructure, different from ATP6V0A2 deficiency.(12)

At the moment, it is difficult to explain the broad heterogeneity in clinical phenotypes among the different V-ATPase associated diseases. Even mutations in *TMEM199* and *CCDC115*, whose gene products are probably interacting in humans, result in different phenotypes. It seems plausible to attribute these differences to different functions of the V-ATPase. On the basis of our experiments, we propose a role for *TMEM199* in Golgi homeostasis. However, it remains to be investigated whether this function is mediated through deficient proton transport via an effect on the V-ATPase or whether *TMEM199* exerts additional roles in ER-to-Golgi transport.

► **Figure 4. Localization of *TMEM199*** *TMEM199* cDNA, compatible with Gateway Technology (Life Technologies), was purchased from Harvard Medical School. HeLa cells were transfected with FuGENE HD Transfection Reagent (Promega), grown on coverslips coated with poly-L-Lysine (Sigma), and incubated overnight. After permeabilization and fixation, cells were stained with fluorescently labeled antibodies against V5 (green in merge) and organelle markers (magenta in merge). Shown are representative cells for the V5 antibody, organelle markers, and a merge with DAPI stain (blue), including a 3-fold magnification. Co-localization is indicated by white in the merged channel. The graphs show the fluorescence intensity profiles along the cross-sections indicated. Scale bars represent 5 μm . Organelle markers used are as follows: anti-V5-Tag (dilution 1:200, Life Technologies, #R960-25), anti-PDI (1:500, Abcam, #ab3672), anti-ERGIC-53 (1:200, Sigma-Aldrich, #E1031), anti-Giantin (1:1,000, BioLegend, #prb-114c), anti- BetaCOP (1:1,000, Abcam, #ab2899), and anti-Sec31a (1:500, Sigma-Aldrich, #HPA005457)



3

We have shown that prioritization of exome data based on functional knowledge of abnormal protein glycosylation can successfully elucidate previously unknown Golgi homeostasis defects. Protein interaction maps can be a useful tool for further identification of novel candidate proteins. During our studies, a protein interaction map of *Drosophila melanogaster* identified interactions between CG7071 (the fruit fly TMEM199) and multiple V-ATPase subunits.⁽³¹⁾ Recently, an ongoing effort to map the human interactome reported similar protein-protein interactions in humans (accessed via BioGRID, see Web Resources). Such interactomes will be of great benefit for disease-gene prioritization in cohorts of families with genetically unsolved cases of type 2 CDG.

In conclusion, we used comparative genomics to uncover TMEM199 as a protein involved in Golgi homeostasis, most likely with at least a partial role in V-ATPase functioning. TMEM199 deficiency should be considered in individuals with unexplained mildly elevated serum ATs, elevated ALP, hepatic steatosis, hypercholesterolemia, and low serum ceruloplasmin. We suggest screening for abnormal glycosylation in individuals with these symptoms.

Accession Numbers

The accession numbers for the pathogenic variants c.92G>C, c.20C>A, and c.40G>C; 376-1G>A reported in this paper are ClinVar: SCV000257475, SCV000257473, and SCV000257476, respectively.

Acknowledgments

We would like to thank the CDG-affected families for their participation in this study. We would also like to thank the group of Dr. Y. Guerardel and Prof. C. Biot for their generous donation of ManNAI. This work was financially supported by grants from the Institute of Genetic and Metabolic Disease (to D.J.L., R.J.R., and J.A.V.), the Dutch Organization for Scientific Research (ZONMW Medium Investment Grant 40-00506-98-9001 and VIDI Grant 91713359 to D.J.L. and VENI grant to A.G.H.), the Metakids foundation (J.C.J., M.v.S., J.P.H.D., and D.J.L.), the AMC graduate school Ph.D scholarship (M.A.W.v.d.B.), the Dr. Karel-Lodewijk Verleysen Award (J.C.J. and J.P.H.D.), the French National Agency (ANR SOLV-CDG to F.F.), and by grant ERARE11-135 of the ERANet for Research Programs on Rare Diseases Joint Transnational Call 2011 (EURO-CDG).

Web Resources

The URLs for data presented herein are as follows:

Alamut, <http://www.interactive-biosoftware.com/>

BioGRID, <http://thebiogrid.org>

BLAST, <http://blast.ncbi.nlm.nih.gov/Blast.cgi>

ClinVar, <https://www.ncbi.nlm.nih.gov/clinvar/>

Constrained Consensus TOPology prediction server, <http://cctop.enzim.ttk.mta.hu/>

dbSNP, <http://www.ncbi.nlm.nih.gov/projects/SNP/>

ExAC Browser, <http://exac.broadinstitute.org>

GenBank, <http://www.ncbi.nlm.nih.gov/genbank/>

Harvard PlasmID database, <https://plasmid.med.harvard.edu/>

PLASMID/Home.jsp

ImageJ, <http://imagej.nih.gov/ij>

Jalview, <http://www.jalview.org>

MutationTaster, <http://www.mutationtaster.org/>

OMIM, <http://www.omim.org/>

PolyPhen-2, genetics.bwh.harvard.edu/pph2/

SIFT, <http://sift.jcvi.org>

SNPcheck, <https://secure.ngri.org.uk/SNPCheck/snpcheck.htm>

TISGolgi, tisbio.wix.com/tisbio

UCSC Human Genome Browser, <http://genome-euro.ucsc.edu/index.htm>

References

1. Yang, Y., Muzny, D.M., Reid, J.G., Bainbridge, M.N., Willis, A., Ward, P.A., Braxton, A., Beuten, J., Xia, F., Niu, Z., et al. (2013). Clinical whole-exome sequencing for the diagnosis of mendelian disorders. *N. Engl. J. Med.* 369, 1502–1511.
2. MacArthur, D.G., Manolio, T.A., Dimmock, D.P., Rehm, H.L., Shendure, J., Abecasis, G.R., Adams, D.R., Altman, R.B., Antonarakis, S.E., Ashley, E.A., et al. (2014). Guidelines for investigating causality of sequence variants in human disease. *Nature* 508, 469–476.
3. Javed, A., Agrawal, S., and Ng, P.C. (2014). Phen-Gen: combining phenotype and genotype to analyze rare disorders. *Nat. Methods* 11, 935–937.
4. Timal, S., Hoischen, A., Lehle, L., Adamowicz, M., Huijben, K., Sykut-Cegielska, J., Paprocka, J., Jamroz, E., van Spronsen, F.J., Körner, C., et al. (2012). Gene identification in the congenital disorders of glycosylation type I by whole-exome sequencing. *Hum. Mol. Genet.* 21, 4151–4161.
5. De Matteis, M.A., and Luini, A. (2011). Mendelian disorders of membrane trafficking. *N. Engl. J. Med.* 365, 927–938.
6. Ohtsubo, K., and Marth, J.D. (2006). Glycosylation in cellular mechanisms of health and disease. *Cell* 126, 855–867.
7. Freeze, H.H., Chong, J.X., Bamshad, M.J., and Ng, B.G. (2014). Solving glycosylation disorders: fundamental approaches reveal complicated pathways. *Am. J. Hum. Genet.* 94, 161–175.
8. Foulquier, F., Amyere, M., Jaeken, J., Zeevaert, R., Schollen, E., Race, V., Bammens, R., Morelle, W., Rosnoblet, C., Legrand, D., et al. (2012). TMEM165 deficiency causes a congenital disorder of glycosylation. *Am. J. Hum. Genet.* 91, 15–26.
9. Rosnoblet, C., Legrand, D., Demaegd, D., Hacine-Gherbi, H., de Bettignies, G., Bammens, R., Borrego, C., Duvet, S., Morsomme, P., Matthijs, G., and Foulquier, F. (2013). Impact of disease-causing mutations on TMEM165 subcellular localization, a recently identified protein involved in CDG-II. *Hum. Mol. Genet.* 22, 2914–2928.
10. Miller, V.J., and Ungar, D. (2012). Re'COG'nition at the Golgi. *Traffic* 13, 891–897.
11. Kornak, U., Reynders, E., Dimopoulou, A., van Reeuwijk, J., Fischer, B., Rajab, A., Budde, B., Nürnberg, P., Foulquier, F., Lefeber, D., et al.;ARCLDebré-type Study Group (2008). Impaired glycosylation and cutis laxa caused by mutations in the vesicular H⁺-ATPase subunit ATP6V0A2. *Nat. Genet.* 40, 32–34.
12. Huchtagowder, V., Morava, E., Kornak, U., Lefeber, D.J., Fischer, B., Dimopoulou, A., Aldinger, A., Choi, J., Davis, E.C., Abuelo, D.N., et al. (2009). Loss-of-function mutations in ATP6V0A2 impair vesicular trafficking, tropoelastin secretion and cell survival. *Hum. Mol. Genet.* 18, 2149–2165.
13. Marshansky, V., Rubinstein, J.L., and Grüber, G. (2014). Eukaryotic V-ATPase: novel structural findings and functional insights. *Biochim. Biophys. Acta* 1837, 857–879.
14. Altschul, S.F., Madden, T.L., Schafer, A.A., Zhang, J., Zhang, Z., Miller, W., and Lipman, D.J. (1997). Gapped BLAST and PSI-BLAST: a new generation of protein database search programs. *Nucleic Acids Res.* 25, 3389–3402.
15. Szklarczyk, R., Wanschers, B.F., Cuypers, T.D., Esseling, J.J., Riemersma, M., van den Brand, M.A., Gloerich, J., Lasonder, E., van den Heuvel, L.P., Nijtmans, L.G., and Huynen, M.A. (2012). Iterative orthology prediction uncovers new mitochondrial proteins and identifies C12orf62 as the human ortholog of COX14, a protein involved in the assembly of cytochrome c oxidase. *Genome Biol.* 13, R12.
16. Graham, L.A., Hill, K.J., and Stevens, T.H. (1998). Assembly of the yeast vacuolar H⁺-ATPase occurs in the endoplasmic reticulum and requires a Vma12p/Vma22p assembly complex. *J. Cell Biol.* 142, 39–49.

17. Forgac, M. (2007). Vacuolar ATPases: rotary proton pumps in physiology and pathophysiology. *Nat. Rev. Mol. Cell Biol.* 8, 917–929.
18. Stránecký, V., Hoischen, A., Hartmannová, H., Zaki, M.S., Chaudhary, A., Zudaire, E., Nosková, L., Baresová, V., Pristoupilová, A., Hodanová, K., et al. (2013). Mutations in ANTXR1 cause GAPO syndrome. *Am. J. Hum. Genet.* 92, 792–799.
19. Vissers, L.E., de Ligt, J., Gilissen, C., Janssen, I., Steehouwer, M., de Vries, P., van Lier, B., Arts, P., Wieskamp, N., del Rosario, M., et al. (2010). A de novo paradigm for mental retardation. *Nat. Genet.* 42, 1109–1112.
20. Calvo, P.L., Pagliardini, S., Baldi, M., Pucci, A., Sturiale, L., Garozzo, D., Vinciguerra, T., Barbera, C., and Jaeken, J. (2008). Long-standing mild hypertransaminasaemia caused by congenital disorder of glycosylation (CDG) type IIx. *J. Inher. Metab. Dis.* 31 (Suppl 2), S437–S440.
21. Vanbeselaere, J., Vicogne, D., Matthijs, G., Biot, C., Foulquier, F., and Guerardel, Y. (2013). Alkynyl monosaccharide analogues as a tool for evaluating Golgi glycosylation efficiency: application to Congenital Disorders of Glycosylation (CDG). *Chem. Commun. (Camb.)* 49, 11293–11295.
22. Jansen, J.C., Cirak, S., Van Scherpenzeel, M., Timal, S., Reunert, J., Rust, S., Perez, B., Vicogne, D., Krawitz, P., Wada, Y., et al. (2016). CCDC115 deficiency causes a disorder of Golgi homeostasis characterized by abnormal protein glycosylation. *Am. J. Hum. Genet.* 98, this issue, 316–328.
23. Ramachandran, N., Munteanu, I., Wang, P., Ruggieri, A., Rilstone, J.J., Israelian, N., Naranian, T., Paroutis, P., Guo, R., Ren, Z.P., et al. (2013). VMA21 deficiency prevents vacuolar ATPase assembly and causes autophagic vacuolar myopathy. *Acta Neuropathol.* 125, 439–457.
24. Borthwick, K.J., Kandemir, N., Topaloglu, R., Kornak, U., Bakkaloglu, A., Yordam, N., Ozen, S., Mocan, H., Shah, G.N., Sly, W.S., and Karet, F.E. (2003). A phenocopy of CAII deficiency: a novel genetic explanation for inherited infantile osteopetrosis with distal renal tubular acidosis. *J. Med. Genet.* 40, 115–121.
25. Karet, F.E., Finberg, K.E., Nelson, R.D., Nayir, A., Mocan, H., Sanjad, S.A., Rodriguez-Soriano, J., Santos, F., Cremers, C.W., Di Pietro, A., et al. (1999). Mutations in the gene encoding B1 subunit of H⁺-ATPase cause renal tubular acidosis with sensorineural deafness. *Nat. Genet.* 21, 84–90.
26. Smith, A.N., Skaug, J., Choate, K.A., Nayir, A., Bakkaloglu, A., Ozen, S., Hulton, S.A., Sanjad, S.A., Al-Sabban, E.A., Lifton, R.P., et al. (2000). Mutations in ATP6N1B, encoding a new kidney vacuolar proton pump 116-kD subunit, cause recessive distal renal tubular acidosis with preserved hearing. *Nat. Genet.* 26, 71–75.
27. Kortüm, F., Caputo, V., Bauer, C.K., Stella, L., Ciolfi, A., Alawi, M., Bocchinfuso, G., Flex, E., Paolacci, S., Dentici, M.L., et al. (2015). Mutations in KCNH1 and ATP6V1B2 cause Zimmermann-Laband syndrome. *Nat. Genet.* 47, 661–667.
28. Frattini, A., Orchard, P.J., Sobacchi, C., Gilliani, S., Abinun, M., Mattsson, J.P., Keeling, D.J., Andersson, A.K., Wallbrandt, P., Zecca, L., et al. (2000). Defects in TCIRG1 subunit of the vacuolar proton pump are responsible for a subset of human autosomal recessive osteopetrosis. *Nat. Genet.* 25, 343–346.
29. Li, Y.P., Chen, W., Liang, Y., Li, E., and Stashenko, P. (1999). Atp6i-deficient mice exhibit severe osteopetrosis due to loss of osteoclast-mediated extracellular acidification. *Nat. Genet.* 23, 447–451.
30. Guillard, M., Dimopoulou, A., Fischer, B., Morava, E., Lefeber, D.J., Kornak, U., and Wevers, R.A. (2009). Vacuolar H⁺-ATPase meets glycosylation in patients with cutis laxa. *Biochim. Biophys. Acta* 1792, 903–914.
31. Guruharsha, K.G., Rual, J.F., Zhai, B., Mintseris, J., Vaidya, P., Vaidya, N., Beekman, C., Wong, C., Rhee, D.Y., Cenaj, O., et al. (2011). A protein complex network of *Drosophila melanogaster*. *Cell* 147, 690–703.

Supplementary files

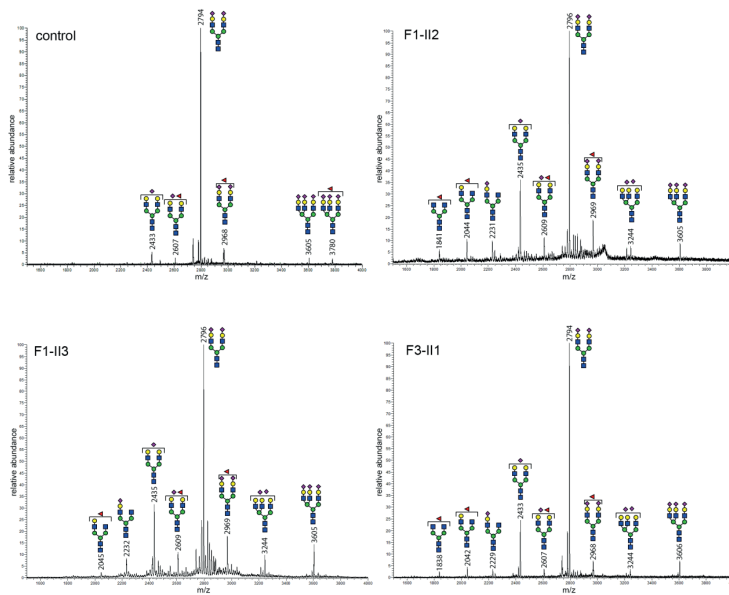


Figure S1 MALDI mass spectrometry profiles of total serum N-glycans of a healthy control and TMEM199 deficient individuals F1-II2, F1-II3 and F3-II1. An increase in hypoglycosylated glycans can be seen for all affected individuals when compared to a healthy control. Most notably the glycans with theoretical masses of 2433 m/z and 2228 m/z are increased, indicating loss of one sialic acid (2433 m/z) or one sialic acid plus one galactose (2228m/z).

Table S1 quantifications of transferrin Isoelectric focusing

		0-sialo (%)	1-sialo (%)	2-sialo (%)	3-sialo (%)	4-sialo (%)	5-sialo (%)	6-sialo (%)
Control		0.0-3.2	0.0-5.0	3.3-7.6	4.9-10.6	47.3-62.7	18.7-31.5	3.2-7.8
range								
(n=60)								
Family	indi-							
	vidual							
F1	II2	2.85	7.07 †	16.46 †	24.38 †	33.58 ↓	13.49 ↓	2.17 ↓
	II3	1.28	4.53	15.60 †	27.26 †	34.64 ↓	13.77 ↓	2.92 ↓
F2	II2	1.31	3.51	11.18 †	21.95 †	49.53 ↓	10.54 ↓	1.98 ↓
F3	II1	1.4	3.9	13.6 †	27.6 †	38.7 ↓	12.4 ↓	2.5

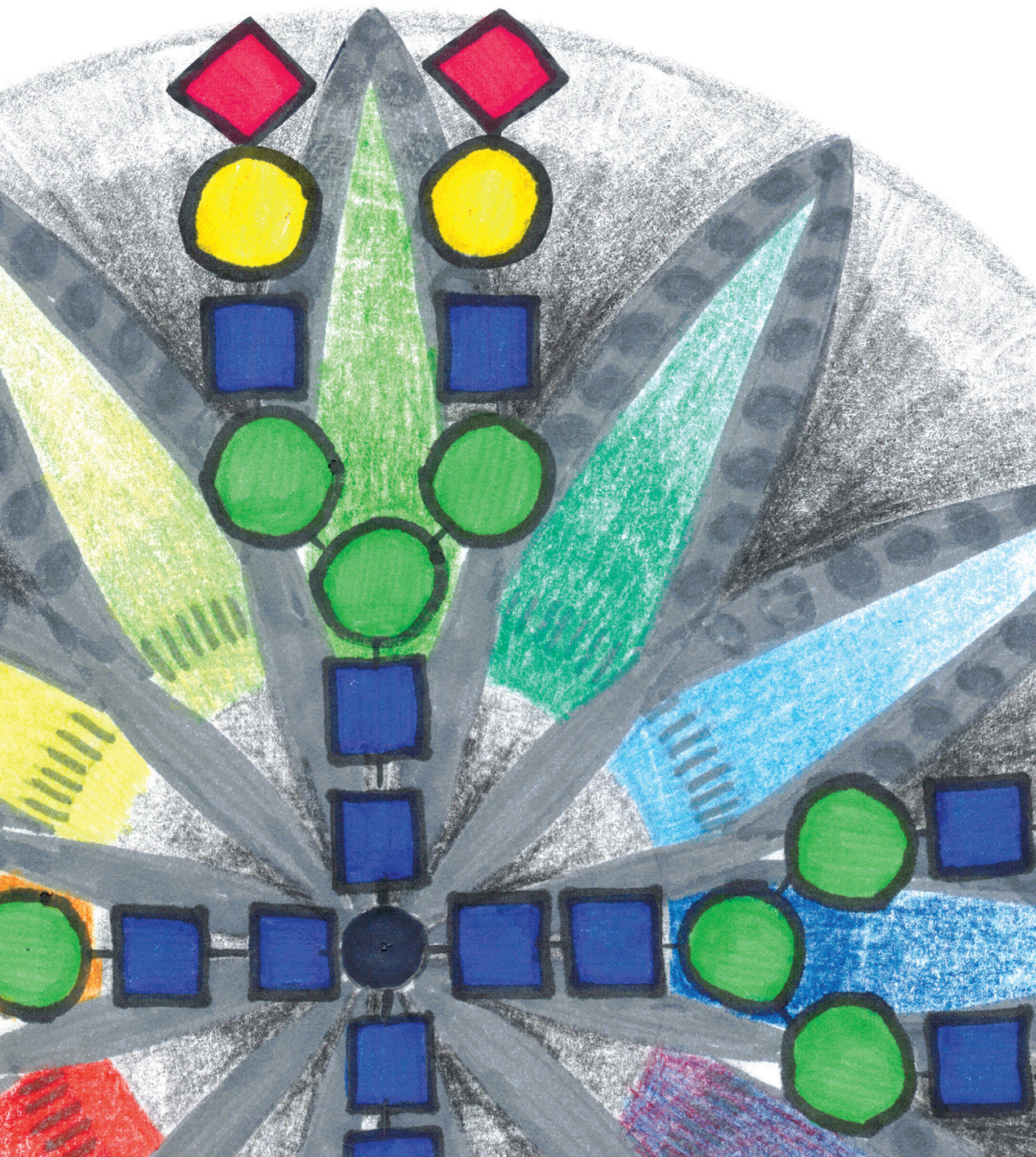
Table S2 quantifications of Apolipoprotein C-III Isoelectric focusing

			0-sialo (%)	1-sialo (%)	2-sialo (%)
Control range	Age 0-1		0.2-4.5	42.7-69.8	26.2-56.7
	Age 1-18		1.4-9.5	48.5-75.2	21.0-45.8
	Age >18		1.8-7.6	47.4-73.6	20.2-46.5
Family	individual	Age at analysis			
F1	II2	17	5.1	83.9 ↑	11.0 ↓
	II3	9	5.9	81.7 ↑	12.6 ↓
F2	II2	>18	7.2	65.5	27.3
F3	II1	12	3.5	85.3 ↑	11.2 ↓

3

Table S3 Glycan structures (peak numbers associated with Figure 3C)

Peak	Structure	Predicted mass (amu)
1		79555
2		79265
3		79104
4		78973
5		78811
6		78649

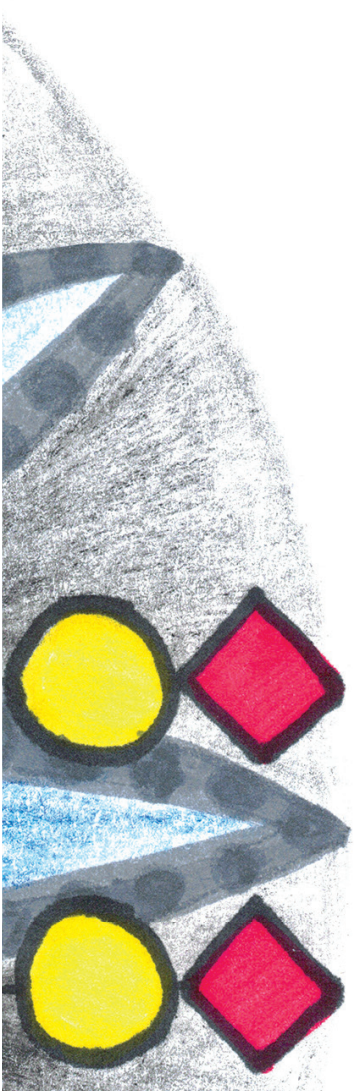


CHAPTER 4

NAFLD Phenotype in Patients With V-ATPase Proton Pump Assembly Defects

Jos C. Jansen, David Wolthuis, Monique van Scherpenzeel, Vlad Ratziu, Joost P.H. Drenth, Dirk J. Lefeber

Based on: Cell Mol Gastroenterol Hepatol. 2018 Jan 18;5(3):415-417.
e1.



Abstract

NAFLD is a common liver disease with a multifactorial etiology with hepatic steatosis as a signature lesion. Secondary causes for NAFLD are important to recognize because of their clear different clinical trajectory. In this review, we describe rare genetic variants in *CCDC115*, *TMEM199*, and *ATP6AP1* that can result in hepatic steatosis. These genes encode assembly factors of the vacuolar H⁺ ATPase proton pump and their deficiency results in abnormal Golgi homeostasis with subsequent abnormal protein glycosylation. Patients present with elevated aminotransferases and alkaline phosphatase and steatosis on liver biopsy. Hepatosplenomegaly is present in a subgroup and progression to cirrhosis with acute liver failure necessitating liver transplantation has been reported. The extra-hepatic phenotype includes dyslipidemia, muscular hypotonia, recurrent infections, and cognitive impairment. In light of these novel findings, V-ATPase assembly factor deficiencies should be recognized as a cause for secondary NAFLD and additionally provide valuable new insights in NAFLD disease mechanisms. We hypothesize a role for defective intracellular lipid metabolism via COPI and COPII vesicles to explain the hepatic phenotype.

Introduction

Nonalcoholic fatty liver disease (NAFLD) is a very common chronic liver disease marked by hepatic fat accumulation. In many patients, fat accumulation triggers hepatic inflammation and liver cell injury, a condition termed non-alcoholic steatohepatitis (NASH). NASH can promote fibrogenesis and evolve towards cirrhosis and primary liver cancer and is therefore considered the progressive extension of NAFLD.

Considerable heterogeneity has been recognized in patients with NAFLD. Most patients carry several features of the metabolic syndrome such as insulin resistance. However, well documented cases of NAFLD are not associated with the metabolic syndrome (Table 1).(1, 2) For these cases of secondary NAFLD, the mechanism of steatogenesis appears to be independent of insulin resistance and adipose tissue expansion. Known inborn errors of metabolism to cause NAFLD are hypo/a betalipoproteinemia, lysosomal acid lipase deficiency, or Wilson disease.(3-5) Additionally, infections, surgical interventions, and drug-induced steatohepatitis have been recognized.(6-10)

Table 1. Secondary causes of NAFLD

Drug-induced fatty liver disease
- Tamoxifen
- Amiodarone
- Atypical antipsychotic drugs
- Many others
Inflammatory causes
- Infectious causes: Hepatitis C virus-associated fatty liver
- Non-infectious causes: auto-immune hepatitis, psoriasis, coeliac disease
Endocrine causes
- Hypopituitarism
- Hypothyroidism
- Hypogonadism
Inborn errors of metabolism
- Wolman disease
- Genetic haemochromatosis
- Wilson disease
- A/hypo-betalipoproteinaemia
- α 1-antitrypsin deficiency
Others
- Acquired haemochromatosis
- Starvation, parenteral nutrition

Secondary causes of NAFLD are important to recognize as their natural history, associated symptoms, and overall management differ from that of primary NAFLD.

In this review, we describe a recently discovered group of genetic defects in assembly factors of the vacuolar H⁺ ATPase (V-ATPase), the intracellular proton pump. These defects result in abnormal protein glycosylation due to impaired Golgi trafficking and a complex phenotype, dominated by hepatic steatosis, which often is the primary manifestation of disease. We will discuss the process of protein glycosylation, the function of the V-ATPase complex and the mechanisms of hepatic lipid build-up in view of these novel disorders and propose that CCDC115-, TMEM199-, and ATP6AP1 deficiency are established as a cause of secondary NAFLD.

Protein glycosylation

Glycans are compounds of covalently linked monosaccharides and are one of four basic components of cells (in addition to nucleic acids, proteins, and lipids). (11) They serve multiple purposes including stabilization of folded proteins, intercellular communication, protein trafficking, and modulation of protein or lipid properties.(12) The attachment of a glycan to a protein or lipid is termed glycosylation and is a complex and highly regulated form of post translational modification.(13) Glycosylation starts in the endoplasmatic reticulum (ER) where the glycan build up and *en bloc* transfer to the nascent protein or lipid take place. If correctly folded, the newly formed glycoprotein travels to the Golgi apparatus (or simply 'Golgi'). In the Golgi, modification of the glycan takes place which results in the finished glycoprotein ready to be transported to other cellular compartments or into the bloodstream.(12)

Primary glycosylation defects

Primary glycosylation defects are congenital defects of glycosylation (CDG). This group encompasses more than 100 monogenic defects and is rapidly expanding. (14) Overall prevalence rates are unknown, but exome sequencing data predict a carriership of 20% and a prevalence of 1-2/1.000 persons for all known CDG genes.(14) All defects are inherited in an (X-linked) autosomal recessive pattern and result in a complex heterogenic phenotype.

CDG are classified based on an Endoplasmatic reticulum (ER)- or Golgi-located

defect. One of the disease mechanisms of Golgi-located CDG is based on imbalance of Golgi homeostasis.(14) In these patients, abnormal glycosylation is a result of an improper electrolyte balance or defective trafficking of glycosyltransferases, part of the Golgi glycosylation machinery.(15-17)

Diagnostics

The field of glycosylation research (or 'glycomics') is challenging because of its complex and dynamic nature. Recent advances in techniques for glycoanalysis such as high-resolution mass spectrometry has led to an increased understanding of function and regulation of glycans.(18)

In gastroenterology and hepatology, glycomics was mostly limited to identification of biomarkers for liver cirrhosis, hepatocellular carcinoma, or colorectal cancer. (19-21) More recently, genetic studies implicated glycosylation genes in IBD and polycystic liver disease.(22)(23) To what extent aberrant glycosylation plays a part in these pathomechanisms remains to be identified.

Diagnostics for CDG are based on glycosylation properties of transferrin. Traditionally, iso-electric focusing was used for rapid determination of the two glycans attached to transferrin. Although this provided a quick and cheap entry test of the glycosylation state of transferrin, (and extrapolation to whole body glycosylation) more detailed insight in glycan build-up was required. Mass spectrometry of intact glycoprotein transferrin affords new insights into glycosylation patterns and has successfully been employed for discovery, diagnostics, and/or monitoring of other CDG subtypes.(24, 25) Next generation sequencing has greatly accelerated identification of new CDG.(26) Declining costs and increased availability will lead to an increased use of genomic sequencing in parallel with glycomics to identify CDG patients.

TMEM199-, CCDC115-, and ATP6AP1 deficiency

As the main site for protein synthesis, the liver is frequently affected in CDG patients and elevated aspartate aminotransferase (AST) and alanine aminotransferase (ALT) serum levels are a common finding.(23) Recently, three CDG subtypes with a predominant liver phenotype have been discovered through advanced genetic studies.(27-29) Patients with pathogenic variants in the V-ATPase assembly factors *TMEM199* (MIM: 616829), *CCDC115* (MIM: 616828), or *ATP6AP1* (MIM: 300972) have defective glycosylation based on abnormal Golgi

homeostasis and a phenotype that contains elements of NAFLD and Wilson disease (Figure 1).

Non-hepatic symptoms such as hypercholesterolemia (for all defects), neurodegenerative symptoms (CCDC115 and ATP6AP1 deficiency) and hypogammaglobulinemia (ATP6AP1 deficiency) may also be present (Table 2).

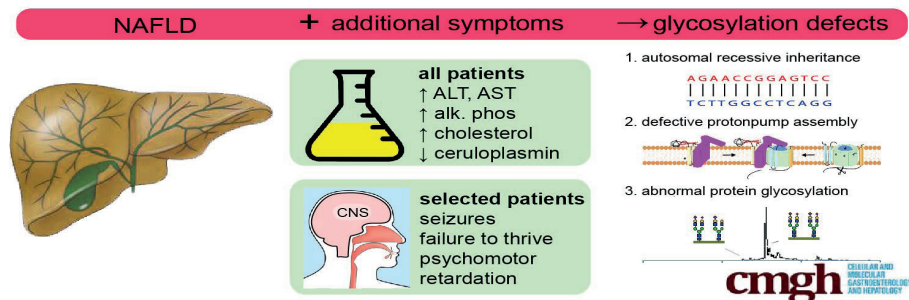


Figure 1. Hepatic symptoms of V-ATPase assembly factor deficiencies A summary of hepatic symptoms to expect in patients with V-ATPase assembly factor deficiencies. On gross examination, the liver may be enlarged with signs of NAFLD. Biochemically, elevated aminotransferases and alkaline phosphatase and low ceruloplasmin are seen in plasma. Liver biopsy shows steatosis and copper accumulation. Structurally, dilation of the ER and the Golgi apparatus are present.

Clinical spectrum

Four patients, three adolescents and one adult, belonging to three families with a TMEM199 deficiency have been reported.(27) Table2 provides an overview of the different genotypes found to date. Two brothers were diagnosed with mildly elevated aminotransferases during routine check-up at adolescence. An adult male was diagnosed with unexplained elevation of aminotransferases and alkaline phosphatase (AP) for 21 years prior to discovery of abnormal Golgi glycosylation.(30) The fourth patient was diagnosed at the age of three months with benign idiopathic hypotonia. At the age of six years her aminotransferases were elevated and at the age of 13 abnormal Golgi glycosylation was detected. All patients presented with similar symptoms: mildly elevated aminotransferases (<5x upper limit of normal), elevated AP, and hepatic steatosis, clinically resembling NAFLD. Serum levels of ceruloplasmin were below 20 mg/dl, consistent with Wilson disease. Hepatic dry copper weight of one patient was 90 $\mu\text{g/g}$ (normal <40 $\mu\text{g/g}$, for Wilson disease > 250 $\mu\text{g/g}$). Cholesterol (range 182 \square 337 mg/dl) and low-density lipoprotein- cholesterol (range 111 -277 mg/dl) were

elevated. Liver biopsy showed mild steatosis and minimal fibrosis.(4) On follow-up aminotransferase levels were reduced but AP and cholesterol remained elevated and ceruloplasmin remained low.

Table 2. Genotype overview of V-ATPase assembly factor deficiencies

Gene symbol (Gene ID)	Approved gene name (MIM)	Locus	Disorder (MIM)	Inheritance	Known pathogenic mutations	Protein change
<i>TMEM199</i> (NM_152464.2)	Trans-membrane protein 199 (616815)	17q11.2	TMEM199-CDG (616829)	Auto-somal recessive	c.20C>A c.[40G>C];[376-1G>A] c.92G>C	p.Ala7Glu p.[Ala14Pro];[p.0?] p.Arg31Pro
<i>CCDC115</i> (NM_032357.3)	Coiled-coil domain-containing protein 115 (613734)	2q21.1	CCDC115-CDG (616828)	Auto-somal recessive	c.92T>C c.31G>T c.[92T>C];[(?-258)_(*1245_?) del]	p.Leu31Ser p.Asp11Tyr p.[Leu31Ser];[p.0?]
<i>ATP6AP1</i> (NM_001183.5)	H+ transporting, lysosomal, accessory protein 1 (300197)	Xq28	AT-P6AP1-CDG (300972)	X-linked recessive	c.1284G>A c.431T>C c.1036G>A c.938A>G	p.Met428Ile p.Leu144Pro p.Glu346Lys p.Tyr313Cys

Parallel to discovery of *TMEM199* mutations, *CCDC115* mutations in eight patients from five families (Table 2) were also described.(29) All patients developed symptoms during early infancy. Clinical features of *CCDC115* deficiency overlap with that of *TMEM199* deficiency. All patients displayed liver involvement with increased aminotransferases and alkaline phosphatase, low ceruloplasmin, and hypercholesterolemia. *CCDC115* deficient patients develop neonatal jaundice, major hepatosplenomegaly, and psychomotor disability within the first months after birth, resembling lysosomal storage diseases. Patients may have mild dysmorphic features, facilitating diagnosis at an early age. The outcome of liver biopsy analysis was highly variable, encompassing the whole NAFLD spectrum from steatosis to cirrhosis. In one patient hepatic copper was increased at 125 µg/g dry weight, an increase that is insufficient for the diagnosis of Wilson disease. Three out of eight patients developed severe liver injury. Two underwent liver transplantation and one developed multi-organ failure and transplantation was omitted.

Eleven patients from six families with ATP6AP1 deficiency were diagnosed within their first year of life. They share a liver phenotype that is compatible with TMEM199- and CCDC115 deficiency. Findings on liver biopsies varied from normal liver histology to severe cirrhosis. Hepatosplenomegaly was present in patients from most families. ATP6AP1 deficiency is defined by the combination of liver injury and immunodeficiency. Almost all patients had a phenotype of recurrent bacterial infections with hypogammaglobulinemia and leukopenia.

Table 3. Extra-hepatic symptoms of V-ATPase assembly factor deficiencies

Extra-hepatic symptoms	TMEM199-CDG	CCDC115-CDG	ATP6AP1-CDG
Dysmorphic facial features	-	+	-
Psychomotor disability	+/-	+	+/-
Neurological symptoms			
- Hypotonia	+/-	+	+/-
- Seizures	-	-	+/-
- Sensineural hearing loss	-	-	+
Hematologic symptoms			
- abnormal coagulation factors	+/-	+/-	n.a.
- anemia	n.a.	+/-	n.a.
- leukopenia	n.a.	n.a.	+
- hypogammaglobulinemia	-	-	+
Creatine Kinase	n.a.	n.a.	
Splenomegaly	-	+	+
Hypoglycemia	n.a.	+/-	n.a.
Hypercholesterolemia	+	+	n.a.
Bone anomalies	-	-	-

Treatment

As with most CDG, treatment of V-ATPase assembly factor deficiencies is empirical. Treatment of TMEM199 deficiency was not indicated for three out of four patients as AST, ALT, and AP regressed to normal. A fourth patient received antiepileptics for recurrent seizures. Zinc treatment was tried in a patient with CCDC115 deficiency without avail. ATP6AP1 deficient patients develop hypogammaglobulinemia, successfully treated by IV immunoglobulines. Liver

transplantation was tried in two patients from the same *CCDC115*-deficient family. For a nine-year old girl transplantation was successful and normalization of aminotransferases and glycosylation was noted after transplantation. Unfortunately, her brother's transplant got rejected twice and he died at the age of nine.

Assembly of the V-ATPase

To better understand the pathogenicity of defects in V-ATPase assembly factors, a short summary of V-ATPase physiology is necessary. For a detailed review regarding structure and function we refer the reader to sources elsewhere. (31, 32) The V-ATPase is the main proton pump of the secretory pathway. Apart from acidification of the Golgi and lysosomes, it is involved in a large number of cellular functions such as protein trafficking and membrane fissuring.

The V-ATPase consists of 14 core units divided between two domains: a transmembrane V0 domain and a cytosolic V1 domain. The V1 domain provides the energy for the V0 domain to translocate protons. The V0 domain consists of a proteolipid ring (made from c, c', and c'' subunits) and a cage structure made from subunit a. An additional d subunit provides the link between the V0 and V1 domains (Figure 2).

Little is known how the mammalian V-ATPase is constructed and regulated and most knowledge comes from yeast studies. Assembly of the V0 domain is regulated by at least four ER-resident proteins: Vph2p (yeast homolog of TMEM199) and Vma22p (homolog of *CCDC115*) stabilize the cage structure, Voa1p (homolog of ATP6AP1) and Vma21p (homolog of *VMA21*) stabilize the proteolipid ring and Vma21p chaperone the V0 domain from the ER to the Golgi.

TMEM199 and *CCDC115* are located in the ER-to-Golgi intermediate complex (ERGIC) and Coatamer Protein Complex 1 (COP1) vesicles in HeLa- and primary hepatoma cells.(27, 29) TMEM199, 208 amino acids small, is a transmembrane protein and shares a conserved Vma12 domain throughout species. TMEM199 was identified as a nuclear envelope transmembrane protein with a fraction distributed to endosomes in human leukocytes.(33) *CCDC115* is a 181 amino acid small protein with two coiled coil domains. It is expressed mainly in the liver, heart, kidney, and testis and immunofluorescence studies located mouse *Ccdc115* to endo/lysosomal structures.(34) Yeast studies confirm a transient interaction between the yeast homologs of TMEM199 and *CCDC115* and the V-ATPase a-subunit.(35)

ATP6AP1 is located on the X chromosome and encodes the 470 amino acid long Ac45 protein. Ac45 is widely accepted as a V-ATPase accessory protein and has been studied extensively in *Xenopus laevis* (frog) hormone-secreting cells and mouse osteoclasts.^{20,21} Ac45 is cleaved by furin in two fragments in the early secretory pathway.(36, 37) After cleavage, the cytosolic C-terminal fragment traffics to secretory vesicles, along with the V-ATPase.(38)

Recent studies demonstrate that the C-terminal fragment of human Ac45 shares homology with Voa1p, a yeast V-ATPase assembly factor.(28) Ac45 is located in the ER and ERGIC and probably interacts with the c' subunit of the proteolipid ring in yeast and mouse osteoclasts.(39, 40) In frog melanotrope cells, overexpression resulted in lower pH in granules and subsequent cell-specific effects, possible due to increased secretion efficiency.(39, 41, 42) Knockdown of Ac45 in mouse osteoclasts resulted in increased pH, impaired lysosomal trafficking, and lysosomal exocytosis.(43)

Mass spectrometric analysis of serum transferrin derived from TMEM199, CCDC115, and ATP6AP1 deficient patients show abnormal N-glycosylation with loss of sialic acids and galactose from glycans. Additionally, isoelectric focusing of Apolipoprotein CIII demonstrated loss of sialic acids, indicative for abnormal O-glycosylation.

VMA21 is the human homolog of yeast Vma21p. VMA21 deficiency (MIM: 310440) is the cause of XMEA (Myopathy, X-linked, with Excessive Autophagy) a disorder dominated by a neuromuscular phenotype.

In yeast, Vma21p escorts the V0 complex out of the ER in COPII vesicles. After delivering the V0 domain to the Golgi, Vma21p dissociates and is retrieved to the ER by an ER retention motif, which is absent in mammalian VMA21.(44) Interestingly, Vma21p was implicated in abnormal lipid homeostasis.(45, 46) Human VMA21 locates to the ER-to-Golgi region and missense mutations lead to decreased formation of V0 complexes and increased numbers of autolysosomes, characteristic for the XMEA phenotype.(47)

Proposed cellular model of V-ATPase assembly factors

Based on the data mentioned above we propose a model where these four proteins aid in the assembly of the V-ATPase V0 domain in humans. CCDC115 and TMEM199 stabilize the a-subunit during assembly and VMA21 and cleaved

Ac45 stabilize the c-ring and guide the V0 domain (or the holocomplex with the V1 domain) to the Golgi. VMA21, and possibly CCDC115 and TMEM199 are then transported back via COPI vesicles (Figure 2).

Of note, only VMA21 has been proven to be a bonafide assembly factor in humans. The experimental evidence that assigns a role of TMEM199, CCDC115, and Ac45 as human V-ATPase assembly factors still needs to be generated. There are several lines of evidence that do support this hypothesis. First, these proteins are reciprocal best hits of their yeast homolog in BLAST searches. Second, TMEM199, CCDC115, and Ac45 (and additional V-ATPase associated proteins) are interacting partners established in high throughput protein-protein interaction studies in drosophila as well as in human. ((48) and in the Biogrid database (www.thebiogrid.org)). Third, all proteins share the ER-to-Golgi region as location and lastly, patients with defects in either TMEM199, CCDC115, and ATP6AP1 have a very similar phenotype in common.

Defects in V-ATPase assembly factors lead to abnormal glycosylation because they impact ER-to-Golgi protein trafficking. Indeed, V-ATPase assembly factors co-localize with COPI, COPII, and ERGIC markers indicating a function in early protein transport. In addition, serum from patients with a –V-ATPase assembly factors have a specific glycosylation pattern, indicative for abnormal Golgi protein trafficking.

Disturbed protein trafficking in the ER-to-Golgi region in NAFLD pathogenesis

Hepatic steatosis is common to all identified V-ATPase assembly factor deficiencies. Lipid droplets (LDs) are the main cellular storage compartment of TGs and play an important role in steatogenesis.(49, 50) Their role as a dynamic organelle has been established by identification of multiple LD associated proteins (LDAPs), present on the LD surface.(51-53) For a comprehensive review on lipid droplets we refer the reader elsewhere.(53) Because of the emerging role of COPI complex in hepatic lipid metabolism and the colocalization of CCDC115 and TMEM199 (and possibly ATP6AP1) in COPI vesicles we focus on the effect of COPI on LDAPs trafficking and the Sterol Regulatory Element-Binding Proteins (SREBPs) pathway. Additionally, VLDL transport from the ER to the Golgi occurs through COPII vesicles and is also dependent on accurate ER-to-Golgi trafficking.

Here, we provide an update on COPI and COPII vesicles regarding steatogenesis and hypothesize that defects in *CCDC115*, *TMEM199*, and *ATP6AP1* result in altered functioning of these vesicles resulting in the steatotic phenotype.

The COPI Complex and SREBPs

The COPI complex mediates retrograde protein transport within Golgi stacks and between *cis*-Golgi and ER.(54) Recently the structure of the COPI vesicle was determined with a resolution of 13 Å revealing a tight network of eight subunits recruited *en bloc* to form nascent vesicles.(55) These subunits are built on small GTPase Arf1 which is an activator of COPI assembly.

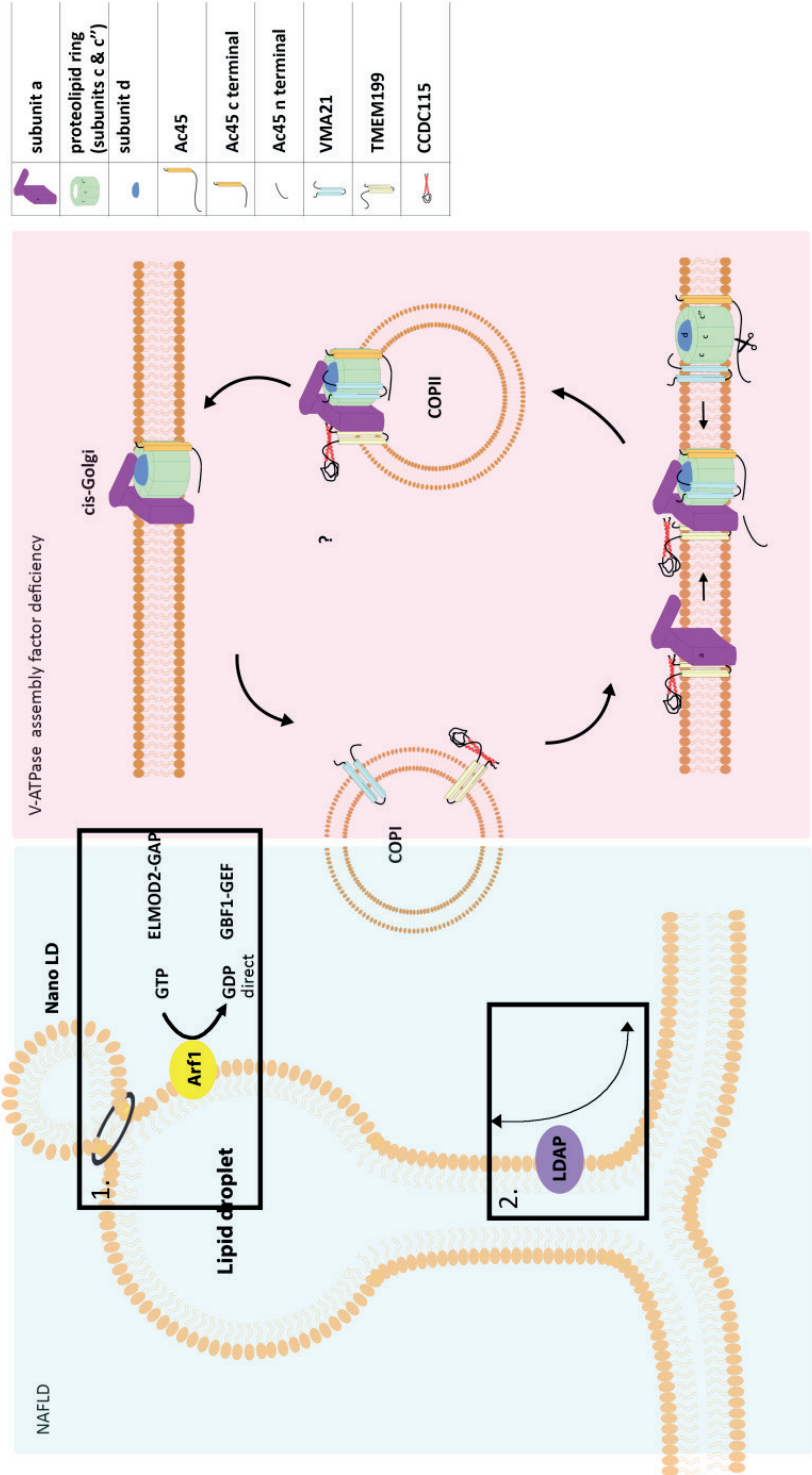
The COPI complex is involved in the Sterol Regulatory Element-Binding Proteins (SREBPs) pathway, the main transcriptional regulator for hepatic lipogenesis (SREBP1) and for cholesterol metabolism (SREBP2).(56) SREBPs reside in the ER membrane as inactive precursors. Upon sterol-deficient conditions SREBPs translocate to the Golgi via SCAP, an escorting protein, and COPII vesicles. In the Golgi, specific proteases cleave SREBP to release a transcription factor domain which is translocated to the nucleus for lipogenic transcription. Recent data show that even under sterol rich conditions a fraction of the SCAP-SREBP complex escapes the ER and that COPI retrograde transport is needed for retrieval.(57) Inhibition of COPI complexes by siRNAs results in an increased activity of SREBPs and increased TG contents.(57) We hypothesize that retrograde COPI transport is affected by V-ATPase assembly factor deficiency resulting in increased activity of SREBPs, similar to COPI knockdown. Interestingly, loss-of-function mutations in *COPA* have recently been associated with a phenotype of autoimmune interstitial lung, joint, and kidney disease (MIM 616414) but steatosis has not been described.(58)

Presence of the COPI complex, Arf1, GBF1, and ELMOD2 on the LD surface has been confirmed by proteomics and co-localization studies.(51, 52, 59-61) GBF1 activates and ELMOD2 deactivates Arf1.(61, 62) Interestingly, GBF1 has been described to interact with LDAP ATGL, but data are not consistent.(63)(64) Knockdown of COPI, Arf1, or GBF1 by siRNA results in increased cellular triglycerides levels and absent levels of LDAPs ATGL and Perilipin 2 on the LD surface.(59, 63-65) In line with these findings, knockdown of ELMOD2 results in increased LD-surface ATGL and decreased TG levels.(61)

COPI can function on a phospholipid monolayer and buds of 60 nm nanoLDs. (66) These data suggest a non-canonical role for the GBF1-Arf1-COPI complex on the LD surface: by budding off of nano-lipid particles from the LD surface, this complex lowers surface tension and thereby supplies energy for membrane-bridge formation and subsequent translocation of LDAPs GPAT4, DGAT2, and *brummer* (fly homolog of ATGL) from the ER to LD (Figure 2). (60, 67) Absence of ATGL on LDs results in decreased lipolysis. (59) Again, dysfunction of COPI vesicles due to TMEM199 or CCDC115 deficiency can have a similar effect as knockdown of COPI and thus result in hepatic steatosis. Further research will be needed to see if this is a direct effect of TMEM199, CCDC115, and ATP6AP1 on COPI functioning, COPI vesicle trafficking or if this is an effect of attenuated non-canonical V-ATPase functioning.

VLDL transport through COPII vesicles

Very low-density lipoproteins (VLDLs) are synthesized in hepatocytes and responsible for export of TGs to other parts of the body. VLDL synthesis is dependent on the availability of TGs and microsomal triglyceride transfer protein (MTP). The importance of MTP in VLDL synthesis is highlighted by the development of hepatic steatosis in abetalipoproteinemia (MIM: 200100) patients due to a genetic defect in *MTP*. (68) LDAPs also play an important role as they transfer the triacylglycerols from the LD to the ER. (50) After correct assembly, VLDL particles are exported to the Golgi in a COPII-dependent manner. However, this is mediated by alternative COPII vesicles compared to routinely processed proteins. (69) Mutations in *Sar1b*, an assembly factor of COPII vesicles, result in chylomicron retention disease (MIM: 246700) with intracellular accumulation of chylomicrons. (70) There is limited data on events after fusion with Golgi membrane. For example, the issue regarding Golgi-located lipidation of VLDL particles has not been resolved yet. (71) Transport from the *trans*-Golgi network to the plasma membrane occurs via specialized vesicles. (72) However, comparable to intra-Golgi processing, this part of the secretory pathway has not been investigated to a level that allows to demonstrate the effects of disturbances in Golgi homeostasis. It is possible that defects in V-ATPase assembly factors impair COPII trafficking of VLDL particles resulting in hepatic steatosis. An alternative explanation is that intra Golgi trafficking of the lipidation machinery is impaired by defective Golgi trafficking resulting in diminished VLDL secretion and thus hepatic steatosis. More research is needed to elucidate this issue.



◀**Figure 2. COPI vesicles in NAFLD pathogenesis and V-ATPase assembly factors** The left pane depicts current model of COPI and hepatic lipid processing. 1. COPI is involved in budding of nano lipid droplets (LD). Arf1 acts as an initiator of COPI assembly and is activated by GBF1-GEF via replacement of GDP by GTP and deactivated by ELMOD2-GAP. As a result of nano-LD formation lipid droplet surface tension is lowered resulting in 2. The formation of membrane bridges and relocation of LD associated proteins to the LD for lipolysis. The right pane shows the VO domain of the V-ATPase is assembled in the ER membrane. TMEM199 and CCDC115 stabilize subunit a. Ac45 and VMA21 stabilize the proteolipid ring. These four V-ATPase assembly factors then transport the VO domain to the cis-Golgi via COPII vesicles. Retrograde transport of VMA21 (and possibly TMEM199 and CCDC115) is mediated by COPI coated vesicles. Our model is that V-ATPase assembly factor deficiencies result in defective retrograde Golgi transport by inhibiting COPI or COPII function or by affecting one of its regulators Arf1, GBF1, or ELMOD2. When COPI function is hampered nano-LD formation is not initiated ultimately resulting in decreased lipolysis and increased hepatic cellular triglycerides levels.

Conclusion

The V-ATPase assembly factor deficiencies are a new group of inborn errors of metabolism that have to be considered in the differential diagnosis of secondary NAFLD. The hepatic phenotype ranges from mild impairment to end-stage liver disease necessitating liver transplantation. We propose a multifaceted etiology based on abnormal Golgi apparatus homeostasis. This can lead to defective COPI and COPII vesicle-mediated protein and lipid trafficking in combination with abnormal glycosylation. Screening can easily be done via glycoanalytical techniques. Better awareness of these genetic defects will improve patient outcome and provide new insights in the etiology of NAFLD.

Author's contributions

JCJ, DW drafted the manuscript, tables and figures, MvS reviewed the manuscript, VR, JPHD and DL designed and reviewed the manuscript. MvS received funding from the Netherlands Organisation for Scientific Research (VENI grant 016168079). VR serves as a Scientific Advisor of Phenex Pharmaceuticals AG, Galmed Pharmaceuticals Ltd., Genfit SA and Tobira Therapeutics, Inc. JPHD has served on advisory boards of AbbVie, Gilead, Intercept. His Department receives research funding from Falk, Abbvie, Ipsen, and Novartis. All reimbursements go to the Radboudumc.

References

1. Ratziu V, Bellentani S, Cortez-Pinto H, Day C, Marchesini G. A position statement on NAFLD/NASH based on the EASL 2009 special conference. *Journal of hepatology*. 2010;53(2):372-84.
2. European Association for the Study of the L, European Association for the Study of D, European Association for the Study of O. EASL-EASD-EASO Clinical Practice Guidelines for the management of non-alcoholic fatty liver disease. *Journal of hepatology*. 2016;64(6):1388-402.
3. Bernstein DL, Hulkova H, Bialer MG, Desnick RJ. Cholesteryl ester storage disease: review of the findings in 135 reported patients with an underdiagnosed disease. *Journal of hepatology*. 2013;58(6):1230-43.
4. Roberts EA, Schilsky ML, American Association for Study of Liver D. Diagnosis and treatment of Wilson disease: an update. *Hepatology*. 2008;47(6):2089-111.
5. Lee J, Hegele RA. Abetalipoproteinemia and homozygous hypobetalipoproteinemia: a framework for diagnosis and management. *Journal of inherited metabolic disease*. 2014;37(3):333-9.
6. Schumacher JD, Guo GL. Mechanistic review of drug-induced steatohepatitis. *Toxicology and applied pharmacology*. 2015;289(1):40-7.
7. Al-Shahwani NH, Sigalet DL. Pathophysiology, prevention, treatment, and outcomes of intestinal failure-associated liver disease. *Pediatric surgery international*. 2017;33(4):405-11.
8. Bruno S, Maisonneuve P, Castellana P, Rotmensz N, Rossi S, Maggioni M, et al. Incidence and risk factors for non-alcoholic steatohepatitis: prospective study of 5408 women enrolled in Italian tamoxifen chemoprevention trial. *Bmj*. 2005;330(7497):932.
9. Adinolfi LE, Rinaldi L, Guerrera B, Restivo L, Marrone A, Giordano M, et al. NAFLD and NASH in HCV Infection: Prevalence and Significance in Hepatic and Extrahepatic Manifestations. *International journal of molecular sciences*. 2016;17(6).
10. Dash A, Figler RA, Sanyal AJ, Wamhoff BR. Drug-induced steatohepatitis. *Expert opinion on drug metabolism & toxicology*. 2017;13(2):193-204.
11. Ohtsubo K, Marth JD. Glycosylation in cellular mechanisms of health and disease. *Cell*. 2006;126(5):855-67.
12. Dalziel M, Crispin M, Scanlan CN, Zitzmann N, Dwek RA. Emerging principles for the therapeutic exploitation of glycosylation. *Science*. 2014;343(6166):1235681.
13. Hart GW, Copeland RJ. Glycomics hits the big time. *Cell*. 2010;143(5):672-6.
14. Freeze HH, Chong JX, Bamshad MJ, Ng BG. Solving glycosylation disorders: fundamental approaches reveal complicated pathways. *American journal of human genetics*. 2014;94(2):161-75.
15. Foulquier F, Amyere M, Jaeken J, Zeevaert R, Schollen E, Race V, et al. TMEM165 deficiency causes a congenital disorder of glycosylation. *American journal of human genetics*. 2012;91(1):15-26.
16. Kornak U, Reynders E, Dimopoulou A, van Reeuwijk J, Fischer B, Rajab A, et al. Impaired glycosylation and cutis laxa caused by mutations in the vesicular H⁺-ATPase subunit ATP6V0A2. *Nature genetics*. 2008;40(1):32-4.
17. Miller VJ, Ungar D. Re'COG'nition at the Golgi. *Traffic*. 2012;13(7):891-7.
18. van Scherpenzeel M, Steenbergen G, Morava E, Wevers RA, Lefeber DJ. High-resolution mass spectrometry glycoprofiling of intact transferrin for diagnosis and subtype identification in the congenital disorders of glycosylation. *Translational research : the journal of laboratory and clinical medicine*. 2015;166(6):639-49 e1.

19. Callewaert N, Van Vlierberghe H, Van Hecke A, Laroy W, Delanghe J, Contreras R. Noninvasive diagnosis of liver cirrhosis using DNA sequencer-based total serum protein glycomics. *Nature medicine*. 2004;10(4):429-34.
20. Blomme B, Van Steenkiste C, Callewaert N, Van Vlierberghe H. Alteration of protein glycosylation in liver diseases. *Journal of hepatology*. 2009;50(3):592-603.
21. Sethi MK, Fanayan S. Mass Spectrometry-Based N-Glycomics of Colorectal Cancer. *International journal of molecular sciences*. 2015;16(12):29278-304.
22. Theodoratou E, Campbell H, Ventham NT, Kolarich D, Pucic-Bakovic M, Zoldos V, et al. The role of glycosylation in IBD. *Nature reviews Gastroenterology & hepatology*. 2014;11(10):588-600.
23. Janssen MJ, Waanders E, Woudenberg J, Lefeber DJ, Drenth JP. Congenital disorders of glycosylation in hepatology: the example of polycystic liver disease. *Journal of hepatology*. 2010;52(3):432-40.
24. Van Scherpenzeel M, Timal S, Ryman D, Hoischen A, Wuhler M, Hipgrave-Ederveen A, et al. Diagnostic serum glycosylation profile in patients with intellectual disability as a result of MAN1B1 deficiency. *Brain : a journal of neurology*. 2014;137(Pt 4):1030-8.
25. Tegtmeyer LC, Rust S, van Scherpenzeel M, Ng BG, Losfeld ME, Timal S, et al. Multiple phenotypes in phosphoglucomutase 1 deficiency. *The New England journal of medicine*. 2014;370(6):533-42.
26. Timal S, Hoischen A, Lehle L, Adamowicz M, Huijben K, Sykut-Cegielska J, et al. Gene identification in the congenital disorders of glycosylation type I by whole-exome sequencing. *Human molecular genetics*. 2012;21(19):4151-61.
27. Jansen JC, Timal S, van Scherpenzeel M, Michelakakis H, Vicogne D, Ashikov A, et al. TMEM199 Deficiency Is a Disorder of Golgi Homeostasis Characterized by Elevated Aminotransferases, Alkaline Phosphatase, and Cholesterol and Abnormal Glycosylation. *American journal of human genetics*. 2016;98(2):322-30.
28. Jansen EJ, Timal S, Ryan M, Ashikov A, van Scherpenzeel M, Graham LA, et al. ATP6AP1 deficiency causes an immunodeficiency with hepatopathy, cognitive impairment and abnormal protein glycosylation. *Nature communications*. 2016;7:11600.
29. Jansen JC, Cirak S, van Scherpenzeel M, Timal S, Reunert J, Rust S, et al. CCDC115 Deficiency Causes a Disorder of Golgi Homeostasis with Abnormal Protein Glycosylation. *American journal of human genetics*. 2016;98(2):310-21.
30. Calvo PL, Pagliardini S, Baldi M, Pucci A, Sturiale L, Garozzo D, et al. Long-standing mild hypertransaminasaemia caused by congenital disorder of glycosylation (CDG) type Iix. *Journal of inherited metabolic disease*. 2008;31 Suppl 2:S437-40.
31. Marshansky V, Rubinstein JL, Gruber G. Eukaryotic V-ATPase: novel structural findings and functional insights. *Biochimica et biophysica acta*. 2014;1837(6):857-79.
32. Cotter K, Stransky L, McGuire C, Forgac M. Recent Insights into the Structure, Regulation, and Function of the V-ATPases. *Trends in biochemical sciences*. 2015;40(10):611-22.
33. Korfali N, Wilkie GS, Swanson SK, Srsen V, Batrakou DG, Fairley EA, et al. The leukocyte nuclear envelope proteome varies with cell activation and contains novel transmembrane proteins that affect genome architecture. *Molecular & cellular proteomics : MCP*. 2010;9(12):2571-85.
34. Pellicano F, Inglis-Broadgate SL, Pante G, Ansorge W, Iwata T. Expression of coiled-coil protein 1, a novel gene downstream of FGF2, in the developing brain. *Gene expression patterns : GEP*. 2006;6(3):285-93.
35. Graham LA, Hill KJ, Stevens TH. Assembly of the yeast vacuolar H⁺-ATPase occurs in the endoplasmic reticulum and requires a Vma12p/Vma22p assembly complex. *The Journal of cell biology*. 1998;142(1):39-49.

36. Louagie E, Taylor NA, Flamez D, Roebroek AJ, Bright NA, Meulemans S, et al. Role of furin in granular acidification in the endocrine pancreas: identification of the V-ATPase subunit Ac45 as a candidate substrate. *Proceedings of the National Academy of Sciences of the United States of America*. 2008;105(34):12319-24.
37. Jansen EJ, van Bakel NH, Olde Loohuis NF, Hafmans TG, Arentsen T, Coenen AJ, et al. Identification of domains within the V-ATPase accessory subunit Ac45 involved in V-ATPase transport and Ca²⁺-dependent exocytosis. *The Journal of biological chemistry*. 2012;287(33):27537-46.
38. Schoonderwoert VT, Jansen EJ, Martens GJ. The fate of newly synthesized V-ATPase accessory subunit Ac45 in the secretory pathway. *European journal of biochemistry / FEBS*. 2002;269(7):1844-53.
39. Feng H, Cheng T, Pavlos NJ, Yip KH, Carrello A, Seeber R, et al. Cytoplasmic terminus of vacuolar type proton pump accessory subunit Ac45 is required for proper interaction with V(0) domain subunits and efficient osteoclastic bone resorption. *The Journal of biological chemistry*. 2008;283(19):13194-204.
40. Ryan M, Graham LA, Stevens TH. Voa1p functions in V-ATPase assembly in the yeast endoplasmic reticulum. *Molecular biology of the cell*. 2008;19(12):5131-42.
41. Jansen EJ, Hafmans TG, Martens GJ. V-ATPase-mediated granular acidification is regulated by the V-ATPase accessory subunit Ac45 in POMC-producing cells. *Molecular biology of the cell*. 2010;21(19):3330-9.
42. Jansen EJ, Scheenen WJ, Hafmans TG, Martens GJ. Accessory subunit Ac45 controls the V-ATPase in the regulated secretory pathway. *Biochimica et biophysica acta*. 2008;1783(12):2301-10.
43. Yang DQ, Feng S, Chen W, Zhao H, Paulson C, Li YP. V-ATPase subunit ATP6AP1 (Ac45) regulates osteoclast differentiation, extracellular acidification, lysosomal trafficking, and protease exocytosis in osteoclast-mediated bone resorption. *Journal of bone and mineral research : the official journal of the American Society for Bone and Mineral Research*. 2012;27(8):1695-707.
44. Malkus P, Graham LA, Stevens TH, Schekman R. Role of Vma21p in assembly and transport of the yeast vacuolar ATPase. *Molecular biology of the cell*. 2004;15(11):5075-91.
45. Fei W, Alfaro G, Muthusamy BP, Klaassen Z, Graham TR, Yang H, et al. Genome-wide analysis of sterol-lipid storage and trafficking in *Saccharomyces cerevisiae*. *Eukaryotic cell*. 2008;7(2):401-14.
46. Fei W, Shui G, Gaeta B, Du X, Kuerschner L, Li P, et al. Fld1p, a functional homologue of human seipin, regulates the size of lipid droplets in yeast. *The Journal of cell biology*. 2008;180(3):473-82.
47. Ramachandran N, Munteanu I, Wang P, Ruggieri A, Rilstone JJ, Israelian N, et al. VMA21 deficiency prevents vacuolar ATPase assembly and causes autophagic vacuolar myopathy. *Acta neuropathologica*. 2013;125(3):439-57.
48. Guruharsha KG, Rual JF, Zhai B, Mintseris J, Vaidya P, Vaidya N, et al. A protein complex network of *Drosophila melanogaster*. *Cell*. 2011;147(3):690-703.
49. Okumura T. Role of lipid droplet proteins in liver steatosis. *Journal of physiology and biochemistry*. 2011;67(4):629-36.
50. Goh VJ, Silver DL. The lipid droplet as a potential therapeutic target in NAFLD. *Seminars in liver disease*. 2013;33(4):312-20.
51. Bartz R, Zehmer JK, Zhu M, Chen Y, Serrero G, Zhao Y, et al. Dynamic activity of lipid droplets: protein phosphorylation and GTP-mediated protein translocation. *Journal of proteome research*. 2007;6(8):3256-65.
52. Guo Y, Walther TC, Rao M, Stuurman N, Goshima G, Terayama K, et al. Functional genomic screen reveals genes involved in lipid-droplet formation and utilization. *Nature*. 2008;453(7195):657-61.
53. Thiam AR, Farese RV, Jr., Walther TC. The biophysics and cell biology of lipid droplets. *Nature*

- reviews *Molecular cell biology*. 2013;14(12):775-86.
54. Brandizzi F, Barlowe C. Organization of the ER-Golgi interface for membrane traffic control. *Nature reviews Molecular cell biology*. 2013;14(6):382-92.
 55. Dodonova SO, Diestelkoetter-Bachert P, von Appen A, Hagen WJ, Beck R, Beck M, et al. VESICULAR TRANSPORT. A structure of the COPI coat and the role of coat proteins in membrane vesicle assembly. *Science*. 2015;349(6244):195-8.
 56. Xu X, So JS, Park JG, Lee AH. Transcriptional control of hepatic lipid metabolism by SREBP and ChREBP. *Seminars in liver disease*. 2013;33(4):301-11.
 57. Takashima K, Saitoh A, Funabashi T, Hirose S, Yagi C, Nozaki S, et al. COPI-mediated retrieval of SCAP is crucial for regulating lipogenesis under basal and sterol-deficient conditions. *Journal of cell science*. 2015;128(15):2805-15.
 58. Watkin LB, Jessen B, Wiszniewski W, Vece TJ, Jan M, Sha Y, et al. COPA mutations impair ER-Golgi transport and cause hereditary autoimmune-mediated lung disease and arthritis. *Nature genetics*. 2015;47(6):654-60.
 59. Beller M, Sztalryd C, Southall N, Bell M, Jackle H, Auld DS, et al. COPI complex is a regulator of lipid homeostasis. *PLoS biology*. 2008;6(11):e292.
 60. Wilfling F, Thiam AR, Olarte MJ, Wang J, Beck R, Gould TJ, et al. Arf1/COPI machinery acts directly on lipid droplets and enables their connection to the ER for protein targeting. *eLife*. 2014;3:e01607.
 61. Suzuki M, Murakami T, Cheng J, Kano H, Fukata M, Fujimoto T. ELMOD2 is anchored to lipid droplets by palmitoylation and regulates adipocyte triglyceride lipase recruitment. *Molecular biology of the cell*. 2015;26(12):2333-42.
 62. Wright J, Kahn RA, Sztul E. Regulating the large Sec7 ARF guanine nucleotide exchange factors: the when, where and how of activation. *Cellular and molecular life sciences : CMLS*. 2014;71(18):3419-38.
 63. Ellong EN, Soni KG, Bui QT, Sougrat R, Golinelli-Cohen MP, Jackson CL. Interaction between the triglyceride lipase ATGL and the Arf1 activator GBF1. *PLoS one*. 2011;6(7):e21889.
 64. Takashima K, Saitoh A, Hirose S, Nakai W, Kondo Y, Takasu Y, et al. GBF1-Arf-COPI-ArfGAP-mediated Golgi-to-ER transport involved in regulation of lipid homeostasis. *Cell structure and function*. 2011;36(2):223-35.
 65. Soni KG, Mardones GA, Sougrat R, Smirnova E, Jackson CL, Bonifacino JS. Coatomer-dependent protein delivery to lipid droplets. *Journal of cell science*. 2009;122(Pt 11):1834-41.
 66. Thiam AR, Antony B, Wang J, Delacotte J, Wilfling F, Walther TC, et al. COPI buds 60-nm lipid droplets from reconstituted water-phospholipid-triacylglyceride interfaces, suggesting a tension clamp function. *Proceedings of the National Academy of Sciences of the United States of America*. 2013;110(33):13244-9.
 67. Wilfling F, Wang H, Haas JT, Krahmer N, Gould TJ, Uchida A, et al. Triacylglycerol synthesis enzymes mediate lipid droplet growth by relocalizing from the ER to lipid droplets. *Developmental cell*. 2013;24(4):384-99.
 68. Wetterau JR, Aggerbeck LP, Bouma ME, Eisenberg C, Munck A, Hermier M, et al. Absence of microsomal triglyceride transfer protein in individuals with abetalipoproteinemia. *Science*. 1992;258(5084):999-1001.
 69. Siddiqi SA. VLDL exits from the endoplasmic reticulum in a specialized vesicle, the VLDL transport vesicle, in rat primary hepatocytes. *The Biochemical journal*. 2008;413(2):333-42.
 70. Levy E. Insights from human congenital disorders of intestinal lipid metabolism. *Journal of lipid research*. 2015;56(5):945-62.

71. Tiwari S, Siddiqi SA. Intracellular trafficking and secretion of VLDL. *Arteriosclerosis, thrombosis, and vascular biology*. 2012;32(5):1079-86.
72. Hossain T, Riad A, Siddiqi S, Parthasarathy S, Siddiqi SA. Mature VLDL triggers the biogenesis of a distinct vesicle from the trans-Golgi network for its export to the plasma membrane. *The Biochemical journal*. 2014;459(1):47-58.

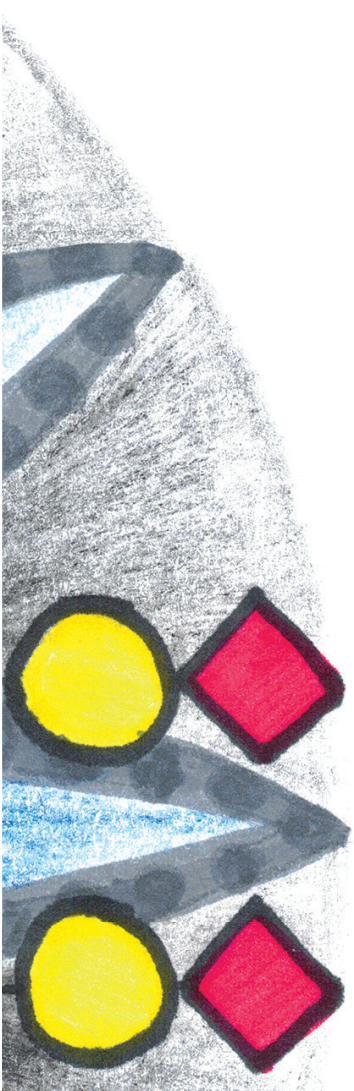


CHAPTER 5

Screening for abnormal glycosylation in a cohort of adult liver disease patients

Jos C. Jansen, Bart van Hoek, Herold J. Metselaar, Aad P. van den Berg, Fokje Zijlstra, Karin Huijben, Monique van Scherpenzeel, Joost P.H. Drenth, Dirk J. Lefeber

J Inherit Metab Dis. 2020 Jun 18. doi: 10.1002/jimd.12273. Online ahead of print



Abstract

Congenital Disorders of Glycosylation (CDG) are a rapidly expanding group of rare genetic defects in glycosylation. In a novel CDG subgroup of Vacuolar-ATPase assembly defects various degrees of hepatic injury have been described, including end stage liver disease. However, the CDG diagnostic workflow can be complex as liver disease per se may be associated with abnormal glycosylation. Therefore, we collected serum samples of patients with a wide range of liver pathology to study the performance and yield of two CDG screening methods. Our aim was to identify glycosylation patterns that could help to differentiate between primary and secondary glycosylation defects in liver disease.

To this end, we analyzed serum samples of 1042 adult liver disease patients. This cohort consisted of 567 liver transplant candidates and 475 chronic liver disease patients. Our workflow consisted of screening for abnormal glycosylation by transferrin isoelectric focusing (tIEF), followed by in-depth analysis of the abnormal samples with quadruple time-of-flight mass spectrometry (QTOF-MS).

Screening with tIEF resulted in identification of 247 (26%) abnormal samples. QTOF-MS analysis of 110 of those did not reveal glycosylation abnormalities comparable with those seen in V-ATPase assembly factor deficiencies. However, two patients presented with isolated sialylation deficiency. Fucosylation was significantly increased in liver transplant candidates compared to healthy controls and patients with chronic liver disease.

In conclusion, a significant percentage of patients with liver disease presented with abnormal CDG screening results, however, not indicative for a V-ATPase assembly factor defect. Advanced glycoanalytical techniques assist in the dissection of secondary and primary glycosylation defects.

Keywords N-glycosylation, hyperfucosylation, end-stage liver disease, V-ATPase assembly factor deficiencies, Congenital Disorders of Glycosylation

Take home message

Secondary glycosylation defects are common in liver disease and advanced glycoanalytics are needed to differentiate these from primary glycosylation defects such as the V-ATPase assembly factor deficiencies.

Introduction

Congenital Disorders of glycosylation (CDG) are a group of inborn errors of metabolism characterized by abnormal glycosylation. Most CDG share a multisystem phenotype with dysmorphic features, failure to thrive and neurological symptoms.(1) Involvement of the liver is frequent in CDG but usually not the dominant feature. (2)

In recent years, a novel subgroup of CDG patients has emerged that presents predominantly with a hepatic phenotype. (3-7) Pathological variants in this group are in genes that code for assembly factors of the vacuolar -ATPase (V-ATPase), the proton pump for intracellular acidification. The glycosylation pattern resembles a type 2 CDG with loss of sialic acid and galactose. The hepatic clinical spectrum ranges from mildly elevated serum transaminases and steatosis, resembling non-alcoholic fatty liver disease, to cirrhosis and end-stage liver disease warranting liver transplantation (LTx).

Liver cirrhosis develops as a response to chronic liver injury. The central pathological event in cirrhosis is deposition of extracellular matrix increasing hepatic flow resistance with ensuing hepatocyte dysfunction.(8) Patients with cirrhosis have a high risk of decompensation of their liver disease. It can develop in end-stage liver disease (ESLD), necessitating (LTx)

Abnormal glycosylation is a known phenomenon in chronic liver disease and can be used to discriminate between different fibrosis stages and cirrhosis and provides an interesting and non-invasive alternative for liver biopsy.(9). Abnormal glycan structures of liver-derived proteins such as transferrin (TF) and haptoglobin have been described in alcoholic liver disease, non-alcoholic steatohepatitis and primary sclerosing cholangitis.(10-12) These abnormalities include hyperfucosylation due to increased fucosyltransferase activity and hyposialylation as a result of lower sialyltransferase activity.

Traditionally, new CDG patients are identified through isoelectric focusing of TF (tIEF).(13) TF possesses two biantennary glycans at amino acids Asn432 and Asn630, both negatively charged because of the terminal sialic acids.(14) tIEF uses loss of these sialic acids to separate the various isoforms. A disadvantage of tIEF is that it only provides information on desialylation and not for example on hypogalactosylation and fucosylation. The use of quadruple time-of-flight mass-spectrometry (QTOF-MS) may overcome this disadvantage by providing in-depth high-resolution information on the glycans attached to TF.(15)

The primary aim of this study was to identify glycosylation patterns that could help to differentiate between primary and secondary glycosylation defects in liver disease within a cohort of adult patients with end-stage liver disease. As a secondary aim, we studied to what extent liver disease affects CDG screening.

Materials and methods

Selection of liver disease patients, sample selection and ethical considerations

We collected 1042 samples from patients with an established chronic liver disease from four Dutch tertiary referral hospitals. (Figure 2) Samples were collected in the period 1993 to 2013. We specifically targeted ESLD patients who were evaluated and waitlisted for LTx. These samples were provided by Erasmus MC in Rotterdam (n= 264), LUMC in Leiden (n=142) and UMCG in Groningen (n=155). All samples were drawn and aliquoted preceding LTx.

Chronic liver disease samples (n=410), without ESLD, were provided by the Radboudumc in Nijmegen and by the LUMC (n=65, all with a diagnosis of auto-immune hepatitis). These patients were seen at the outpatient clinic for diagnosis and treatment of a range of liver diseases. Patients with viral hepatitis (infectious hepatitis B, C or E) were excluded from analysis as we hypothesized that the presence of underlying CDG would be unlikely in this patient population. Samples from healthy controls (n=40) were obtained from the local bloodbank. All samples were stored at -80°C till analysis.

Material was collected in agreement with the Dutch code of conduct for responsible use of human tissue (Dutch Federation of Biomedical Scientific Societies, www.federa.org). All experiments were performed in accordance with the guidelines and regulations of the Ethics Committee of the Radboudumc. Approval was documented in case file 2018-5012.

Study design and workflow

We first performed tIEF of the collected samples to identify global N-glycosylation defects with hyposialylation. Sixty-one samples were excluded prior to tIEF: 24 samples because they were drawn after liver transplantation, 21 were of very poor quality and unsuitable for further workup, 5 samples were wrongly allocated, 10 patients were <18 years of age at time of sampling and one sample was from a patient with an established diagnosis of CDG.

We defined abnormal TF sialylation as an increased percentage of hyposialylated TF isoforms compared with the main isoform, tetrasialoTF. Control ranges were used from the clinical diagnostic protocol, derived by tIEF of 59 healthy control samples: asialoTF 0-3.2%; monosialoTF 0-5.0%; disialoTF 3.3-7.6%; trisialoTF 4.9-10.6%; pentasialoTF 18.7-31.5%.

If applicable, we designated the profile type 1 or type 2 CDG based on international consensus. Type 1 CDG has increased asialo- and disialo TF isoforms, indicating loss of 1 or 2 glycans. Type 2 CDG has hyposialylation for all TF isoforms.(16)

Abnormal tIEF samples were selected for further work-up with QTOF-MS. Quality criteria for inclusion of the sample included an abundance of >50.000 amu of the intact TF glycoprotein (79556 amu). We selected peaks corresponding to a known TF isoform with an abundance of >1000. The relative abundance of these peaks was calculated based on their percentage relative to total abundance. Figure 1 shows a typical tIEF and QTOF-MS pattern and depicts the nomenclature of the glycosylation isoforms used throughout this manuscript.

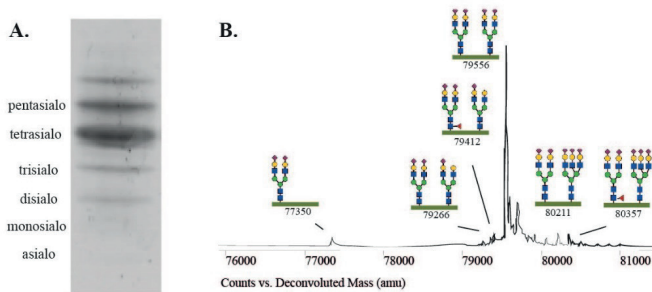


Figure 1. Overview of a normal tIEF and QTOF-MS profile. A. Typical tIEF pattern. The most abundant fraction correlates with the intact TF glycoprotein. B Typical QTOF-MS profile of intact TF with two attached glycans. Shown are the most commonly encountered glycans. The green horizontal bar corresponds with the amino acid backbone. The peak at 79556 amu correlates with the intact TF glycoprotein. The legend for the monosaccharides is: blue square: N-acetylglucosamine, red triangle: fucose, green circle: mannose, yellow circle: galactose, purple diamond: sialic acid.

Sample preparation for N-glycan analysis

Transferrin isoelectric focusing

All samples were analyzed with tIEF to determine abnormal sialylation of TF. tIEF was performed as described before. (14) Briefly, serum or plasma samples were incubated with iron and applied to a 5-7 pH gradient gel for electrophoresis. After completion, gels were incubated with 2.5 $\mu\text{l}/\text{cm}^2$ anti-TF antibody (Dako

#A0061, Carpinteria, CA USA) and visualized with Coomassie blue. Data analysis was performed with Image Quant Software (TotalLab, Newcastle upon Tyne, UK)

TF polymorphisms were recognized by doubled bands for all isoforms. For confirmation, neuraminidase treatment was applied on samples with ambiguous isoelectric patterns. (14)

Nano liquid chromatography-chip (C8)- quadruple time of flight mass spectrometry (QTOF-MS)

Mass spectrometry analysis was performed as described before.(15) First, beads were loaded with anti-TF antibody (Dako #A0061, Carpinteria, CA USA) and stored in 20% ethanol. Prior to usage, beads were washed 4 times with a Tris-HCl (pH 7) solution. Next, 100 µl of a 1:10 plasma sample dilution in 0.9% sodiumchloride was mixed with beads and incubated for 20 minutes under continuous shaking at 3000 rpm/min. Subsequently beads were washed four times with Tris-HCl (pH 7) solution. For elution, 1 µl of Tris-HCl pH 9 solution was added to the sample followed by 50 µl elution buffer (0.1M Glycine-HCl pH 2.7). After spinning and verification of neutral pH, 2µl sample was injected into the microfluidic 6540 HPLC-chip-QTOF instrument (Agilent Technologies, Santa Clara, CA, USA). For data analysis of QTOF-MS profiles Agilent Mass Hunter Qualitative Analysis software (v. B.04.00) was used.

Statistical analysis

For statistical analysis SPSS Statistics v. 22 (IBM Corporation, Armonk, NY, USA) was used. Due to non-linearity of our data we used the non-parametric Kruskal-Wallis test for comparisons of more than two groups and the Mann-Whitney U test when there were two groups. P-values were adjusted for multiple testing with the Bonferroni method.

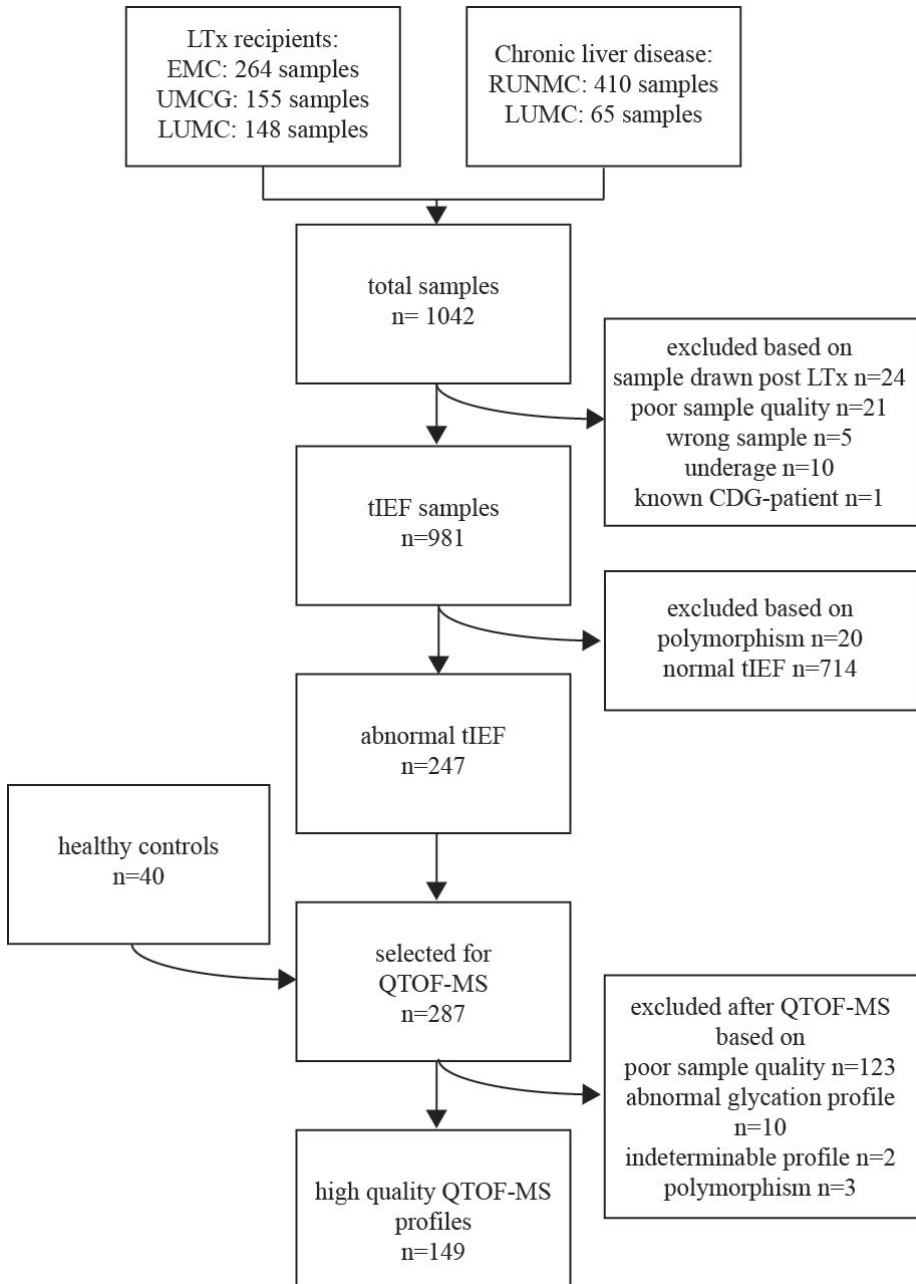


Figure 2. Flowchart of the study design.

Results

A total of 1042 samples were collected, 567 samples of LTx candidates and 475 samples of patients with CLD. Figure 2 shows a flowchart of the study design. We included 981 samples for further N-glycan analysis with tIEF. After tIEF, 744 samples including 20 samples with a confirmed polymorphism were excluded based on a normal profile

Subsequently, QTOF-MS was performed on 247 samples and 40 healthy controls. After QTOF-MS analysis, 125 samples were excluded because the main peak (at 79556 amu) was of insufficient abundance, 10 samples were excluded because of an abnormal glycation profile and 3 because of a TF polymorphism (of which 2 were not identified with tIEF and one was a healthy control). In total, 110 patient samples and 39 healthy control samples were of sufficient quality for interpretation of the glycosylation profile. Table 1 shows patient characteristics for the selected samples. Supplementary table 1 shows tIEF and QTOF-MS results for all samples with an abnormal tIEF profile.

tIEF screening of 961 samples of liver disease patients shows mild glycosylation abnormalities

Out of 961 samples we analyzed using tIEF, 247 samples (26%) had hyposialylation compared to our controls. Of these samples, 175 (70%) had a solitary increased percentage of the trisialoTF isoform, 42 (17%) had an elevated percentage of monosialoTF isoform and 4 (2%) had an elevated percentage of the disialoTF isoform. Mixed combinations of elevated isoforms occurred in 26 (11%) samples. (Figure 3a) None of the samples had increased percentages of all isoforms. One sample had slightly increased percentages of the asialo and the disialoTF isoform and did not reach the values to be suggestive for type 1 CDG. The mixed profiles can be compatible with a CDG type 2 profile, however, in most samples the increase in percentage is subtle (Figure 3b).

Table 1. Patient characteristics

	tIIEF selected samples (n=961)		QTOF-MS selected samples (n=149)		
	LTx (n=511)	CLD (n=450)	LTx (n=76)	CLD (n=34)	HC (n=39)
Mean age (years)	48.5 (SD 12.2)	50.0 (SD 15.5)	52.6 (SD 12.0)	51.8 (SD 13.2)	47.1 (SD 14.2)
Male sex	283 (55.4%)	211 (46.9%)	50 (65.8%)	15 (44.1%)	21 (53.8%)
Etiology					
Acute liver failure	38 (7.4%)	2 (0.4%)	1 (1.3%)	0	n.a.
Alcohol liver disease	121 (23.7%)	20 (4.4%)	35 (46.1%)	6 (17.6%)	n.a.
Auto-immune hepatitis	39 (7.6%)	152 (33.8%)	3 (3.9%)	15 (44.1%)	n.a.
Cholestatic liver disease	157 (30.7%)	42 (9.3%)	11 (14.5%)	0	n.a.
Cryptogenic cirrhosis	54 (10.6%)	20 (4.4%)	10 (13.2%)	1 (2.9%)	n.a.
Metabolic disease	26 (5.1%)	7 (1.6%)	7 (9.2%)	0	n.a.
NASH	10 (2.0%)	36 (8.0%)	0	3 (8.8%)	n.a.
Other	61 (11.9%)	36 (8.0%)	8 (10.5%)	2 (5.9%)	n.a.
Unknown	5 (1.0%)	5 (1.1%)	1 (1.3%)	0	n.a.
Gilbert	-	25 (5.6%)	0	2 (5.9%)	n.a.
Viral hepatitis	-	94 (20.9%)	0	5 (14.7%)	n.a.
DILI	-	11 (2.4%)	0	0	n.a.

LTx = Liver transplant recipient, CLD = Chronic liver disease, NASH = non-alcoholic steatohepatitis, DILI = drug induced liver injury. HC = healthy controls, SD= standard deviation, n.a. = not applicable

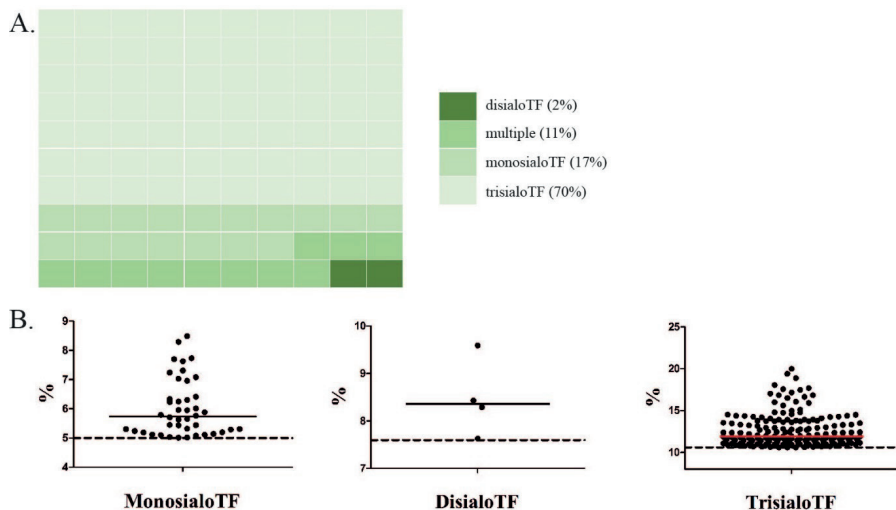


Figure 3. Abnormal tIEF result. A. Waffle chart that shows the distribution of the abnormal tIEF samples. B. Individual medians for the abnormal samples per TF isoform. The dotted line represents upper limit of normal based on internal standards.

QTOF-MS analysis of preselected liver disease patients did not identify profiles compatible with V-ATPase assembly factor defects.

Of the 110 high quality QTOF-MS profiles, none had a distinguishable type 1 CDG pattern. The peak associated with non-glycosylated TF (peak 75140) was only present in one LTx patient with progressive familial intrahepatic cholestasis syndrome (1.2% of total glycan abundance), one CLD patient with auto-immune hepatitis (1.1%) and three HC (all <1% total glycan abundance). Both patients had a normal percentage of asialoTF in tIEF screening and the six patients with an elevated asialoTF fraction with tIEF analysis did not have a detectable peak with mass 75140, corresponding to non-glycosylated transferrin. Peak 77350, which corresponds to loss of one glycan, was present in all but five samples and was not significantly different among the groups (data not shown). We did not identify samples that showed typical glycan structural abnormalities that are seen in type 2 CDG profiles and did not identify a pattern compatible with a V-ATPase assembly factor deficiency.

We identified two samples (2/110 = 1.8%) with clearly elevated trisialo TF isoform abundance. The first patient in the CLD group was a female, age 55 at sampling, who was seen at the outpatient clinic for hepatic steatosis. Her profile showed an elevated trisialo TF isoform of 15.0%, (median for the CLD group is 2.0%)

and presence of an additional isoform (mass 78976, corresponding with loss of 2 sialic acids). There were no signs of other glycosylation abnormalities. The second patient was a male liver transplant recipient diagnosed with alpha-1 anti-trypsin deficiency. At age of sampling he was 28 years old. His QTOF-MS profile showed an increase in the trisialo TF isoform of 12,4% (median for the LTx group is 1.9%) and also an increased loss of 2 sialic acids (mass 78976). For both patients, we could not detect transferrin glycoforms with missing galactose residues, as for example seen in the V-ATPase assembly defects.

tIEF but not QTOF-MS shows that loss of one sialic acid is more frequent and more severe in LTx candidates compared to CLD patients and HC

To see what the effect is of liver disease on desialylation we compared the tIEF screening results between LTx and CLD samples. Table 2 shows the medians for all isoforms. The prevalence of several isoforms was statistically significantly different between these groups, but medians were within the normal range. Only the LTx group had a median of the trisialo TF isoform above the upper limit of normal and significantly higher than in the chronic liver disease group (11.8% vs 10.4%, $p < 0.001$). An abnormal tIEF pattern was more frequently seen in LTx candidates compared to CLD patients (175/511=34% vs. 72/450=16%, Chi square p -value =0.000).

Table 2. medians of the different tIEF TF isoforms

	Abnormal samples (n=247)					
	CLD (n=72)		LTx (n=175)		MWU	
TF Isoform	Range (%)	Median (%)	SD	Median (%)	SD	p-value
Asialo	0.0-3.2	0.94	1.02	1.24	0.79	0.001
Mono	0.0-5.0	4.84	2.52	2.02	1.74	0.000
Di	3.3-7.6	5.25	1.21	5.27	1.39	0.588
Tri	4.9-10.6	10.40	3.07	11.84	2.25	<0.001
Tetra	47.3 - 62.7	52.63	6.71	52.67	5.72	0.476
Penta	18.7 - 31.5	20.78	3.94	19.95	3.44	0.038

TF=Transferrin, CLD=chronic liver disease, LTx=liver transplantation, MWU: Mann Whitney U test, SD=standard deviation

Next, we aimed to gain more insight in desialylation with QTOF-MS. QTOF-MS provides additional detail on glycan composition. To investigate desialylation we used the combined abundance of the trisialo and the fucosylated trisialo TF isoform. Comparison of these combined peaks among the three groups only showed a slight statistically significant difference between the LTx and CLD groups (Supp. Table 2). However, because of the broad standard deviations we conclude that overall desialylation is not different between LTx candidates, CLD patients and healthy controls. In conclusion, based on these data, desialylation is more prominent in LTx candidates when measured with tIEF, but this data is not reproduced with QTOF-MS.

Hyperfucosylation is more pronounced in end-stage liver disease than in chronic liver disease

Hyperfucosylation of liver derived proteins is a known phenomenon in a variety of liver diseases. Therefore, we calculated the fucosylation ratio for the trisialo and pentasialo TF isoforms. (Figure 4 and Supp. Table 2). Fucosylation of the tetrasialo TF isoform was not reliably detectable because of overlap with other nearby peaks. Figure 4 shows that the ratios are higher for the LTx samples compared to the HC and the CLD samples ($p < 0.0001$ for both). These data indicate that hyperfucosylation of TF is more pronounced in end-stage liver disease compared to chronic liver disease and healthy controls.

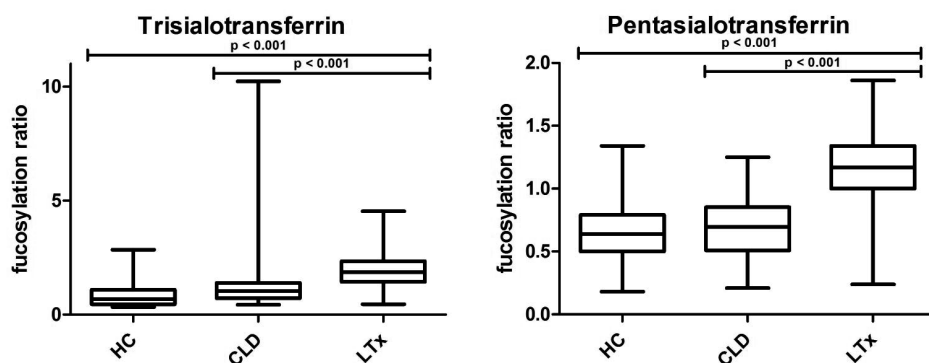


Figure 4. Boxplots of the fucosylation ratio of the tri- and pentasialo QTOF-MS isoforms. The left graph shows the fucosylation ratio of trisialotransferrin, or peak 79266. The right graph shows the fucosylation ratio of pentasialotransferrin, or peak 80211. We used a Kruskal-Wallis test for calculation of p-values. HC=healthy controls, CLD=chronic liver disease, LTx=liver transplantation

Discussion

In our retrospective analysis of a cohort of 1042 liver disease patients we found a significant percentage of patients with altered CDG screening results by serum transferrin isoelectric focusing. However, we did not find clear evidence for the presence of a CDG due to V-ATPase assembly factor defects. We found that hyperfucosylation is more pronounced in LTx patients compared to those with milder liver disease and healthy controls, thereby showing that high-resolution mass spectrometry aids the discrimination between secondary and primary glycosylation abnormalities in CDG screening.

Screening for possible primary glycosylation defects

Initial screening with tIEF resulted in identification of 247 (26%) , mostly mild, abnormal patterns. We did not identify a typical CDG type 1 pattern, which we anticipated, as to date there are no known type 1 CDG associated with a mild hepatic phenotype.(1) The majority of samples had an increase in the trisialo TF isoform. None had an increase of all isoforms, a feature of most type 2 CDG. However, based on these tIEF results we could not rule out a V-ATPase assembly factor deficiency as mild abnormalities have been described. QTOF-MS analysis did not confirm desialylation as seen in tIEF and did not show patterns compatible with type 1 CDG or V-ATPase assembly factor deficiencies. Similarly, no samples with loss of galactose were observed. Therefore, we conclude that our analysis did not identify novel patients with a V-ATPase assembly factor defect.

A possible reason for this might be that prevalence is too low for detection within our cohort. The exact prevalence of the whole group of CDG is unknown but is estimated at 0.1 – 0.5 / 100.000 in Europe. This number is based on recent data from the European CDG network that estimated that there is a total number of 2500 recognized CDG patients in Europe. (1) However, these observations are based on patients with a multisystem phenotype. The discovery of the V-ATPase-CDG subgroup with a very mild hepatic phenotype could indicate that the prevalence is much higher. We speculated that this subgroup would be enriched in a population that covers the full spectrum of liver disease severity, but no cases were detected.

Another reason might be that glycosylation defects of CDG patients who survive into adulthood can become milder, or even normalize, over time. (17-

19). Spontaneous normalization of the glycosylation profile has not yet been investigated for V-ATPase-CDG. However, spontaneous normalization of serum transaminases has been described with this condition. (4)

We identified two patients with an abnormally high percentage of the isoform with loss of one sialic acid. The reason for this abnormal pattern remains unknown. Glycosylation defects in SLC35A1-CDG (OMIM 603585), a defect in the CMP-sialic acid transporter, show pure desialylation effects (15, 20). However, the phenotype of SLC35A1-CDG is mostly neurological with dysmorphic features, not hepatic.

Also, the presence of bacterial sialidase in serum can lead to hyposialylation of TF. This has been described for *Streptococcus pneumoniae*- associated hemolytic ureum syndrome.(21). However, hemolytic uremic syndrome is primarily a disease of infancy and early childhood and the incidence in the adult population is extremely low.

Another option is that these patients have an as yet unrecognized type of CDG. Our study design did not allow us to further investigate this as we did not have access to fresh plasma, fibroblasts or parental DNA to perform adequate genetic analyses and functional studies.

Glycosylation defects in liver disease

Desialylation has been mostly studied in the context of alcoholic liver disease. Indeed, the Carbohydrate Deficient Transferrin (CDT) test to identify chronic alcohol intake is based on desialylation of transferrin. Analysis of CDT in abstaining patients with various degrees of liver disease shows a correlation of high CDT percentages with the Child-Pugh score.(22)

The pathophysiological mechanism behind alcohol-induced hypoglycosylation is not fully elucidated. Some studies suggest a primary ER defect (23, 24). Other studies suggest an effect on the Golgi apparatus.(25, 26). One study investigated gene expression of glycosylation genes in NASH but found mixed results with upregulation of *ST6GAL2* and downregulation of *ST6GAL1*.(11)

Hyperfucosylation of liver derived proteins has been most extensively studied in hepatocellular carcinoma patients. (27-30) Indeed, fucosylated alpha-fetoprotein is an established disease marker for HCC in the setting of cirrhosis.(31) Here we

show that fucosylation of transferrin is elevated in samples from LTx candidates compared to CLD patients and healthy controls.

Hyperfucosylation of transferrin was shown to be the cause of chromatographic abnormalities in CDT testing, or so-called “di-tri-bridging” (i.e. poor resolution of disialoTF from trisialoTF).(32) Di-tri-bridging is associated with liver disease and is more frequent in cirrhosis than in non-cirrhotics.(33)

Somewhat older data exists on fucosylation of haptoglobin in liver disease and shows hyperfucosylation in patients with alcoholic liver disease and primary biliary cholangitis.(34) A more recent paper showed increased hyperfucosylated glycans on haptoglobin in HCC as well as in cirrhosis. (35)

Previous work on serum glycan analysis in liver cirrhosis identified increased hypogalactosylation and increased modification of the serum N-glycome with a bisecting N-acetylglucosamine.(9) Log ratios of different glycans could with good sensitivity and specificity discriminate between early fibrosis and cirrhosis. A follow-up study showed that undergalactosylation was due to the IgG-derived glycan fraction.(36) This is in line with our data that did not show undergalactosylation in any sample. Also, no glycans were observed within our cohort with a bisecting N-acetylglucosamine. This might be explained by protein specific glycosylation.

Strengths and limitations

One strength of our study was that we included a wide range of liver disease patients for analysis. We took care to include patients with mild liver disease but also those with advanced chronic liver disease in need for LTx. Our efforts led to the establishment of a large sample size of over 1000 liver disease patients which adds to the robustness of the study. Additionally, we were able to screen these samples with high resolution mass spectrometry that provided in depth analysis of the intact transferrin glycoprotein, including fucosylation, loss of galactose and the absence of complete glycans.

A limitation of our study is because of its retrospective character. We had access to collected serum samples but were not in possession of fresh plasma or fibroblasts of patients to perform whole-exome sequencing, run a CDG-panel, or perform functional studies. We detected two patients with an increased trisialoTF isoform. Although the cause for this elevation is unknown, we believe

that the QTOF-MS analysis ruled out abnormal glycosylation due to a defect in V-ATPase-CDG. However, we cannot completely exclude another, possibly novel, CDG.

Another limitation of our study is the high percentage of exclusion of samples resulting from low abundance of serum TF in the samples. A possible explanation could be that low serum TF is associated with cirrhosis.(37, 38). Additionally, the effect of long term storage on stability of TF is unknown.

Recommendations

Differentiating primary from secondary glycosylation defects in patients with liver dysfunction can be challenging. Previously analysis of total plasma N-glycans suggested that hyperfucosylation was increased in a single liver disease patient but not in primary CDG.(39) This study expands these findings to a large patient group and thus transferrin hyperfucosylation pattern could guide clinicians in decision making.

Our current research exposes caveats in tIEF as a primary diagnostic step. We show that 26% of tiEF samples were abnormal, but these samples did not show a clear type 2 CDG pattern upon QTOF-MS analysis. An important message is that tIEF screening can be false positive because of liver dysfunction.

We suggest caution when interpreting tIEF result in patients with a suspected CDG and liver disease and recommend maintaining a low-threshold to use advanced glycoanalytic methods, preferably in an expertise center. A clear hyperfucosylated pattern is more suggestive for a secondary cause and loss of galactose more suggestive for a primary glycosylation defect. When only sialylation is decreased, we suggest a repeat sample to rule out the involvement of exogenous sialidase and a critical review of the phenotype to rule out a CDG with known hyposialylation.

Conclusion

Our screening study did not identify V-ATPase assembly factor defects in a cohort of severe liver disease, but we show that end-stage liver disease is associated with hyperfucosylation of transferrin. We confirm that regular CDG screening with tIEF can be complicated by liver disease, itself is associated with mildly abnormal tIEF profiles

Acknowledgments

This work was supported by the Dr. Karel-Lodewijk Verleysen Award (JD) and the Dutch Organization for Scientific Research (ZONMW) Medium Investment grant 40-00506-98-9001 (DL)

Conflict of Interest

All authors state no conflict of interest.

Author contributions

JJ, MvS, JD and DL design the study. JJ, FZ and KH performed the experiments. BvH, HM, AvdB and JD provided samples and collected data. JJ, JD and DL wrote the manuscript. All authors critically reviewed the manuscript.

References

1. Peanne R, de Lonlay P, Foulquier F, Kornak U, Lefeber DJ, Morava E, et al. Congenital Disorders of glycosylation (CDG): Quo vadis? *European journal of medical genetics*. 2018;61(11):643-63.
2. Marques-da-Silva D, Dos Reis Ferreira V, Monticelli M, Janeiro P, Videira PA, Witters P, et al. Liver involvement in congenital disorders of glycosylation (CDG). A systematic review of the literature. *Journal of inherited metabolic disease*. 2017;40(2):195-207.
3. Jansen JC, Cirak S, van Scherpenzeel M, Timal S, Reunert J, Rust S, et al. CCDC115 Deficiency Causes a Disorder of Golgi Homeostasis with Abnormal Protein Glycosylation. *American journal of human genetics*. 2016;98(2):310-21.
4. Jansen JC, Timal S, van Scherpenzeel M, Michelakakis H, Vicogne D, Ashikov A, et al. TMEM199 Deficiency Is a Disorder of Golgi Homeostasis Characterized by Elevated Aminotransferases, Alkaline Phosphatase, and Cholesterol and Abnormal Glycosylation. *American journal of human genetics*. 2016;98(2):322-30.
5. Jansen EJ, Timal S, Ryan M, Ashikov A, van Scherpenzeel M, Graham LA, et al. ATP6AP1 deficiency causes an immunodeficiency with hepatopathy, cognitive impairment and abnormal protein glycosylation. *Nature communications*. 2016;7:11600.
6. Rujano MA, Cannata Serio M, Panasyuk G, Peanne R, Reunert J, Rymen D, et al. Mutations in the X-linked ATP6AP2 cause a glycosylation disorder with autophagic defects. *The Journal of experimental medicine*. 2017;214(12):3707-29.
7. Cannata Serio M, Graham LA, Ashikov A, Larsen LE, Raymond K, Timal S, et al. sMutations in the V-ATPase assembly factor VMA21 cause a congenital disorder of glycosylation with autophagic liver disease. *Hepatology*. 2020.
8. Tsochatzis EA, Bosch J, Burroughs AK. Liver cirrhosis. *Lancet*. 2014;383(9930):1749-61.
9. Callewaert N, Van Vlierberghe H, Van Hecke A, Laroy W, Delanghe J, Contreras R. Noninvasive diagnosis of liver cirrhosis using DNA sequencer-based total serum protein glycomics. *Nature medicine*. 2004;10(4):429-34.
10. Blomme B, Van Steenkiste C, Callewaert N, Van Vlierberghe H. Alteration of protein glycosylation in liver diseases. *Journal of hepatology*. 2009;50(3):592-603.
11. Clarke JD, Novak P, Lake AD, Hardwick RN, Cherrington NJ. Impaired N-linked glycosylation of uptake and efflux transporters in human non-alcoholic fatty liver disease. *Liver international : official journal of the International Association for the Study of the Liver*. 2017;37(7):1074-81.
12. Culver EL, van de Bovenkamp FS, Derksen NIL, Koers J, Cargill T, Barnes E, et al. Unique patterns of glycosylation in immunoglobulin subclass G4-related disease and primary sclerosing cholangitis. *Journal of gastroenterology and hepatology*. 2019;34(10):1878-86.
13. Francisco R, Marques-da-Silva D, Brasil S, Pascoal C, Dos Reis Ferreira V, Morava E, et al. The challenge of CDG diagnosis. *Molecular genetics and metabolism*. 2019;126(1):1-5.
14. Guillard M, Wada Y, Hansikova H, Yuasa I, Vesela K, Ondruskova N, et al. Transferrin mutations at the glycosylation site complicate diagnosis of congenital disorders of glycosylation type I. *Journal of inherited metabolic disease*. 2011;34(4):901-6.
15. van Scherpenzeel M, Steenbergen G, Morava E, Wevers RA, Lefeber DJ. High-resolution mass spectrometry glycoprofiling of intact transferrin for diagnosis and subtype identification in the congenital disorders of glycosylation. *Translational research : the journal of laboratory and clinical medicine*. 2015;166(6):639-49 e1.
16. Lefeber DJ, Morava E, Jaeken J. How to find and diagnose a CDG due to defective N-glycosylation. *Journal of inherited metabolic disease*. 2011;34(4):849-52.

17. Wolthuis DF, Janssen MC, Cassiman D, Lefeber DJ, Morava E. Defining the phenotype and diagnostic considerations in adults with congenital disorders of N-linked glycosylation. *Expert review of molecular diagnostics*. 2014;14(2):217-24.
18. Ng BG, Buckingham KJ, Raymond K, Kircher M, Turner EH, He M, et al. Mosaicism of the UDP-galactose transporter SLC35A2 causes a congenital disorder of glycosylation. *American journal of human genetics*. 2013;92(4):632-6.
19. Westphal V, Kjaergaard S, Davis JA, Peterson SM, Skovby F, Freeze HH. Genetic and metabolic analysis of the first adult with congenital disorder of glycosylation type Ib: long-term outcome and effects of mannose supplementation. *Molecular genetics and metabolism*. 2001;73(1):77-85.
20. Martinez-Duncker I, Dupre T, Piller V, Piller F, Candelier JJ, Trichet C, et al. Genetic complementation reveals a novel human congenital disorder of glycosylation of type II, due to inactivation of the Golgi CMP-sialic acid transporter. *Blood*. 2005;105(7):2671-6.
21. Scobell RR, Kaplan BS, Copelovitch L. New insights into the pathogenesis of Streptococcus pneumoniae-associated hemolytic uremic syndrome. *Pediatric nephrology*. 2019.
22. DiMartini A, Day N, Lane T, Beisler AT, Dew MA, Anton R. Carbohydrate deficient transferrin in abstaining patients with end-stage liver disease. *Alcoholism, clinical and experimental research*. 2001;25(12):1729-33.
23. Flahaut C, Michalski JC, Danel T, Humbert MH, Klein A. The effects of ethanol on the glycosylation of human transferrin. *Glycobiology*. 2003;13(3):191-8.
24. Cottalasso D, Domenicotti C, Traverso N, Pronzato M, Nanni G. Influence of chronic ethanol consumption on toxic effects of 1,2-dichloroethane: glycolipoprotein retention and impairment of dolichol concentration in rat liver microsomes and Golgi apparatus. *Toxicology*. 2002;178(3):229-40.
25. Gong M, Garige M, Hirsch K, Lakshman MR. Liver Galbeta1,4GlcNAc alpha2,6-sialyltransferase is down-regulated in human alcoholics: possible cause for the appearance of asialoconjugates. *Metabolism: clinical and experimental*. 2007;56(9):1241-7.
26. Ghosh P, Liu QH, Lakshman MR. Long-term ethanol exposure impairs glycosylation of both N- and O-glycosylated proteins in rat liver. *Metabolism: clinical and experimental*. 1995;44(7):890-8.
27. Pompach P, Brnakova Z, Sanda M, Wu J, Edwards N, Goldman R. Site-specific glycoforms of haptoglobin in liver cirrhosis and hepatocellular carcinoma. *Molecular & cellular proteomics : MCP*. 2013;12(5):1281-93.
28. Zhang D, Huang J, Luo D, Feng X, Liu Y, Liu Y. Glycosylation change of alpha-1-acid glycoprotein as a serum biomarker for hepatocellular carcinoma and cirrhosis. *Biomark Med*. 2017;11(5):423-30.
29. Huang Y, Zhou S, Zhu J, Lubman DM, Mechref Y. LC-MS/MS isomeric profiling of permethylated N-glycans derived from serum haptoglobin of hepatocellular carcinoma (HCC) and cirrhotic patients. *Electrophoresis*. 2017;38(17):2160-7.
30. Verhelst X, Dias AM, Colombel JF, Vermeire S, Van Vlierberghe H, Callewaert N, et al. Protein Glycosylation as a Diagnostic and Prognostic Marker of Chronic Inflammatory Gastrointestinal and Liver Diseases. *Gastroenterology*. 2020;158(1):95-110.
31. Sato Y, Nakata K, Kato Y, Shima M, Ishii N, Koji T, et al. Early recognition of hepatocellular carcinoma based on altered profiles of alpha-fetoprotein. *The New England journal of medicine*. 1993;328(25):1802-6.
32. Landberg E, Astrom E, Kagedal B, Pahlsson P. Disialo-trisialo bridging of transferrin is due to increased branching and fucoylation of the carbohydrate moiety. *Clinica chimica acta; international journal of clinical chemistry*. 2012;414:58-64.

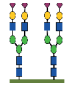
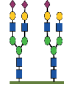
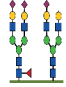
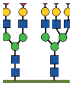
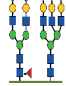
33. Stewart SH, Reuben A, Anton RF. Relationship of Abnormal Chromatographic Pattern for Carbohydrate-Deficient Transferrin with Severe Liver Disease. *Alcohol and alcoholism*. 2017;52(1):24-8.
34. Mann AC, Record CO, Self CH, Turner GA. Monosaccharide composition of haptoglobin in liver diseases and alcohol abuse: large changes in glycosylation associated with alcoholic liver disease. *Clinica chimica acta; international journal of clinical chemistry*. 1994;227(1-2):69-78.
35. Zhu J, Lin Z, Wu J, Yin H, Dai J, Feng Z, et al. Analysis of serum haptoglobin fucosylation in hepatocellular carcinoma and liver cirrhosis of different etiologies. *Journal of proteome research*. 2014;13(6):2986-97.
36. Vanderschaeghe D, Laroy W, Sablon E, Halfon P, Van Hecke A, Delanghe J, et al. GlycoFibroTest is a highly performant liver fibrosis biomarker derived from DNA sequencer-based serum protein glycomics. *Molecular & cellular proteomics : MCP*. 2009;8(5):986-94.
37. 37. Bruns T, Nuraldeen R, Mai M, Stengel S, Zimmermann HW, Yagmur E, et al. Low serum transferrin correlates with acute-on-chronic organ failure and indicates short-term mortality in decompensated cirrhosis. *Liver international : official journal of the International Association for the Study of the Liver*. 2017;37(2):232-41.
38. Viveiros A, Finkenstedt A, Schaefer B, Mandorfer M, Scheiner B, Lehner K, et al. Transferrin as a predictor of survival in cirrhosis. *Liver transplantation : official publication of the American Association for the Study of Liver Diseases and the International Liver Transplantation Society*. 2018;24(3):343-51.
39. Guillard M, Morava E, van Delft FL, Hague R, Korner C, Adamowicz M, et al. Plasma N-glycan profiling by mass spectrometry for congenital disorders of glycosylation type II. *Clinical chemistry*. 2011;57(4):593-602.

Supplementary files

Supplementary Table 1 is in an online depository accessible via this link:

<https://onlinelibrary.wiley.com/doi/10.1002/jimd.12273>

Supplementary Table 2. Medians of different TF isoforms measured with QTOF-MS

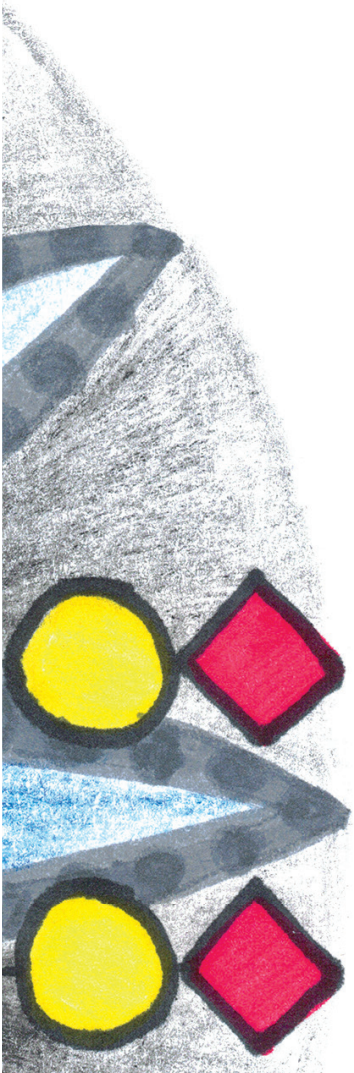
Peaks (amu)	structure	HC (n=39) Median (SD)	CLD (n=34) Median (SD)	LTx (n=76) Median (SD)	K-W test	HC/CLD	HC/LTx	CLD/LTx
79556		72.9 (6.3)	78.8 (4.9)	67.9 (7.3)	<0.001	0.006	0.040	<0.001
79266		3.0 (1.1)	2.0 (2.5)	1.9 (1.6)	<0.001	0.034	<0.001	0.918
79412		1.9 (0.8)	1.9 (1.7)	3.3 (1.6)	<0.001	1.0	<0.001	<0.001
79266+ 79412		5.2 (1.2)	4.0 (2.7)	5.2 (2.0)	0.029	0.273	1.0	0.024
80211		6.1 (1.3)	8.7 (1.9)	5.1 (1.4)	<0.001	<0.001	0.007	<0.001
80357		3.5 (1.1)	5.8 (1.75)	5.8 (1.4)	<0.001	<0.001	<0.001	1.0
Fucosylation ratio								
Trisialo		0.7 (0.6)	1.0 (1.9)	1.8 (1.0)	<0.001	1.0	<0.001	<0.001
Penta sialo		0.6 (0.3)	0.7 (0.2)	1.2 (0.3)	<0.001	1.0	<0.001	<0.001

HC=healthy controls, CLD=chronic liver disease, LTx=liver transplantation, K-W=Kruskal Wallis test, SD=standard deviation



CHAPTER 6

Discussion and conclusion



The main aims of this dissertation were (1) identification and characterization of the pathogenic variants in families with abnormal Golgi glycosylation and a phenotype dominated by liver disease and (2) to explore glycosylation in liver disease. To accomplish these goals, the following research questions were postulated:

1. Can we find the pathogenic gene(s) in three families with abnormal glycosylation?
2. Can we correlate the phenotype of *CCDC115* and *TMEM199* deficiency to more common hepatic diseases?
3. Can screening in a pre-selected patient group identify patients with hepatic injury due to congenital glycosylation disorders?

Answers to these research questions were provided in the chapters 2 to 5. In the next paragraphs each research question will be discussed separately followed by future perspectives and a research agenda.

Chapter	Main findings	Implications	Limitations
2 and 3	<ul style="list-style-type: none"> • 12 patients from 8 families were clustered based on comparable hepatic phenotype and glycosylation defects • Comparative genomics identified TMEM199 and CCDC115 as the human orthologs of yeast V-ATPase assembly factors Vph2p and Vma22p • NGS revealed pathogenic variants in <i>CCDC115</i> and <i>TMEM199</i> • CCDC115 and TMEM199 localize to the ER-to-Golgi region • (TMEM199 only) Ultrastructural hepatocyte analysis shows dilated Golgi and steatosis 	<ul style="list-style-type: none"> • Defects in CCDC115 and TMEM199 are recognized as a new type 2 CDG • Clinicians should be aware of CCDC115- and TMEM199 deficiency in patients with abnormal glycosylation, elevated liver enzymes and hepatosplenomegaly • Additional indirect evidence for the link between V-ATPase and abnormal glycosylation 	<ul style="list-style-type: none"> • All observations are in skin fibroblasts and HeLa cells, not in hepatocytes or hepatocyte-derived cell cultures
4	<ul style="list-style-type: none"> • This narrative review summarizes the findings of chapter 2 and 3 and puts them into perspective 	<ul style="list-style-type: none"> • Increased awareness among hepatologists 	<ul style="list-style-type: none"> • Few patients • Large gaps in knowledge regarding function and pathogenicity
5	<ul style="list-style-type: none"> • No CDG were found • Hyperfucosylation is associated with end-stage liver disease 	<ul style="list-style-type: none"> • CDG screening can be hampered by synchronous liver disease 	<ul style="list-style-type: none"> • Fair amount of drop-out due to low-quality samples • Sample size not large enough for CDG detection

HC=healthy controls, CLD=chronic liver disease, LTx=liver transplantation, K-W=Kruskal Wallis test, SD=standard deviation

1. Can we find the pathogenic gene(s) in three families with abnormal glycosylation?

In this thesis we used an alternative strategy, yeast homology, for identification of pathogenic variants in exome sequencing data of patients with abnormal Golgi glycosylation. Clustering was possible because of a similar hepatic phenotype of these patients. We identified *CCDC115* and *TMEM199* as new proteins involved in abnormal Golgi-located N-glycosylation.

New strategies for disease gene identification

In the introduction I explained different strategies to identify pathogenic variants in exome sequencing data. In chapter 2 and 3 we describe how we used knowledge of the yeast proteome as a tool to find pathogenic variants. Exon 1 of two *TMEM199* deficient patients was incompletely covered. This type of technical failure will occur much less in the future as techniques improve. A homozygous variant in *CCDC115* was not recognized in the candidate list. With the increased availability of genome sequencing (and with that, the large increase in called variants) new challenges arise. How to deal with exome data of high quality without (or with too much) likely pathogenic candidates? Here I will discuss potential strategies on different cellular levels.

Comparative genomics

The transfer of knowledge from one species to another is a valuable tool in disease gene identification and common practice since the first sequenced genomes. Orthologs are genes derived by a speciation event (in contrast to paralogs, which are derived from a duplication event).(1) The general consensus among comparative genomic researchers is that orthologs have similar function among species.(2) One of the assumptions in comparative genomics is reciprocity, two orthologous genes are more similar to each other than to any other gene. (3) Orthology prediction is one of the cornerstones of comparative genomics and a multitude of models are available to predict orthology.(2) We used an iterative orthology prediction model for yeast proteins based on reciprocity already successfully utilized for mitochondrial proteins (Figure 1).(4)

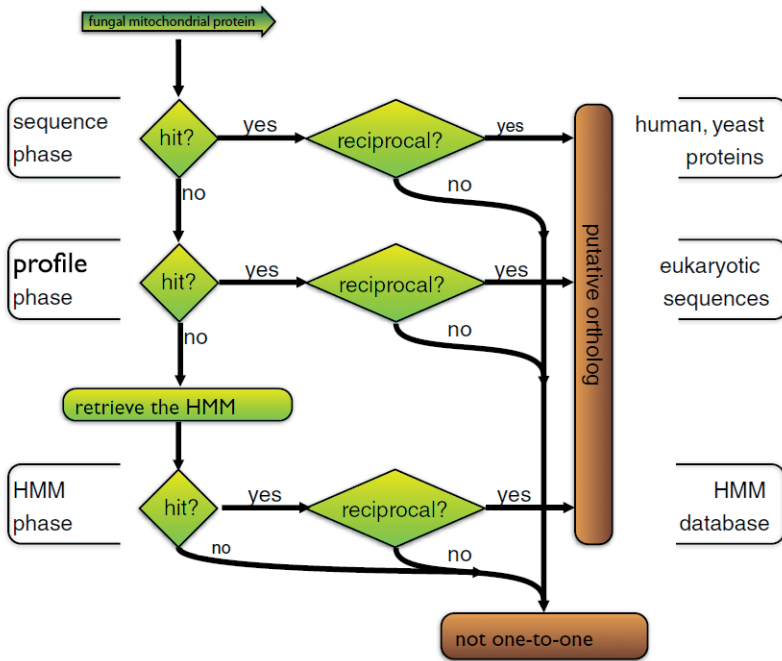


Figure 1 flow chart regarding reciprocity. Derived from Szklarczyk et al, Genome Biol, 2012 (4)

Proteomics

On proteome level several large scale projects were (and are) undertaken to map human protein-protein interactions (PPIs).⁽⁵⁻⁸⁾ These maps can aid in recognition of potential new targets. All these projects share their data in easy-to-use online databases.⁽⁹⁾ Yeast 2 hybrid PPI is the oldest technique to study PPIs and depends on proximity of a split transcription factor. Disadvantages are that the proteins must be able to enter the yeast nucleus and it provides an indirect readout. More recent techniques involve affinity purification with beads or agarose, washing, fractioning and mass spectrometry analysis. Advantages are high-throughput and scalability. Disadvantages are that temporal interactions easily get lost and that the sample can become contaminated resulting in false positive identification. Although these PPI databases give a hint, additional experiments will always be required. For example, the BioGrid network gives interactions for all V-ATPase assembly factors with an uncharacterized protein, KIAA2013. Exome sequencing data of CDG patients without a genetic diagnose was tested for variants in KIAA2013, but no pathogenic variants were identified.

Glycomics

Usually, a severe phenotype in infancy triggers genetic investigations for inborn errors of metabolism, including congenital glycosylation disorders. This has always been dependent on isoelectric focusing and thus the glycosylation pattern of transferrin. The success of this method is exemplified by the amount of discovered CDG. As explained in the introduction, QTOF-MS of the intact transferrin protein broadened the spectrum of glycosylation disorders, not dependent on the number of sialic acids. A disadvantage of this method is tissue and/or protein specificity. New methods are being developed to analyse the glycopeptides and will provide new valuable insights in these matters. Additionally, experimental designs identified new proteins associated with abnormal glycosylation, such as TMEM59 and TMEM115. (10, 11) These genes should be a target for screening in patients with abnormal glycosylation.

2. Can we correlate the phenotype of CCDC115 and TMEM199 deficiency to more common hepatic diseases?

As a consequence of our search strategy, yeast homology, little is known on the function of both proteins in human. In chapter 2 and 3 we show that dysfunction leads to abnormal Golgi-located glycosylation, indicating a detrimental effect on the Golgi. The phenotype, with hepatic steatosis and mild copper accumulation, provides addition (indirect) evidence for a role in hepatic lipid metabolism and copper metabolism. In chapter 4 we reviewed V-ATPase assembly factor functions and explored their effects on hepatic lipid metabolism and correlated CCDC115 and TMEM199 deficiency with NAFLD. The conclusion was that protein trafficking plays a significant role in hepatic lipid metabolism and we hypothesize a possible role for abnormal COPI trafficking as a common etiology.

Differences between yeast and human

Chapters 2 and 3 show that CCDC115 and TMEM199 are highly conserved within the eukaryotes and that homology detection was reciprocal with Vma22p and Vph2p, indicative for orthology. Most research on their function was conducted in *S. cerevisiae* and reviewed in chapter 4. After our publications came out, one paper was published on TMEM199 and CCDC115 in HeLa cells.(12) In this paper, reciprocal immunoprecipitation of TMEM199 and CCDC115 was proven.

Furthermore, depletion of either protein resulted in decreased lysosomal protein degradation and decreased acidification of endosomal compartments. Although no direct evidence is available yet, it seems likely that human TMEM199 and CCDC115 are V0 assembly factors just as their yeast orthologs.

Vph2p and Vma22p are ER-dedicated and have no known additional functions. However, it seems that TMEM199 and CCDC115 gained additional, yet uncharacterized, functions. Vph2p and Vma22p are located in the ER and not in COPI or COPII vesicles in yeast, in contrast to Vma21p which was demonstrated to shuttle between the ER and the Golgi. Epitope-tagged CCDC115 and TMEM199 were located outside the ER primarily in the ERGIC and the ER-to-Golgi transport vesicles. One possible explanation for this difference could be that V0 domain assembly takes place in the ERGIC. Another option is that assembly takes place in the ER and CCDC115 and TMEM199 chaperone the V0 domain via ERGIC vesicles to the Golgi. In this model, partial co-localization with COPII markers could indicate diffusion from the ER to the ERGIC, which is microtubuli independent. A lack of co-localization with ER-marker PDI could be due to unknown environmental or experimental factors. Complete or partial colocalization with COPI, COPII, Golgi and ERGIC markers predict that CCDC115 and TMEM199 travel with the V0 domain to the cis-Golgi, similar to Vma21p. However, both proteins lack a clear ER-retention motif. Co-localization with the V-ATPase was not possible due to lack of good-functioning antibodies.

Non-canonical V-ATPase functions

The V-ATPase is a highly conserved proton pump designed by Nature hundreds of millions years ago present in all eukaryotes.(13) The last decades additional functions besides acidification were discovered. It is a possibility that V-ATPase assembly factors play a direct or regulatory role in non-canonical functions of the V-ATPase. These included intracellular signaling through Wnt and Notch pathways, mTORC1 activation with subsequent cell growth and autophagy.(14-16) It will be interesting to discover if and how CCDC115 and TMEM199 influence these non-canonical functions.

ER-to-Golgi trafficking and non-NAFLD hepatic disorders

Chapter 4 provides in-depth analysis of possible mechanisms for the NAFLD phenotype. NAFLD is not the only disease resembling *CCDC115* and *TMEM199* deficiency. Clinicians also considered Wilson disease and Niemann-Pick C. Additionally, *LAL* deficiency patients also show a similar phenotype. Knowledge on ER-to-Golgi trafficking in these diseases could provide clues for the pathogenesis in *CCDC115* and *TMEM199* deficiency and vice versa.

Wilson disease

Unexplained elevated aminotransferases and low ceruloplasmin triggered several physicians of patients with *CCDC115* and *TMEM199* mutations to consider Wilson disease (WD, MIM: 227900). This autosomal recessively inherited disease is characterized by intracellular copper accumulation leading to hepatic, neurologic and psychiatric symptoms. Here, I will focus on the pathologic effects of WD on the liver. For a comprehensive review on neurological symptoms I refer elsewhere. (17) Patients with WD typically present with liver symptoms between the first and second decade of life, two to five years before neurological symptoms occur. (18) Around 5% of patients with WD are indicated to receive a liver transplantation. (19)

WD is caused by mutations in *ATP7B*, localized in the *trans*-Golgi network (TGN) where it provides copper to enzymes such as ceruloplasmin, which can then be secreted into the bloodstream (20). Furthermore, excessive Cu^{2+} in hepatocytes is removed from the cells by translocation of *ATP7B* to the bile canaliculi. (21) *ATP7B* is primarily expressed in hepatocytes in contrast to its paralog *ATP7A* which is located in all non-hepatic tissues. (22)

Insights on TGN-to-endosome trafficking show that *ATP7A/B* endocytosis is dependent on regulatory transporter proteins such as clathrin, AP-1, AP-2 and Rab22. (23) Interestingly, exocytosis of *ATP7B* in case of excessive copper follows a lysosomal exocytotic pathway, known to be disturbed in *Ac45* knockdown mice. (24, 25) In contrast to post-Golgi trafficking not much is known on ER-to-Golgi and intra Golgi regulation of copper.

Golgi-homeostasis defects in *CCDC115*- and *TMEM199* deficient patients may lead to copper homeostasis defects through different mechanisms. Although not

proven, a general defect of mislocalization or functioning of copper homeostasis proteins could produce the same phenotype. The V-ATPase assembly factors could possibly alter the pH of the TGN thereby influencing the function of ATP7B. The copper binding region of ATP7B is very sensitive for pH fluctuations.(26, 27) Although TGN pH for the V-ATPase assembly factors have yet to be determined, *VMA21* mutations lead to an increase in lysosomal pH.

Lysosomal acid lipase deficiency

Patients with Lysosomal Acid Lipase (LAL) deficiency due to a defect in *LIPA* present with variable degrees of hepatomegaly, dyslipidaemia and liver cell damage. Its prevalence is estimated at 1 to 175.000.(28) Liver damage may vary from slight elevation of aminotransferases to fibrosis and progression to cirrhosis.(29) There is a distinction between severe, infantile-onset LAL-D (Wolman disease; MIM 278000) and the less severe form that usually presents in childhood or even adulthood (Cholesterol Ester Storage Disease (CESD); MIM 278000). Patients with Wolman disease usually die before the age of 1 year, unless they are successfully treated with stem cell transplantation. CESD patients experience morbidity due to atherosclerosis, progressive liver disease, and/or malabsorption.

LAL exhibits an important role in cholesterol and triglyceride homeostasis. In healthy individuals, LAL is located in lysosomes and hydrolyses cholesteryl esters and triglycerides to free cholesterol and fatty acids respectively. The cholesteryl esters and TGs are derived from endocytosed LDL particles. When lysosomal TG levels are low, activity of sterol regulatory element-binding proteins (SREBPs) is increased, leading to upregulation of HMG-CoA reductase.(30) Loss-of-function mutations in LAL-deficiency cause cholesteryl esters and triglycerides accumulation in the lysosome. In reaction to this, under normal levels of triglycerides, the SREBP pathway is activated. Consequently, endogenous cholesterol production is elevated resulting in increased levels of LDL and VLDL.(30)

Niemann-Pick C

CCDC115- and TMEM199 deficiency are hepatically characterized by steatosis and, especially CCDC115 deficiency, hepatomegaly. CCDC115 deficient patients phenotypically resemble lysosomal storage diseases such as Niemann-Pick

disease type C (NPC, MIM 257220). Although characterized as a lysosomal storage disease, in essence, NPC is a cholesterol-trafficking-disease caused by autosomal recessive mutations in *NPC1* or *NPC2*. Prevalence is estimated at 1:150.000.(31) Deficiency in either two leads to accumulation of unesterified cholesterol due to ineffective transportation out of the lysosomes. Secondly, this imbalance in lysosomal lipids results in accumulation of lipids such as sphingomyelin and glucosylceramide.(32) Although NPC has a very heterogeneous presentation, the perinatal and early infantile period are often characterized by prolonged cholestatic icterus and regressing hepatosplenomegaly.(33) Interestingly, a subset of NPC patients develop an acute form of cholestatic jaundice with liver failure, similar to three out of eight *CCDC115* deficient patients.(34)

The mechanism behind cholesterol accumulation is incompletely understood. It is very likely that *NPC1* and *NPC2* act cooperatively; cytosolic *NPC2* binds free cholesterol and presents it to *NPC1*. *NPC1* then, by still unknown mechanism, transports cholesterol out of the lysosome. This process is dependent on functional vimentin, as *NPC1*-deficient cells have a hypophosphorylated form of vimentin with accumulation of Rab9.(35) The role of vimentin in lipid processing has long been known, as vimentin-deficient cells have abnormal lipid trafficking.(36) This is further highlighted by Genome wide associations studies (GWAS) identification of the vimentin-containing loci associated with high total cholesterol levels.(37) In conclusion, although the considerable overlap in phenotype with *CCDC115* deficient patients, a direct link between Golgi homeostasis defects and *NPC1* deficiency is not yet recognized.

3. Can screening in a pre-selected patient group identify more patients with hepatic injury due to congenital glycosylation disorders?

In chapter 5 we hypothesized that the a priori chance of identifying a CDG, and especially the V-ATPase assembly factor deficient CDG, would be increased in a cohort enriched with liver disease. This triggered us to develop a workflow for screening of a cohort consisting of patients with chronic liver disease and liver transplant recipients. In this study of >1000 samples we failed to find a CDG with our workflow. We believe that the main reason for failure is the low prevalence of CDG and even more the subgroup V-ATPase assembly factor deficiencies. As we already described this in chapter 5, we will explore additional explanation in this section.

One possible explanation could be that patients that develop severe liver disease warranting liver transplantation have more progressive disease and are likely to be diagnosed at young age. Indeed, of all *TMEM199*-, *CCDC115*-, and *ATP6AP1* deficient patients only 3 (all 3 *CCDC115* deficient) required liver transplantation. The oldest was 8 years old. Another explanation could be that patients with a mild phenotype (especially *TMEM199*-deficient patients) never require a liver transplantation. These patients would more likely be diagnosed at the outward patient clinic. However, few patients have been described thus far and the clinical spectrum will very likely expand over time.

Off course, when we started the screening project, *CCDC115*-CDG and *TMEM199*-CDG had yet to be discovered and the rationale was based on other potential CDG that can be accompanied by liver disease such as steatosis or fibrosis.(38)

Reflections

This dissertation focuses on the association between glycosylation and liver disease. We believe that with our findings we contributed in unravelling the fascinating science of glycosylation. Strengths of our study result from our excellent collaborations with experts in the field. This allowed us to identify the number of patients we did for the *CCDC115* and *TMEM199* papers in the EUROGLYCAN network. Also, establishing a cohort of >1000 patient samples for screening could only be possible because of collaborations with all national liver transplantation centers. Additionally, a particular strength of all studies is the QTOF-MS, which provides in depth glycan analysis that earlier methods cannot.

Limitations and gaps are stated here and in the research agenda. For the *CCDC115* and *TMEM199* articles, one limitation was that we did not use hepatocyte derived cell cultures as glycosylation is known to be tissue specific. These papers were the first to identify the cause (*CCDC115* and *TMEM199* pathogenic variants) and effect (abnormal glycosylation and a hepatic phenotype). Everything in between still needs to be explored. We started with localization of both proteins. Another group provided evidence for protein interaction and an effect on acidification. Next groups should focus on finding direct evidence that *TMEM199* and *CCDC115* are V-ATPase assembly factors. After that, it will be very interesting to see if both proteins are involved in canonical or non-canonical V-ATPase pathways.

The narrative review was intended to increase awareness among hepatologists and pediatricians. We first wrote an extensive review on the function of the V-ATP

assembly factors (published in this dissertation) but soon realized that this was not for a broad public. Therefore, a concise letter was drafted accompanied by an informative figure. We believe it is essential that awareness is increased as this will shed light on prevalence and the clinical spectrum.

Our screening study did not identify a CDG. A limitation of this study was that a large number of samples had to be excluded because of low quality. As sample age potentially negatively affects quality, we believe it is best to build a prospective database with the drawing of fresh samples and immediate glycoanalysis. Careful patient selection will increase the likelihood for CDG identification. Cut-off values based on liver enzymes, cholesterol and ceruloplasmin seem an obvious choice. Also, there should be a maximum age of 30-40 years as all V-ATPase deficient patients are diagnosed at a relatively young age. Concerning the methods used, we would suggest to abandon tIEF and directly screen with QTOF-MS. Improvements in QTOF-MS workflow makes this possible nowadays.

Future perspectives and conclusions

Identification of TMEM199-CDG and CCDC115-CDG is important for two reasons. The first is that patients with a resembling phenotype get a correct diagnosis. This prevents excessive treatment, such as Zinc, which can potentially be harmful. We are still far away from a treatment for these patients, however, identifying the affected genes is a first step. Treatment options can be pathway specific, for example, modulators of protein trafficking or V-ATPase functioning. This all depends on the function of both proteins. Another exciting option is knock-in of the wildtype gene with CRISPR/Cas9 technology in patient-derived organoids and subsequent retransplantation.⁽³⁹⁾ This technique is still a distinct prospect but could cure metabolic liver disease. More readily available treatments rely on unraveling the function of TMEM199 and CCDC115. Therefore, I believe that future research should focus on establishing the function of both proteins in human by answering questions such as: what is the protein interaction network of both proteins and what are the effects on glycosylation, protein trafficking and the V-ATPase? (See also Box 1). As a secondary important topic, the role of these two proteins, and V-ATPase assembly factors more general, should be studied in more common hepatic diseases, such as NAFLD and WD. This will further our understandings of these diseases and hopefully aid in finding a cure for these patients.

Box 1 Research agenda

Short term

- Elucidation of the interaction of human CCDC115 and TMEM199
- Elucidation of the interaction of both with the V-ATPase
- Elucidation of the protein-protein interaction network for the wildtype and the pathogenic variants
- Establishing the effect on intracellular lipid and copper metabolism
- Establishing the effect on protein transport

Long term

- Establishing an *in vivo* knockout research model
- Exploring possible treatment options for patients
- Increasing CDG awareness among pediatricians and hepatologists

References

1. Kuzniar A, van Ham RC, Pongor S, Leunissen JA. The quest for orthologs: finding the corresponding gene across genomes. *Trends in genetics : TIG*. 2008;24(11):539-51.
2. Sonnhammer EL, Gabaldon T, Sousa da Silva AW, Martin M, Robinson-Rechavi M, Boeckmann B, et al. Big data and other challenges in the quest for orthologs. *Bioinformatics*. 2014;30(21):2993-8.
3. Koonin EV. Orthologs, paralogs, and evolutionary genomics. *Annual review of genetics*. 2005;39:309-38.
4. Szklarczyk R, Wanschers BF, Cuypers TD, Esseling JJ, Riemersma M, van den Brand MA, et al. Iterative orthology prediction uncovers new mitochondrial proteins and identifies C12orf62 as the human ortholog of COX14, a protein involved in the assembly of cytochrome c oxidase. *Genome biology*. 2012;13(2):R12.
5. Hein MY, Hubner NC, Poser I, Cox J, Nagaraj N, Toyoda Y, et al. A human interactome in three quantitative dimensions organized by stoichiometries and abundances. *Cell*. 2015;163(3):712-23.
6. Gupta GD, Coyaud E, Goncalves J, Mojarad BA, Liu Y, Wu Q, et al. A Dynamic Protein Interaction Landscape of the Human Centrosome-Cilium Interface. *Cell*. 2015;163(6):1484-99.
7. Huttlin EL, Bruckner RJ, Paulo JA, Cannon JR, Ting L, Baltier K, et al. Architecture of the human interactome defines protein communities and disease networks. *Nature*. 2017;545(7655):505-9.
8. Kovalski JR, Bhaduri A, Zehnder AM, Neela PH, Che Y, Wozniak GG, et al. The Functional Proximal Proteome of Oncogenic Ras Includes mTORC2. *Molecular cell*. 2019;73(4):830-44 e12.
9. Stark C, Breitkreutz BJ, Reguly T, Boucher L, Breitkreutz A, Tyers M. BioGRID: a general repository for interaction datasets. *Nucleic acids research*. 2006;34(Database issue):D535-9.
10. Ullrich S, Munch A, Neumann S, Kremmer E, Tatzelt J, Lichtenthaler SF. The novel membrane protein TMEM59 modulates complex glycosylation, cell surface expression, and secretion of the amyloid precursor protein. *The Journal of biological chemistry*. 2010;285(27):20664-74.
11. Ong YS, Tran TH, Gounko NV, Hong W. TMEM115 is an integral membrane protein of the Golgi complex involved in retrograde transport. *Journal of cell science*. 2014;127(Pt 13):2825-39.
12. Miles AL, Burr SP, Grice GL, Nathan JA. The vacuolar-ATPase complex and assembly factors, TMEM199 and CCDC115, control HIF1alpha prolyl hydroxylation by regulating cellular iron levels. *eLife*. 2017;6:e22693.
13. Finnigan GC, Hanson-Smith V, Stevens TH, Thornton JW. Evolution of increased complexity in a molecular machine. *Nature*. 2012;481(7381):360-4.
14. Marshansky V, Rubinstein JL, Gruber G. Eukaryotic V-ATPase: novel structural findings and functional insights. *Biochimica et biophysica acta*. 2014;1837(6):857-79.
15. Cotter K, Stransky L, McGuire C, Forgac M. Recent Insights into the Structure, Regulation, and Function of the V-ATPases. *Trends in biochemical sciences*. 2015;40(10):611-22.
16. Meo-Evoli N, Almacellas E, Massucci FA, Gentilella A, Ambrosio S, Kozma SC, et al. V-ATPase: a master effector of E2F1-mediated lysosomal trafficking, mTORC1 activation and autophagy. *Oncotarget*. 2015;6(29):28057-70.
17. Bandmann O, Weiss KH, Kaler SG. Wilson's disease and other neurological copper disorders. *The Lancet Neurology*. 2015;14(1):103-13.
18. Czlonkowska A, Litwin T, Dusek P, Ferenci P, Lutsenko S, Medici V, et al. Wilson disease. *Nat Rev Dis Primers*. 2018;4(1):21.
19. Schilsky ML. Liver transplantation for Wilson's disease. *Annals of the New York Academy of Sciences*. 2014;1315:45-9.

20. Polishchuk R, Lutsenko S. Golgi in copper homeostasis: a view from the membrane trafficking field. *Histochemistry and cell biology*. 2013;140(3):285-95.
21. Nyasae LK, Schell MJ, Hubbard AL. Copper directs ATP7B to the apical domain of hepatic cells via basolateral endosomes. *Traffic*. 2014;15(12):1344-65.
22. Lutsenko S, Barnes NL, Bartee MY, Dmitriev OY. Function and regulation of human copper-transporting ATPases. *Physiological reviews*. 2007;87(3):1011-46.
23. Holloway ZG, Velayos-Baeza A, Howell GJ, Levecque C, Ponnambalam S, Sztul E, et al. Trafficking of the Menkes copper transporter ATP7A is regulated by clathrin-, AP-2-, AP-1-, and Rab22-dependent steps. *Molecular biology of the cell*. 2013;24(11):1735-48, S1-8.
24. Polishchuk EV, Concilli M, Iacobacci S, Chesi G, Pastore N, Piccolo P, et al. Wilson disease protein ATP7B utilizes lysosomal exocytosis to maintain copper homeostasis. *Developmental cell*. 2014;29(6):686-700.
25. Yang DQ, Feng S, Chen W, Zhao H, Paulson C, Li YP. V-ATPase subunit ATP6AP1 (Ac45) regulates osteoclast differentiation, extracellular acidification, lysosomal trafficking, and protease exocytosis in osteoclast-mediated bone resorption. *Journal of bone and mineral research : the official journal of the American Society for Bone and Mineral Research*. 2012;27(8):1695-707.
26. Nilsson L, Aden J, Niemiec MS, Nam K, Wittung-Stafshede P. Small pH and salt variations radically alter the thermal stability of metal-binding domains in the copper transporter, Wilson disease protein. *The journal of physical chemistry B*. 2013;117(42):13038-50.
27. Safaei R, Otani S, Larson BJ, Rasmussen ML, Howell SB. Transport of cisplatin by the copper efflux transporter ATP7B. *Molecular pharmacology*. 2008;73(2):461-8.
28. Carter A, Brackley SM, Gao J, Mann JP. The global prevalence and genetic spectrum of lysosomal acid lipase deficiency: A rare condition that mimics NAFLD. *Journal of hepatology*. 2019;70(1):142-50.
29. Burton BK, Balwani M, Feillet F, Baric I, Burrow TA, Camarena Grande C, et al. A Phase 3 Trial of Sebelipase Alfa in Lysosomal Acid Lipase Deficiency. *The New England journal of medicine*. 2015;373(11):1010-20.
30. Reiner Z, Guardamagna O, Nair D, Soran H, Hovingh K, Bertolini S, et al. Lysosomal acid lipase deficiency--an under-recognized cause of dyslipidaemia and liver dysfunction. *Atherosclerosis*. 2014;235(1):21-30.
31. Wheeler S, Sillence DJ. Niemann-Pick type C disease: cellular pathology and pharmacotherapy. *Journal of neurochemistry*. 2019.
32. Vanier MT. Complex lipid trafficking in Niemann-Pick disease type C. *Journal of inherited metabolic disease*. 2015;38(1):187-99.
33. Vanier MT. Niemann-Pick disease type C. *Orphanet journal of rare diseases*. 2010;5:16.
34. Yerushalmi B, Sokol RJ, Narkewicz MR, Smith D, Ashmead JW, Wenger DA. Niemann-pick disease type C in neonatal cholestasis at a North American Center. *Journal of pediatric gastroenterology and nutrition*. 2002;35(1):44-50.
35. Walter M, Chen FW, Tamari F, Wang R, Ioannou YA. Endosomal lipid accumulation in NPC1 leads to inhibition of PKC, hypophosphorylation of vimentin and Rab9 entrapment. *Biology of the cell / under the auspices of the European Cell Biology Organization*. 2009;101(3):141-52.
36. Sarria AJ, Panini SR, Evans RM. A functional role for vimentin intermediate filaments in the metabolism of lipoprotein-derived cholesterol in human SW-13 cells. *The Journal of biological chemistry*. 1992;267(27):19455-63.

37. Global Lipids Genetics C, Willer CJ, Schmidt EM, Sengupta S, Peloso GM, Gustafsson S, et al. Discovery and refinement of loci associated with lipid levels. *Nature genetics*. 2013;45(11):1274-83.
38. Janssen MJ, Waanders E, Woudenberg J, Lefeber DJ, Drenth JP. Congenital disorders of glycosylation in hepatology: the example of polycystic liver disease. *Journal of hepatology*. 2010;52(3):432-40.
39. Schwank G, Koo BK, Sasselli V, Dekkers JF, Heo I, Demircan T, et al. Functional repair of CFTR by CRISPR/Cas9 in intestinal stem cell organoids of cystic fibrosis patients. *Cell stem cell*. 2013;13(6):653-8.



APPENDICES

English summary

Nederlandse samenvatting

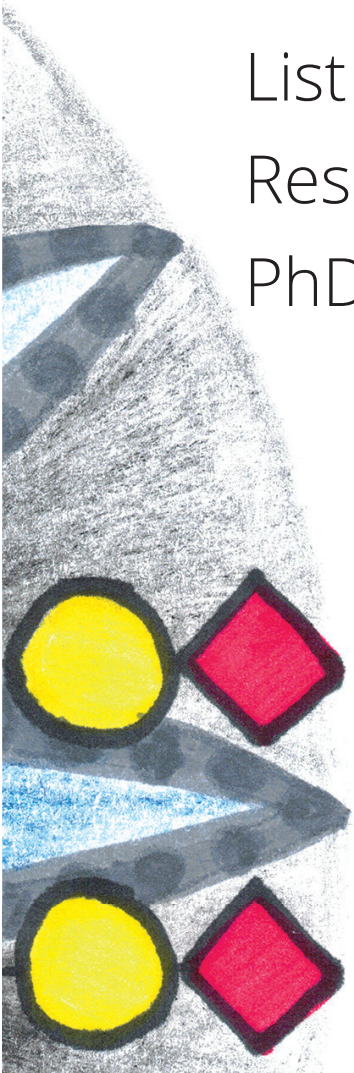
Dankwoord

Curriculum vitae

List of publications

Research data management

PhD Portfolio



English summary

Congenital Disorders of Glycosylation (CDG) are a group of inborn errors of metabolism that affect glycosylation. This group comprises over 100 different monogenic defects and most inherit in an autosomal recessive manner. Classically, patients present at early infancy with a multisystemic phenotype, almost always involving psychomotor functioning and dysmorphic features. As our ability to analyze a patients glycosylation profile increases due to advances in analytical methods, novel CDG are discovered regularly. In this thesis we described identification of two CDG subtypes in patients with a primarily hepatic phenotype. Additionally, we analyzed the glycosylation profile of patients with severe liver disease to see the effects of hepatic injury on glycosylation.

In **chapter 2 and 3** we described the discovery of CCDC115- and TMEM199-deficiency as two new CDG. We identified eight families with a similar hepatic phenotype and mild type 2 glycosylation defects. Regular workup, including whole exome sequencing, failed to identify a clear pathogenic variant. Based on previous knowledge that defects in subunits of the intracellular proton pump (the V-ATPase) cause a CDG, we set out to identify human orthologs of yeast proteins associated with V-ATPase and we identified CCDC115 and TMEM199 as orthologs of V-ATPase assembly factors. Both proteins have an unknown function in human.

We provided evidence that pathogenic variants in both genes are causative for the patients phenotype. Additionally, by using immunofluorescence studies, we showed that both proteins are located in the ER-to-Golgi region in HeLa cells.

Patients shared an overlapping phenotype with elevated serum transaminases, elevated alkaline phosphatase, low ceruloplasmin and hypercholesterolemia. Additionally, hepatosplenomegaly and steatosis were present. Severity of disease ranged from mildly elevated liverenzymes to liver failure warranting liver transplantation.

Chapter 4 is a narrative review on the possible roles and function of both proteins. First, we hypothesized that CCDC115 and TMEM199 are assembly factors of the human V-ATPase. We propose that they work together to stabilize part of the V-ATPase V0-domain and possibly travel with the V0 domain to the Golgi apparatus.

Next, we explored the possible link between *CCDC115*- and *TMEM199* deficiency with hepatic steatosis, a feature seen in all patients. We proposed a model involving COP-coated vesicles, which shuttle proteins to and from the Golgi apparatus and lipid droplets. Ineffective or absent *CCDC115* or *TMEM199* functioning could negatively influence this transport through yet unknown processes. Evidence for this hypothesis is based on (1) the localization of *CCDC115* and *TMEM199* in the ER-to-Golgi region and their co-localization with COP-coated vesicle proteins, (2) a general detrimental effect on Golgi-located glycosylation and (3) the steatotic phenotype of the patients.

In **chapter 5** we set out to screen a cohort of ~1000 patients with liver disease, including patients that needed a liver transplantation and patients that visited the hepatology outpatients clinic. We wanted to see if the glycosylation pattern of transferrin was different in liver disease compared to CDG. A secondary aim was to identify new CDG patients. We show that isoelectric focusing of transferrin is frequently abnormal in patients with liver disease, with 26% of the samples resembling a mild CDG type 2 pattern. Subsequent analysis of these samples with high-resolution mass spectrometry failed to identify clear CDG profiles. We confirmed that hyperfucosylation was associated with severe liver disease. Based on these experiments we suggest caution when interpreting isoelectric focusing results in patients with liver disease and suspected CDG. We did not identify glycosylation profiles that were suggestive of CDG.

In conclusion, in this thesis we showed that mutations in either *CCDC115* or *TMEM199* resulted in a glycosylation disorder and a primarily hepatic phenotype. We proposed that this is due to defective ER-to-Golgi trafficking. Additionally, we showed that severe liver disease can hamper CDG diagnostics and provided evidence for hyperfucosylation as a distinguishing factor. Further research should focus on elucidation of the pathophysiology of both proteins, which hopefully leads to effective treatment options for patients in the near future.

Nederlandse samenvatting

Congenitale defecten van de glycosylering (CDG) is een groep erfelijke stofwisselingsziekten waarbij de glycosylering is aangedaan. Deze groep bevat meer dan 100 verschillende monogene ziekten waarvan de meesten in een autosomaal recessieve manier overerven. Traditioneel presenteren patiënten zich op jonge leeftijd met een multisysteemisch fenotype waarbij bijna altijd de psychomotore ontwikkeling aangedaan is samen met dysmorfe kenmerken. Als gevolg van verbeterde technieken om glycosylering te analyseren worden er tegenwoordig frequent nieuwe CDG-subtypes ontdekt. In dit proefschrift beschrijf ik de identificatie van twee nieuwe CDG-subtypes in patiënten met een primair hepatisch fenotype. Additioneel hebben we glycosyleringsprofielen geanalyseerd van patiënten met ernstig leverfalen om de effecten hiervan op glycosylering te onderzoeken.

In **hoofdstuk 2 en 3** beschrijven we de ontdekking van CCDC115- en TMEM199 deficiëntie. We hebben 8 families geïdentificeerd met een vergelijkbaar hepatisch fenotype en milde type 2 glycosyleringsdefecten. Reguliere work-up, waaronder whole-exome-sequencing, resulteerde niet in een duidelijke pathogene variant. Het is bekend dat defecten in subunits van de intracellulaire protonpomp (de V-ATPase) leiden tot een CDG. Wij zijn op zoek gegaan naar humane orthologen van gist-eiwitten die geassocieerd zijn met de V-ATPase en vonden CCDC115 en TMEM199 als orthologen van twee V-ATPase assemblage eiwitten. Beide eiwitten hebben in mensen een nog onbekende functie.

We tonen bewijs dat beide pathogene varianten een causaal verband hebben met het fenotype. Tevens tonen we middels immunofluorescentie-proeven aan dat beide eiwitten zich in HeLa cellen bevinden in de ER-Golgi regio.

De patiënten hebben een overlappend fenotype met verhoogde serum transaminases en alkalisch fosfatase, verlaagd ceruloplasmine en hypercholesterolemie. Tevens was er sprake van hepatosplenomegalie en steatose. De ernst van symptomen varieerde van mild verhoogde leverenzymen tot leverfalen waarvoor levertransplantatie noodzakelijk was.

Hoofdstuk 4 is een beschrijvende review waarin we mogelijke functies van beide eiwitten beschrijven. Als eerste hypothetiseren we dat CCDC115 en TMEM199 assemblage eiwitten zijn van humaan V-ATPase. We doen een voorstel waarbij beide eiwitten samenwerken om het V0 domein van de V-ATPase te stabiliseren

gedurende assemblage maar ook dat de eiwitten betrokken zijn bij transport van het V0 domein naar het Golgi apparaat.

Als tweede gaan we verder in op de mogelijke associatie van een deficiëntie van CCDC115 en TMEM199 met leversteatose. We stellen een model voor met betrokkenheid van COP-coated vesikels. Deze vesikels verplaatsen eiwitten van en naar het Golgi apparaat en lipide druppels. Ineffectieve of afwezige CCDC115 of TMEM119 werking kan, op een nog onbekende wijze, een negatieve invloed hebben op dit proces. We baseren onze hypothese ten eerste op de locatie van CCDC115 en TMEM199 in de ER-Golgi regio en co-localisatie met eiwitten van COP-coated vesikels. Ten tweede op een gegeneraliseerd nadelig effect op glycosylering in het Golgi apparaat en ten derde op het steatotische fenotype van patiënten.

In **hoofdstuk 5** screenen we een cohort van ~1000 patiënten met leverziekte. Dit zijn patiënten die een levertransplantatie nodig hadden en patiënten die de hepatologie polikliniek bezochten. Ons primaire doel was om het verschil te zien in het glycosyleringsprofiel van transferrine tussen leverziekte en CDG. Het secundaire doel was om nieuwe CDG-patiënten te identificeren. We laten zien dat isoelectrische focusing van transferrine in 26% van de samples afwijkend is in leverziekte en vergelijkbaar is met een mild type 2 CDG profiel. Verdere analyse met hoge-resolutie spectrometrie liet echter geen evidente CDG profielen zien. Wel hebben we bevestigd dat hyperfucosylering geassocieerd is met ernstig leverfalen. Op basis van deze resultaten adviseren wij voorzichtigheid bij het interpreteren van isoelectrische focusing resultaten bij patiënten met leverziekte die verdacht worden van CDG. Er zijn geen glycosyleringsprofielen gevonden die een CDG suggereerden.

Dankwoord

Zo. Nu ik de laatste woorden aan het opschrijven ben valt er langzaam maar zeker een zware last van mijn schouders. Wat een traject heb ik doorlopen, hoge pieken en diepe dalen zijn kenmerkend geweest voor mijn promotietraject. Maar des te meer reden om trots te zijn op het eindproduct! Uiteraard zou dit boekje niet tot stand zijn gekomen zonder de hulp van anderen.

Allereerst wil ik mijn eerste promotor **Prof. Dr. J.P.H. Drenth** bedanken. Beste Joost, bedankt voor het vertrouwen wat ik vanaf het begin tot aan het eind van je heb gekregen. Jouw enthousiasme en werkethos zijn een voorbeeld voor alle junior-onderzoekers (zoals jij arts-onderzoekers noemt). Mijn promotietraject was zeker niet zonder hobbels op de weg. Je hebt op de juiste momenten mij mijn vrijheid gegeven maar ook was je de stok achter de deur wanneer dat nodig was. Heel erg bedankt en ik hoop in de toekomst nog vaak een biertje met je te drinken op een congres of nascholing event.

Ten tweede wil ik mijn tweede promotor **Prof. Dr. D.J. Lefeber** bedanken. Beste Dirk, als net afgestudeerd Geneeskunde student kwam ik met amper enige onderzoekservaring op jouw lab binnen. Jij hebt mij geleerd om te denken als een basaal onderzoeker en met je enthousiasme en geduld (glycosy wat?) mij geïntroduceerd in de wondere wereld van de glycomics. Gedurende mijn promotietraject ben je Professor geworden, een titel die je past. Ik hoop dat we in de toekomst elkaar ooit nog gaan tegenkomen en misschien een mooi glycosyleringsproject gaan opzetten.

Als derde wil ik **Monique van Scherpenzeel** bedanken voor haar begeleiding. Beste Monique, je nam me onder je hoede op het glycomics lab gedurende mijn promotie. Bedankt dat ik altijd bij je kon aankloppen voor vragen of overleg. Het ga je goed met je eigen onderneming!

Verder wil ik alle leden van **de manuscriptcommissie en de corona** van harte bedanken voor het beoordelen van mijn proefschrift en de bereidheid om met mij van gedachten te wisselen gedurende de verdediging.

Alle **co-auteurs** van harte bedankt voor de prettige samenwerking, ik denk dat we een paar mooie publicaties hebben bewerkstelligd!

Rene, Hennie, Jody en Daisy. Zonder jullie zou dit boekje nooit hebben bestaan. Als analisten van het MDL lab hebben jullie mij hands-on begeleid bij

het uitvoeren van alle experimenten. Ik heb altijd met veel plezier met jullie in het lab gestaan en een kaartje gelegd in de pauzes. Bedankt!

Karin, Fokje, Gerrie, Irma, Astrid en Else. Als analisten van het metabool laboratorium zullen jullie af en toe gezucht moeten hebben toen deze Geneeskunde student bij jullie op het lab verscheen. Bedankt voor alle uitleg en hulp bij het pipetteren, runnen en analyseren van de vele gelletjes en massa spectrometrie samples.

Anke, Angel, Amin, Sharita en Walinka. Als promovendi in de glycosyleringsgroep hebben we veel samengewerkt. Bedankt voor alle leuke inhoudelijke discussies tijdens ons wekelijkse journal club en daarbuiten. Anke, Sharita en Walinka, jullie zijn allen goede onderzoekers en ik weet zeker dat jullie goed op jullie plek zullen komen! Angel, thank you very much for your assistance in interpretation of my data, I hope you fare well and will find your place. Amin, thank you for all the pleasant conversations while waiting for results. I hope to see you one day in Kuching!

Vervolgens wil ik de promovendi van de MDL groep bedanken: **Angelique, Dorian, Edgar, Floor, Govert, Hedwig, Isabelle, Karina, Lauranne, Loes, Mark B, Mark L, Marten, Myrthe, Rene, Simon, Titus, Tom, Wybrich, Xavier, Yannick en Yasmijn.** Gedurende de 3 jaar dat ik als promovendus op het RadboudUMC rondliep is deze lijst fors uitgebreid en velen van jullie kan ik tegenwoordig als mijn directe collega's beschouwen. Ik denk dat we met z'n allen iets moois neergezet hebben in het RadboudUMC. Het ontwikkelplan is uitgerold, de high-impact publicaties vlogen ons om de oren en we stonden vooraan op elk congresfeestje! Ik wil twee mensen apart bedanken: Mark B, mijn roomie, bedankt voor het uitbreiden van mijn muzikale kennis, zonder jou had ik nooit van het bestaan van 'Die Antwort' en 'City and Colour' geweten. Mijn onderzoekstijd is door jou een stuk leuker geworden. Goed om te horen dat je helemaal je draai hebt gevonden! Titus, Twijnands, Titus Pullo, vanaf dag 1 konden we het goed vinden. Samen in het vroege treintje op weg naar Nijmegen en weer terug na een vruchtbare onderzoeksdag. Vele uren slap ouwehoeren over van alles van chaperonneren tot Game of Thrones. Ook jij hebt mijn onderzoekstijd en stuk leuker gemaakt. Dank!

Bedankt alle studenten die meegewerkt hebben aan verschillende aspecten van mijn promotie: **Olaf, Floris, Pieter-Paul, David en Hassin.** Ik vond het leuk om jullie onderzoekstages te begeleiden en met jullie samen te werken. Ik wens

jullie het beste voor de toekomst.

Ik wil mijn huidige **collega's van het Jeroen Bosch Ziekenhuis** in 's Hertogenbosch bedanken voor hun support gedurende de 2 jaar dat ik alweer rondloop bij de MDL vakgroep. Tessa en Bob bedankt voor het meedenken en het vertrouwen wat ik van jullie gekregen heb.

Dan van 's Hertogenbosch naar Amsterdam. Ik wil mijn Geneeskundevrienden **Max, Robert en Coty** bedanken voor alle steun gedurende mijn onderzoekstraject. Jullie ongezouten meningen en kritische blikken werden (en worden) zeer gewaardeerd. Ik kijk uit naar nog vele avondjes discussiëren over de gezondheidszorg, het leven en (soms) wat luchtigere onderwerpen.

Daarna van Geneeskunde naar Farmacie: **Evert, Johan, Maarten, Martijn, Niels, Robert en Roland** bedankt! Sinds 2003 zijn wij een hechte vriendengroep. Wat hebben we veel meegemaakt in al die jaren: de collegies Farmacie, het studentenleven in Utrecht, de vele pokeravondjes en uiteraard de memorabele tripjes door heel (Oost-)Europa. Ondanks dat dit alles de laatste jaren steeds moeilijker te plannen is, is het mooi om te zien dat we met z'n allen langzaam volwassen aan het worden zijn. Mijn beide paranimfen, Niels en Johan, wil ik speciaal bedanken. **Niels**, vanaf dag een van het Farmacie introductiekamp beste matties. Samen met Julia, ook (bijna) van het eerste uur, ben jij betrokken geweest bij alle grote gebeurtenissen in mijn leven. Mooi dat we met z'n vieren zo goed kunnen opschieten. Kunnen we straks met de kids aan het strand vakantie vieren, jij surfend en ik met een boek op het strand. In 2015 was ik jouw paranimf. Nu staan we weer quitte. **Johan!** Ook onze geschiedenis gaat ver terug waarbij ik vooral de mooie tijden aan de Obrechtstraat nooit zal vergeten. Sinds je naar het Zuiden bent verhuisd zien we elkaar niet meer dagelijks maar uit het oog is niet uit het hart!

Beste schoonfamilie **Abhilakh Missier**. Dank jullie voor alle support en bemoedigende woorden de laatste jaren.

Lieve **Nicolette, Petra, Marco, Arjan en neefjes**. Lieve zusjes, wat hebben we een moeilijke tijd doorgemaakt afgelopen 2 jaar. Voor mij is dit proefschrift een licht aan het uiteinde van een tunnel waarmee ik een stap voorwaarts gezet heb. Ik hoop dat ik hiermee jullie ook een beetje mee kan nemen de positiviteit in. Bedankt dat jullie altijd voor me klaar staan met adviezen, een luisterend oor of hoe dan ook.

En dan als laatste, mijn allerliefste **Arti**. Sinds 2004 zijn wij onafscheidelijk. We houden beide niet van clichés, maar we zullen elkaar wel aanvullen, of zoiets. Eigenlijk is er teveel waarvoor ik je moet bedanken: het ontwerpen van de prachtige omslag, mij achter mijn broek aan zitten, je geduld, je adviezen en het luisteren naar mijn frustraties. Concluderend, bedankt voor alles! HvJ!

Curriculum vitae

Johannes (Jos) Cornelis Jansen werd op 30 november 1984 geboren te Tiel. Na het behalen van zijn VWO-diploma aan het Rivierenland college in 2003 ging hij, na uitgeloot te zijn voor de studie Geneeskunde, Farmaceutische Wetenschappen studeren aan de Universiteit van Utrecht. In 2006 behaalde hij de titel Bachelor of Science. In hetzelfde jaar werd hij via decentrale selectie geselecteerd voor de studie Geneeskunde aan de Universiteit van Amsterdam. In 2013 behaalde hij cum laude zijn artsenexamen. Direct vanuit de collegebanken ging hij zijn



eerste fulltime betaalde baan aan als arts-onderzoeker in het RadboudUMC te Nijmegen. Onder de leiding van Prof. Dr. J.P.H. Drenth en Prof. Dr. D.J. Lefeber begon hij aan zijn promotietraject naar de associatie tussen glycosylering en leverziekten, waarvan het eindresultaat in dit proefschrift beschreven staat.

In 2016 werd hij aangenomen voor de opleiding tot Maag-, Darm- en Leverarts in de regio Oost. De vooropleiding Interne Geneeskunde rondde hij af in het Jeroen Bosch Ziekenhuis te 's Hertogenbosch onder begeleiding van opleidster Dr. W. Smit. Daarna volgde een jaar in het RadboudUMC onder begeleiding van Dr. M.C.A. van Kouwen.

Sinds 1 februari 2019 volgt hij zijn opleiding tot Maag, Darm- en Leverarts weer in het Jeroen Bosch Ziekenhuis onder begeleiding van opleiders Dr. T.E.H. Römken en Dr. R.C.H. Scheffer. Jos woont in Utrecht met zijn vrouw Arti en hun zontje Indra.

List of publications

Jansen JC, van Hoek B, Metselaar HJ, van den Berg AP, Zijlstra F, Huijben K, van Scherpenzeel M, Drenth JPH, Lefeber DJ. Screening for abnormal glycosylation in a cohort of adult liver disease patients. *Journal of inherited metabolic disease*. 2020.

Cannata Serio M, Graham LA, Ashikov A, Larsen LE, Raymond K, Timal S, Le Meur G, Ryan M, Czarnowska E, **Jansen JC**, He M, Ficicioglu C, Pichurin P, Hasadsri L, Rios-Ocampo WA, Gilissen C, Rodenburg R, Jonker JW, Holleboom AG, Morava E, Veltman JA, Socha P, Stevens TH, Simons M, Lefeber DJ. sMutations in the V-ATPase assembly factor VMA21 cause a congenital disorder of glycosylation with autophagic liver disease. *Hepatology*. 2020.

Jansen JC, Wolthuis D, Van Scherpenzeel M, Ratzu V, Drenth JPH, Lefeber DJ. NAFLD Phenotype in Patients With V-ATPase Proton Pump Assembly Defects. *Cell Mol Gastroenterol Hepatol*. 2018;5(3):415-7 e1.

Jansen JC, Cirak S, van Scherpenzeel M, Timal S, Reunert J, Rust S, Perez B, Vicogne D, Krawitz P, Wada Y, Ashikov A, Perez-Cerda C, Medrano C, Arnoldy A, Hoischen A, Huijben K, Steenbergen G, Quelhas D, Diogo L, Rymen D, Jaeken J, Guffon N, Cheillan D, van den Heuvel LP, Maeda Y, Kaiser O, Schara U, Gerner P, van den Boogert MA, Holleboom AG, Nassogne MC, Sokal E, Salomon J, van den Bogaart G, Drenth JP, Huynen MA, Veltman JA, Wevers RA, Morava E, Matthijs G, Foulquier F, Marquardt T, Lefeber DJ. CCDC115 Deficiency Causes a Disorder of Golgi Homeostasis with Abnormal Protein Glycosylation. *American journal of human genetics*. 2016;98(2):310-21.

Jansen JC, Timal S, van Scherpenzeel M, Michelakakis H, Vicogne D, Ashikov A, Moraitou M, Hoischen A, Huijben K, Steenbergen G, van den Boogert MA, Porta F, Calvo PL, Mavrikou M, Cenacchi G, van den Bogaart G, Salomon J, Holleboom AG, Rodenburg RJ, Drenth JP, Huynen MA, Wevers RA, Morava E, Foulquier F, Veltman JA, Lefeber DJ. TMEM199 Deficiency Is a Disorder of Golgi Homeostasis Characterized by Elevated Aminotransferases, Alkaline Phosphatase, and Cholesterol and Abnormal Glycosylation. *American journal of human genetics*. 2016;98(2):322-30.

Jansen JC, van Dop WA, Fockens P, Lowenberg M. Acute upper abdominal pain after excessive vomiting: Boerhaave's syndrome. *Nederlands tijdschrift voor geneeskunde*. 2013;157(35):A6374.

Research data management

The data that was collected during this thesis was in accordance with principles of the Declaration of Helsinki. All patients that provided samples used for the research in chapter 2 and 3 provided informed consent to their respective clinician. The patient data used for chapter 5 was anonymously provided to J.C. Jansen by participating authors. The research proposal for this study was presented to and approved by the medical and ethical review board Committee on Research Involving Human Subjects Region Arnhem Nijmegen, Nijmegen. The case number assigned was: 2018-5012.

Published data generated or analyzed in this thesis are part of published articles and its additional files are available from the associated corresponding authors on reasonable request. Data for chapters 2, 3 and 5 was stored on a personal space within the network during the course of this thesis. After completion of the thesis, all data was transferred to the Gastroenterology Departments' H-drive (H:\Onderzoekers\Jos Jansen). Exome sequencing files that were used for chapter 2 and 3 were analyzed with permission of the Department of Genetics of the RadboudUMC.

Lab journals were registered, issued and stored by the Department of Translational Metabolic Laboratory of the RadboudUMC. The generated data was coded (JJYYMMDD.X) for traceability. Patient samples that were used in chapter 2,3 and 5 were taken from a general storage facility that was operated by technicians from the Translational Metabolic Laboratory of the RadboudUMC. The patient samples that were provided for the experiments described in chapter 5 were stored in the refrigerator in the Translational Metabolic Laboratory. All other samples, including Western Blots, were stored in the Laboratory of the Gastroenterology and Hepatology department. Based upon reasonable request, these samples can be provided by the technician concerned. Data will be stored for 15 years after termination of the study (May 1, 2016)

PhD Portfolio

Name PhD student: J.C. Jansen
Department: Gastroenterology & Hepatology
Graduate school: Radboud Institute for Molecular Life Sciences
PhD period: 21-05-2013 until 20-05-2016
Promotor(s): Prof. Dr. J.P.H. Drenth
Co-promotor: Prof. Dr. D.J. Lefeber

TRAINING ACTIVITIES	Year(s)	ECTS
Courses & Workshops		
Introduction day RadboudUMC	2013	0.5
RUNMC Introduction for PhD student	2013	2.5
PhD student retreat (poster)	2014	0.75
Workshop: How to write a medical scientific paper	2015	0.2
Seminars & Lectures		
Ravensteijn GI lectures (yearly 6x)	2013 - 2016	1.5
GI-hep meetings (yearly 8x)	2013 - 2016	1.5
(Inter)national Symposia & Congresses		
CDG orphan course, Nijmegen	2013	1.0
NVGE voor- en najaarsvergadering, Veldhoven (3x) (oral and poster)	2013 - 2016	2.0
Joint Glycobiology Meeting, Ghent (oral)	2014	1.0
UEGW, Vienna (poster)	2014	1.0
EURO-CDG & TREATCDG, Madrid (oral)	2015	1.0
AASLD, San Francisco (poster)	2015	1.0
BSPHAN annual meeting, Bristol (oral)	2016	0.75
ESN voorjaarsvergadering, Groningen (oral)		
Other		
Radboud In'to Languages IELTS English Course	2013	2.5
Peer reviews (2x)	2013 - 2014	0.2
GI Journal Club (weekly)	2013 - 2016	12.0
Glycomics Journal Club (weekly)	2013 - 2016	12.0
GI research meetings (weekly)	2013 - 2016	12.0
Organisation of glycoHeidag	2015	1.0
MDL ontwikkelplan	2015 - 2016	5.0
TEACHING ACTIVITIES		
	Year(s)	ECTS
Lecturing		
Supervision and tutoring in the course 'Cardiometabolic'	2013 - 2014	0.4
RAMS Summerschool presentation	2015	0.2
Other		
Student internship coaching, 5 months	2014	1.7
Student internship coaching, 4 months	2014	1.3
Supervision of 2 nd year BMW student	2014	1.75
Student internship coaching, 4 months	2015	1.7
Student internship coaching, 3 months	2015	1.0
TOTAL		68,45

